REPUBLIC OF YEMEN

MINISTRY OF AGRICULTURE AND IRRIGATION

Agro biodiversity and Climate Change Adaptation Project (ACAP)/PSU

Ctr. Reference: ACAP/GEF / CS /9

Project ID: P103922

Global Environment Facility (GEF)

Trust Fund Grant No. TF 096330

Final Report on

Assessment of Historical Climate Data

Prepared by;

Consultant: Civil Aviation & Meteorology Authority-

Yemen Meteorological Service (CAMA/YMS)

Haddah, St., Sana'a
Tel: + 967 1 419774/ 419775
Fax: + 967 1 419770
Email: ymsh-cama@y.net.ye

Submitted to:

The Client: Agro-Biodiversity and Climate Adaptation Project (ACAP) /Global Environment Facility (GEF)

Abu Baker Al Sedeek Street-In front of Rayman School, Sana'a
Tel: + 967 1 441770/450472
Fax: + 967 1 441768
Email: acap@yemen.net.ye

Sana'a, February 2015

For the attention of:
Dr. Mohammed Ali Hassan Farea
Project Technical Specialist
Sana‟a, Yemen
Tel: + 967 1 441770/450472
Cellophane: + 967 770 771 916
Facsimile: +967 1 441768
E-mail: fareamohamed@yahoo.com

Table of Contents

Last of Tables

List of Figures

List of abbreviations

AMIP	Atmospheric Model Inter-comparison Project
AOGCM	Atmospheric Oceanic General Circulation Model
CMIP5	Coupled Model Inter-comparison Project 5th phase
CO2	Carbon dioxide
IPCC	Intergovernmental Panel on Climate Change
RCP45	Representative Concentration Pathway for scenario 45
RCP85	Representative Concentration Pathway for scenario 45
WGCM	Working Group on Couple Modeling

1. Overview of current and future assessments of climate change in the Arabian Peninsula

1.1. Features of the climatic conditions of Yemen and neighboring regions.

The Arabian Peninsula is located in the south-west Asia, occupies an area of about 3.1 millions square kilometers and is the largest Peninsula on the planet. On the west, it is bordered by the Red Sea, the Gulf of Aden in the south and the Arabian Sea in the east - the Gulf of Oman and the Indian Ocean. The Arabian Peninsula comprises of the following states: Bahrain, Yemen, Qatar, Kuwait, United Arab Emirates (UAE), Oman and Saudi Arabia (SA).

The Arabian Peninsula is located between 12 ° and 30 ° N and 35 ° and 60 ° E. The region is characterized by diverse natural conditions and various geophysical structures (Figure 1.1.1), dominated by plains and plateaus in the west and the south-east Mountains (altitude up to 3600m). Most of the territory is occupied by deserts and semi-deserts (Rub 'al Khali, ad-Dahna Desert, Nefud, Tihama et al.), which account for about 89% of the territory.

More than 50 million years ago, Arabian Peninsula was part of African continent. But after rift zone along the Red Sea has been formed, the Peninsula began to move away from the coast of Africa. Powerful geological force contributed to the formation of the new highlands formed along the coast. Along the coast of the Red Sea mountain ranges reaches 3,000 meters in northern Yemen and dominated by the Jabal an Nabi Shuyab (3766 m) - the highest mountain in the Arabian Peninsula.

Figure 1.1.1. – Geographical and Political map of the Arabian Peninsula

The climate of the Arabian Peninsula is one of the most unfavorable climate for human being [1,2]: continental hot dry, subtropical in the north, and tropical in the south. Limited moisture, extreme temperatures and high summer evaporation make this area the most unfit for human life, animals and vegetation. The area is situated in the arid areas in the north where the climate is temperate, with maximum precipitation in winter and tropical climate in the south. The absolute maximum temperature in summer reaches 50 ° C in the desert, winter temperatures range from 11 – 20 °C in the continental part of the peninsula, up to 19 – 28 ° C on the coast of the Red Sea and from 11 – 17 °C along the coast of Persian Gulf. The absolute minimum temperature recorded in Kuwait and Al-Khafji is -2 °C and -6 °C respectively. The climate of southern and central parts of the region is tropical. The Red Sea coast climate belongs to the hottest and humid places in the globe. The temperature over these areas ia at least 15 °C and often exceed 45 °C. The climate over inland and continental areas is dry with average temperature in June – 30 °C and -10 °C in January) [3]. In the desert of Rub 'al Khali destructive hot wind blows sandstorm, raising the temperature to 50 "C and the relative humidity at the same time close to zero.

Rainfall is extremely low: in the south - about 50 mm per year (sometimes there is no rain for several years), about 100 mm annually in tropical areas. A little more rain in the south-west and southeast of the peninsula - here on the slopes of the mountains, observed annual precipitation of about 500 – 700 mm. Long-term drought and dust storms are common. Throughout the year, the Arabian Peninsula is under the influence of the Azores subtropical high pressure, whose influence extends to north as far as southern Syria [4, 5, 6]. As a consequence, in the west of the peninsula and the Red Sea prevails winds of the northern and north-westerly direction, that in winter only change to eastern winds carrying air from Central Asia. These conditions of air masses circulation do not favor precipitation formation [7]. Only in the far north planned transition to a brief period of winter rains associated with the passage of the polar front, and during summer, the extreme south-west rainfall brought by the monsoon winds. The main summer monsoon moisture loses, passing over Ethiopia [8]. During summer on the south coast of the Arabian Peninsula observed transport of air masses from the west (summer monsoon) [9, 10]. In some areas, for several years in a row have observed no rainfall at all or sometimes showers have been observed which results on few tens millimeters of moisture [11]. Almost everywhere, these random rains fall on the winter season. Over the mountains regions, of the internal parts of the Arabian Peninsula little rain have been observed, these areas are desert [12].

1.2. A brief overview of the results of modern research of climate change on the Earth, Arabian Peninsula and Yemen.

According to the degree of importance, factors of climate change include the following:

a) Change in the concentration of greenhouse gases in the atmosphere. Greenhouse gases (Carbon dioxide, water vapor, methane, and others) are responsible for absolving infrared radiation from the Earth's surface and prevent it from scattering in the space. During the XX century, the concentration of carbon dioxide in the atmosphere has increased by a quarter. While there is no proof of exactly whether the increase is caused by human activities or is caused by natural processes, the number of arguments in favor of the first version is large compared to the second version. Particularly, in the late 2007 Nobel Peace Prize was awarded to the Intergovernmental Panel on Climate Change (IPCC), for their research on the influence of anthropogenic gases in the global warming.

b) Changing of landscapes. The nature of the land surface and vegetation on it depends on the number of scattered (reflected) of radiation and, ultimately, the Earth's Albedo. Landscape has significant impact on the agriculture and urbanization.

c) Restructuring of ocean currents. Ocean currents play an important role in the redistribution of heat from the tropical zones of the Earth to the temperate and polar regions. Restructuring of the flow can cause changes in salinity and temperature of individual sections of the oceans. Also global ocean circulation map is changing due to the movements of the continent.

d) Changes in the luminosity of the sun. At this moment, the amount of energy coming from the sun varies very slightly (about 0.1%). However, in the long run, these fluctuations can have a significant impact on the climate and general circulations in general.

e) Strong explosions on the surface of the Earth. Asteroid, large volcanic eruptions, nuclear explosions lead to the release of aerosols into the stratosphere, which absorbs the sun's heat, not allowing it to the surface of the earth, and the dust in the troposphere increases cloudiness, which reflects sunlight into space. These factors together can lead to the so-called nuclear winter lasting from several months to decades.

f) Fluctuations of the Earth's axis. Tilt of Earth's axis relative to its plane is 23.5 ° and experiencing fluctuations in the value of 1° for the hundreds of thousands of years. These changes affect the temperature contrast between the high and low latitudes.

g) Variations of the orbit radius of the Earth. Under the influence of gravitational perturbations of other planets, mean distance from the earth to the sun can vary at the scale of the order of 100 million years. This affects the amount of the sun energy coming from the sun to the earth.

h) Variation of the eccentricity of Earth's orbit. For the same reasons, the long-period fluctuations in the Earth's orbit undergoes elongation, affects the temperature contrast between the hemispheres. Currently, due to the reasons that, the elliptic orbit of the distance from Earth to the Sun changes throughout the year by 3.4%, while the amount of heat energy produced is 7%. Maximum is in January, minimum in July. In the Northern Hemisphere, it reduces seasonal climatic variations, and increases seasonal variations in the South.

i) The reversal of the earth's magnetic field. On average one out of four of a million years, magnetic field of the Earth changes its pole (although the last time such reversal occurred was 780,000 years ago). At the moment of polarity changes of the atmosphere, to a certain extent is protected from the solar wind and cosmic rays.

j) Fluctuations in the intensity of cosmic rays. Cosmic rays ionize atoms in Earth's atmosphere. Ions are used as centers of condensation of water vapor and promote the formation of clouds, which increases the Earth's Albedo. Cosmic ray intensity changes during the motion of the solar system in the Galaxy.

k) The movement of tectonic plates. Continental plates move at a rate of a few centimeters per year. During the 100 million years old stay continents on the planet's surface is radically changing. From time to time all the plates are combined into one huge supercontinent (Pangaea, Gondwana et al.), the greater part of which is set sharply continental climate, which leads to desertification.

All these factors contribute differently to climate change and have different time scales fluctuations forming the full range of climate change on the inter-annual variability to cyclical fluctuations in the tens, hundreds, thousands and millions of years, due to space and geophysical factors [13, 14]. According to recent reports from the 5th IPCC report [15], the main climate factors make the following contributions to its fluctuations, as shown in Figure 1.2.1, where the temperature anomalies (° C) are:

a) The observed global temperature over the period from 1890 to 2010 reanalysis data Hadley Center [16] (black line) and it's smoothing according to Lean [17, 18, 19] (red line), Lockwood [20, 21, 22, 23] (pink line), Folland [24] (green line), Kaufmann [25, 26, 27] (blue line);

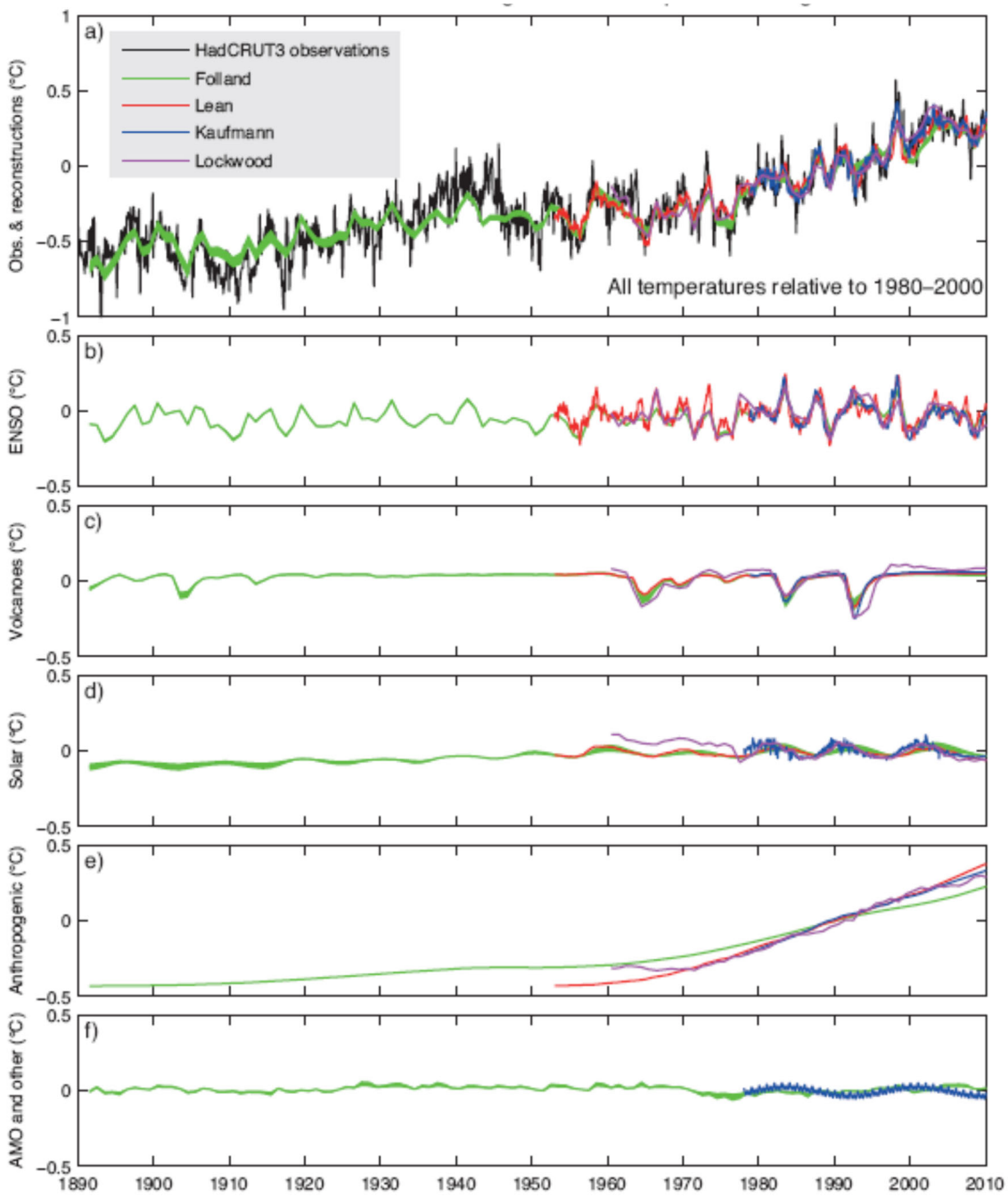

Figure 1.2.1 - Anomalies fluctuations in global temperature and the main factors forming it

b) The index of the El Niño - Southern Oscillation (ENSO);

c) Volcanic activity;

d) Fluctuations in incoming solar radiation;

e) Human impacts;

f) Other factors, including inter-annual Atlantic Oscillation (Folland [24]), fluctuations in 17.5 years and semi-annual fluctuations, the Arctic Oscillation index (Lean [17], Lockwood [20], Lean and Rind [19], Folland [24] Kaufmann [25], Imbers et al. [28]).

Analysis of components, cyclical components in the fluctuations in global temperature and separate it from falling due to natural factors (El Niño, volcanoes, incoming solar radiation), and directed hanging - man-made [29, 30, 31, 32, 33]. Moreover, in recent years, as seen from Figure 1.2, the global temperature has stabilized, due to the decrease in the incoming solar radiation and ENSO index [34, 35, 36, 37, 38, 39, 40, 41, 42]. The division of the global air temperature and its trends as trends on the natural and built components are shown in Figure1.3.

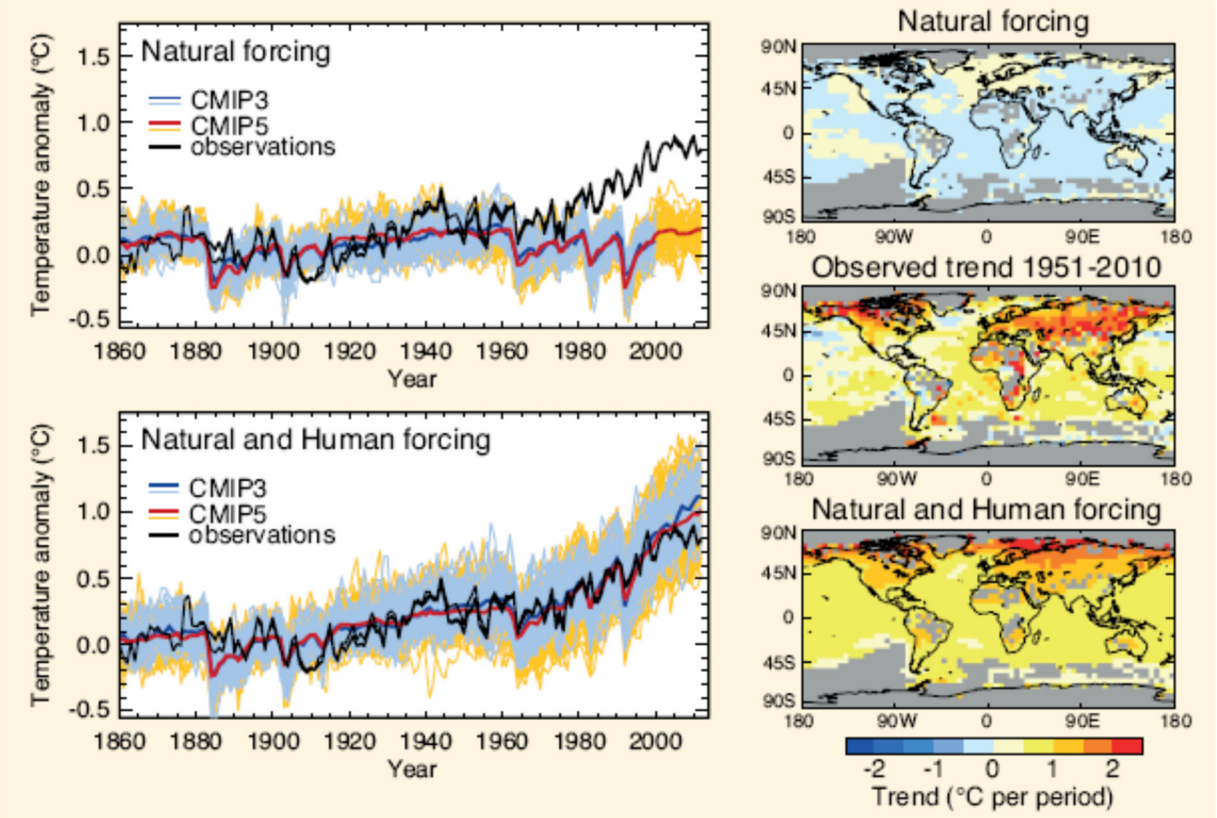

Figure 1.2.2 - Separation of global temperature fluctuations and trends in the spatial distribution of natural and anthropogenic components

In Figure 1.2.2, graphs on the left show the global temperature anomaly (°C) for the period 1860 – 2010, taking into account, only the modeling of natural factors (upper graph) and due to the joint effect of natural and anthropogenic factors (lower graph), according to observations

(black line) and according to the two ensembles of climate models (CMIP3 - blue line for the middle and blue stripe for all models and CMIP5 - red line for the average values of the ensemble, and a yellow stripe for the range obtained in all models) [43, 44, 45, 46].

In general, for the entire period of observation model effectively reproduce the fluctuations in global temperature and therefore we can assume that the temperature rise since the beginning of the 1960s, almost exclusively due to anthropogenic factors. On the right scheme, Figure 1.3 shows the spatial distribution of temperature trends (in ° C for the period) over the Globe only due to natural factors according to modeling based on an ensemble of models CMIP5 (top figure) [47], according to observations (reanalysis) for the period 1951-2010 (Middle figure) [48, 49] and the total simulated temperature due to natural and anthropogenic factors (lower figure).

From a consideration of the drawings and comparing the right part shows that according to models of growth temperature increases from middle to high latitudes, whereas according to the observations of such a law is clearly not observed significant trends of the temperature rise occurs at all latitudes, although expressed locally. On the Arabian Peninsula, as follows from the right middle figure, and there are no trend area and the area of temperature increase, including significant [50, 51].

Spatial trends in precipitation, as the same, the 5th IPCC report [15], even more ambiguous and localized and depend on latitude and time of year [52, 53].

According to the results of the 5th IPCC report also shows that the current climate change is becoming more frequent and anomalous phenomena [54, 55]. So in the WMO Statement on the Status of the Global Climate in 2013 [56] states that in the period from 10 to 15 December rare snowstorm struck separate areas of the Middle East. In Egypt, the snow fell in Cairo for the first time 112 years. In the Republic of Syria, Jordan and Israel as an unprecedented amount of snow fall. Storm accompanied by cold weather on December 15, the temperature dropped to -16 ° C, the lowest temperature to be recorded.

Detailed analysis of climate change annual air temperatures and precipitation in the Arabian Peninsula over the past 30 years was carried out in [57]. For this purpose, considered reanalysis data [58] gridded in Saudi Arabia [59, 60], whose area is 80% of the area of the peninsula obtained from observations at 27 meteorological stations (Figure 1.2.3).

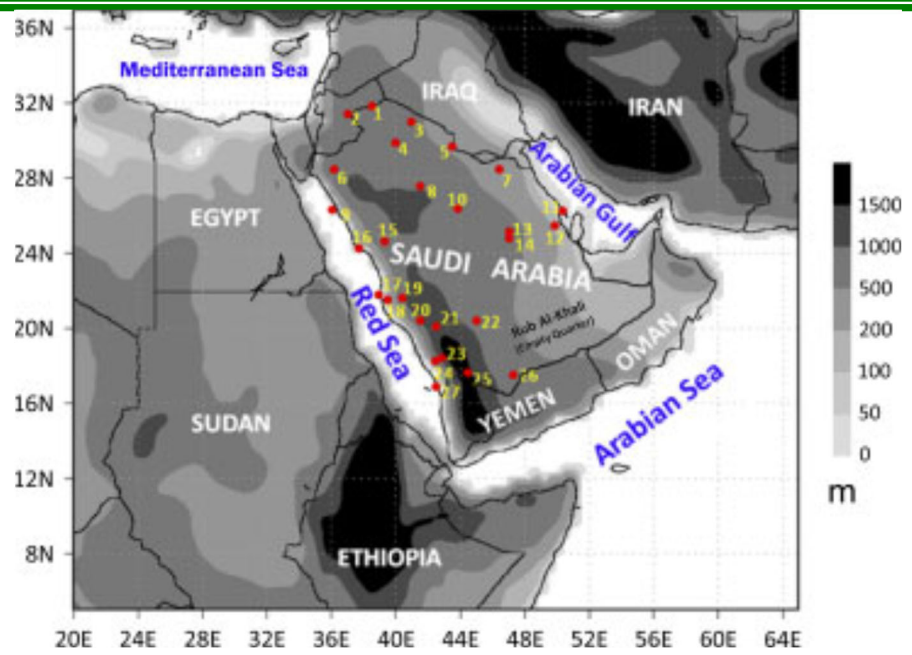

Figure 1.2.3. - Hypsographic map of the Arabian Peninsula with the observation points (red dots) and their numbers

Precipitation data covered both very dry areas with precipitation of 40-80 mm per year (desert region of the Rub al Khali), dry with annual rainfall of 80-150 mm in the center and in the north, and humid areas with rainfall greater than 150 mm in the south-west Peninsula. Average temperatures ranged from relatively high (24-27 ° C) in the center and south of the peninsula to low (<21 ° C) in the north-west and south-west. The study found that rainfall in the second half of the period under review tends to fall at a rate of 47.8 mm per decade, but with a large inter-annual variability. At the same time, the maximum, medium and minimum annual temperatures have increased at a rate of respectively 0.71, 0.60 and 0.48 ° C per decade [61]. The spatial distribution of velocities obtained trends or anomalies in decades (in percent for deposits and in ° C for temperature) are shown in Figure 1.5.

From a consideration of spatial distributions implies that the temperature decade 1980-1989 was abnormally cold decade of 1990-1999. Average, but the last decade of 2000-2009. Abnormally warm, with the largest positive anomalies occur in the center of the peninsula. Spatial and temporal distribution of precipitation and more heterogeneous in each decade of the field can be found both positive and negative anomalies. Thus, in the first decade negative precipitation anomalies are observed in the north and center of the peninsula, and the positive to the south-west. In the last decade, negative anomalies occur in the south-west and north, and the positive - in the center and east. In addition, there are quite extensive areas where rainfall does not change [62].

1.3. Estimates of future climate based on scenarios and GCMs (applications of the CMIP5 results with the assessment of the most appropriate scenario and the model for Yemen).

The main instruments for assessment of future climate are the physical and mathematical models of the general circulation of the atmosphere and ocean with the inclusion of their biological, chemical and other blocks [75, 76, 77]. Climate models like other numerical models are in a period of intense development, which is mainly caused by rapid development of computer technology. The process of inventing climate models is happening all over the World, and therefore it was necessary to develop common rules for models verification, objective being to compare different model skills, their pros and cons as well as their numerical experimental results. For this purpose, in 1990 the international project AMIP was launched and since then comparison of global AOGCM has been carried out between models and against observational data.

AOGCM developed in different countries by different groups of researchers. This gives them opportunity to explore systematic errors in forecasting the current state of the atmosphere and or climate and evaluate the ranges of its possible changes by taking into account the influence of different factors from microscale to mesoscale to synoptic and planetary scales.

Therefore, principal objectives of this paper were to assess the performance of AOGCM, to select the best models for predicting changes in surface air temperature over Yemen and to project the future tas changes under different scenarios.

In 2005-2006 Working Group on joint models between the atmosphere and the ocean (Working Group on Coupled Modeling - WGCM) under AMIP began collecting the results of climate modeling leading research centers around the world. Collected in archives simulation results of the past, present and future climate formed a third phase of the project compared interconnected models (Coupled Model Inter-comparison Project - CMIP3) [79]. In particular, WGCM organized this activity to specialists outside the major centers for climate modeling could use their results for the Fourth Assessment Report of the Intergovernmental Panel on Climate Change (IPCC or the IPCC, 2007).

In general, the simulation results are for IPCC Working Group №1, which seeks to study the physical foundations of the climate system (atmosphere, land, Ocean and sea ice) and the choice of variables that reflect the components of the system and should be archived. This collection of simulation results is called multi-model data sets CMIP3 project of the World

Climate Research Program, (WCRP CMIP3). It represents a comprehensive archive of a large set of data on climate twentieth and twenty-first centuries, and other experiments that almost completely changes the way the analysis of the results of climate modeling for researchers, students and all those interested in the problem of modern climate change.

This current study, for analyzing climate changes over Yemen uses data of 9 AOGCM from CMIP5 under the IPCC and organized by Working Group on Coupled Modeling (WGCM),

Table 1.3.1 Meteorological parameters used include near the surface air temperature and rainfall.

Table 1.3.1 – List of CMIP5 models used in this study, including model identification, group/country and atmospheric resolution

Model ID	Originating group/Country	Resolution (°)
BCC-CM1	Beijing Climate Center, China	2.8×2.8
CanESM2	Canadian Center for Climate Modeling and Analysis	2.8×2.8
CNRM-CM5	National Centre for Meteorological Research	1.41 º ×1.41 º
HadGEM2_AO	Hadley Centre for Climate Prediction, Met Office, UK	1.875×1.25
INM – CM3.0	Institute for Numerical Mathematics (INM)/Russia	2 .0º x1.5 º
IPSL-CM5A-MR	L' Institut Pierre-Simon Laplace (IPSL)/France	3.75×2.5
MIROC5	Japan	1.125×1.12
MPI-ESM-MR	Max Planck Institute for Meteorology, Germany	1.875×1.875
MRI-CGCM3	Japan	1.125 º x1.125 º

All data used in this paper were downloaded from the FTP server of the World Data Climate (WDC) maintained by the Earth System Grid Federation (ESGF) of the US Department Office of Energy Science [2].

For the purpose of selecting the best effective AOGCM, future projections under two RCP scenarios (45 and 85), featured by their respective radiative forcing of 4.5 and 8.5 W m^{-2} by the year 2100 of monthly surface air temperature (tas) fields for the period 2006 – 2100, simulated by different models were verified against simulated tas of recent-past for the period 1856–2005. Verification was done against historical simulations due to the lack of enough and quality observational data in this area under study.

The CO2 concentrations associated with RCP scenarios are expected to reach peak at the end of 21 century ; 538 ppm for medium 4.5 and 936 ppm for high 8.5 [1].

Our main focus was on several periods: the near future period (2016 – 2045), the middle period (2046-2075) and the end of 21st century (2070 – 2099) relative to the reference period (1976 – 2005).

It is important to note that, in this paper, change is the thirty-years mean values in the scenarios (runs) relative to the reference period.

The Climate Data Operators (CDO) was used to manipulate monthly to seasonal tas field and required time interval.

1.3.1. Recent-past climate in Yemen and nearby regions

In this study, for the purpose of quantifying the projections of the future climate change over Yemen and nearby, the climatology means of surface air temperature from nine climate models averaged over reference period for both winter and summer seasons have been used to represent the recent-past climate. Results for a) bcc-csm1-1, b) CanESM2, c) CNRM-CM5, d) HadGEM2-A0, e) inmcm4, f) IPSL-CM5A-MR, g) MIROC5, h) MPI-ESM-MR, and i) MRI-CGCM are shown in figure 1.3.1, left column for (December – February (DJF)) and right for (June – August (JJA)).

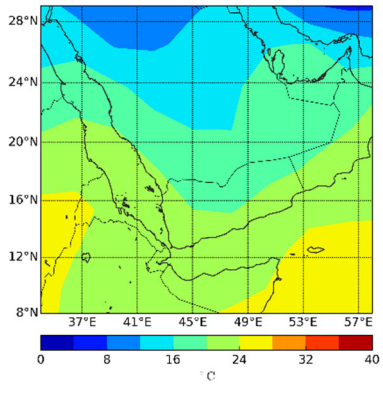

Fig. 1.3.1-a-1: bcc-csm1-1 Winter

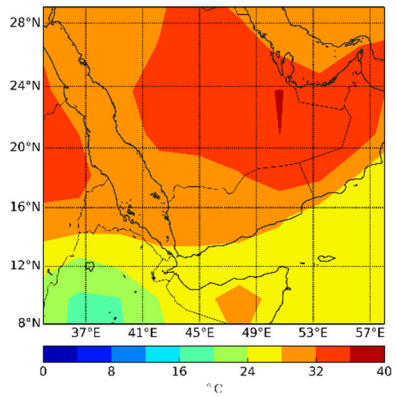

Fig. 1.3.1-a-2: bcc-csm1-1 Summer

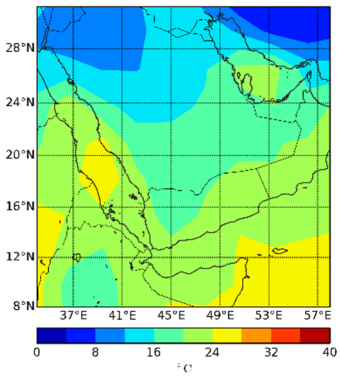

Fig. 1.3.1-b-1: CanESM2 - Winter

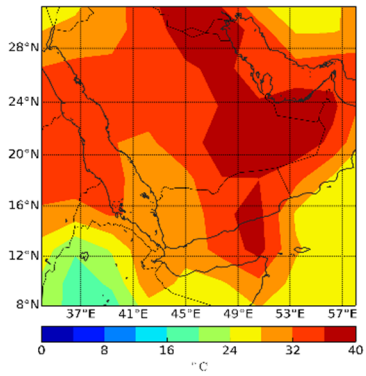

Fig. 1.3.1-b-2: CanESM2 – Summer

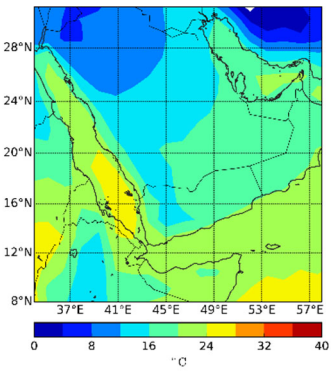

Fig. 1.3.1-c-1: CNRM-CM5 - Winter

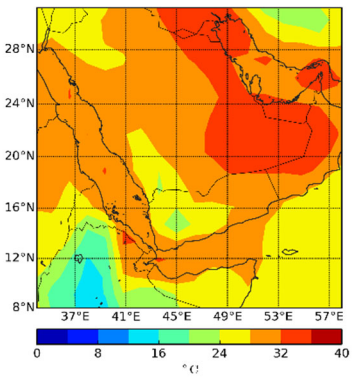

Fig. 1.3.1-c-2: CNRM-CM5 – Summer

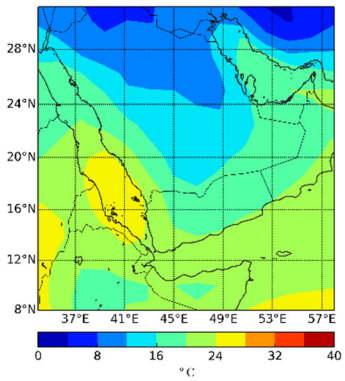

Fig. 1.3.1-d-1: HadGEM2-A0 - Winter

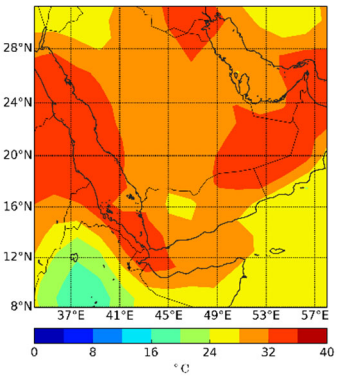

Fig. 1.3.1-d-2: HadGEM2-A0 – Summer

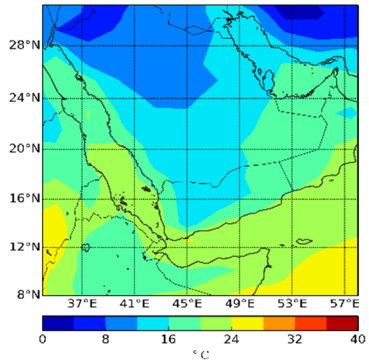

Fig. 1.3.1-f-1: IPSL-CM5A-MR - Winter

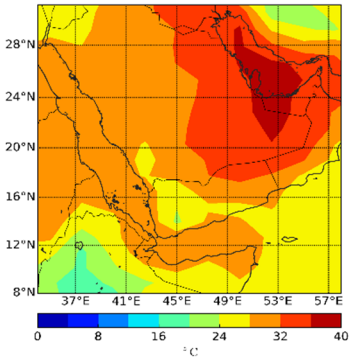

Fig. 1.3.1-f-2: IPSL-CM5A-MR - Summer

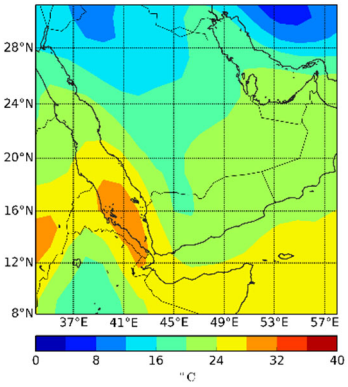

Fig. 1.3.1-g-1: MIROC5 - Winter

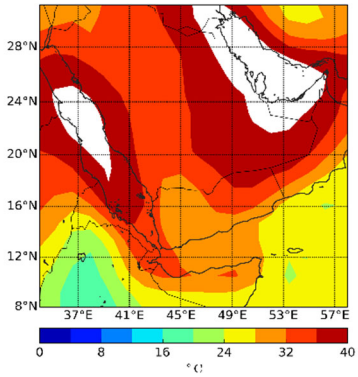

Fig. 1.3.1-g-2: MIROC5- Summer

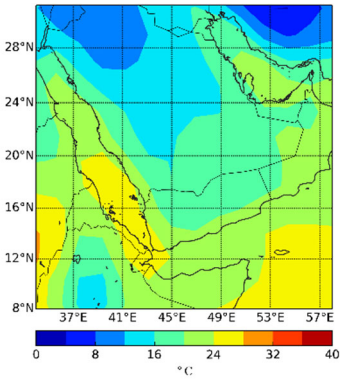

Fig. 1.3.1-h-1: MPI-ESM-MR - Winter

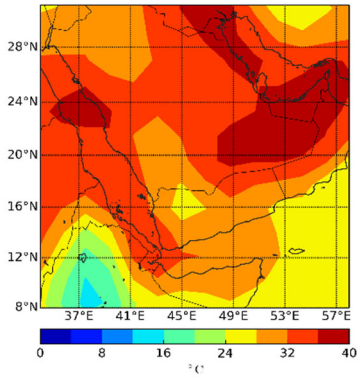

Fig. 1.3.1-h-2: MPI-ESM-MR – Summer

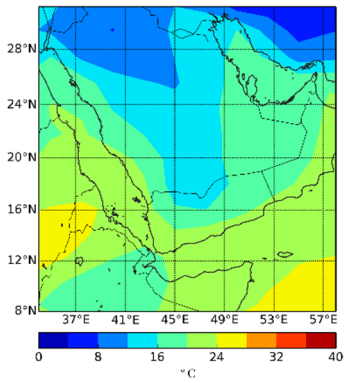

Fig. 1.3.1-i-1: MRI-CGCM – Winter

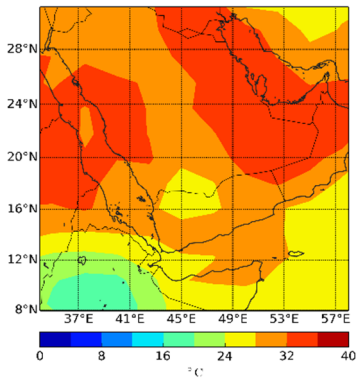

Fig. 1.3.1-i-2: MRI-CGCM – Summer

Spatial map in figs. 1.3.1, depicts that, the seasonal mean near the surface air temperature of the CMIP5 historical experiments is ranging from 0 to 28 ° C for DJF, with relatively low meridional temperature gradients to the north and large gradients to the south, and from 16 to 40 °C for JJA, with relatively large temperature gradients to the north and small gradients to the south.

1.3.2 Projected climate changes by the end of 21 century for scenario RCP85

Spatial distribution of seasonal averaged surface air temperature (°C) over Yemen and nearby regions for the 2070-2099 period relative to reference period for DJF and JJA seasons left and right columns respectively. Performance of CMIP5 models has been compared against historical experiment for two seasons DJF and JJA for near future period and by the end of 21st century. Results according to model performance have been presented in figs. 1.3.2, and table 1.3.1.

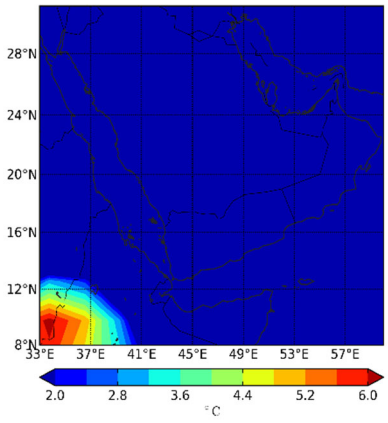

Fig. 1.3.2-a-1: INMCM4 – Winter

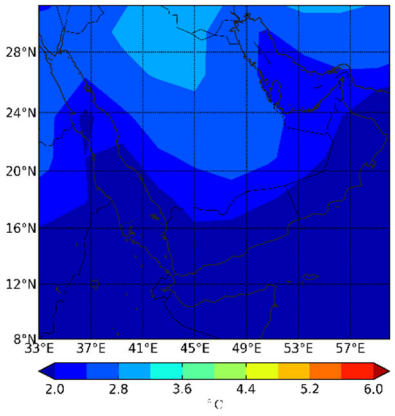

Fig. 1.3.2-a-2: INMCM4 – Summer

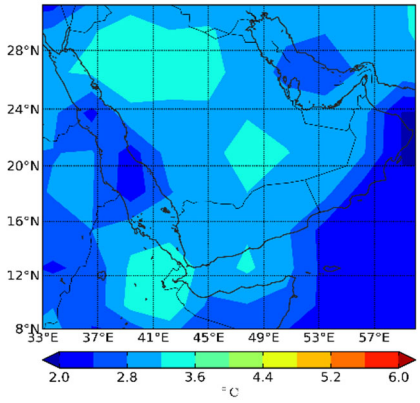

Fig. 1.3.2-b-1: MPI-ESM-MR – Winter

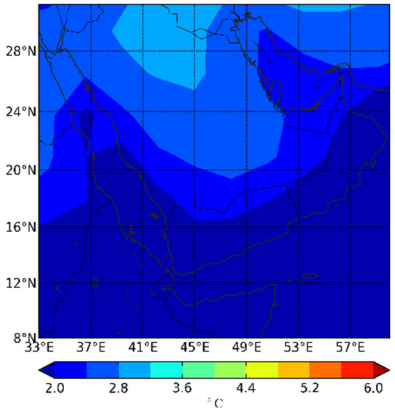

Fig. 1.3.2-b-2: MPI-ESM-MR – Summer

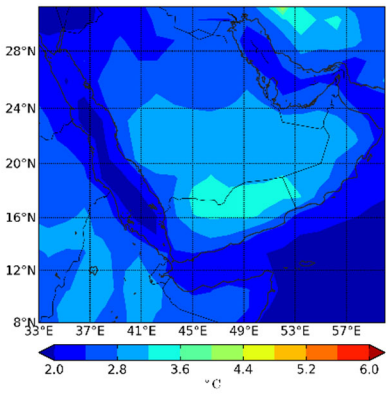

Fig. 1.3.2-c-1: CNRM-CM5 – Winter

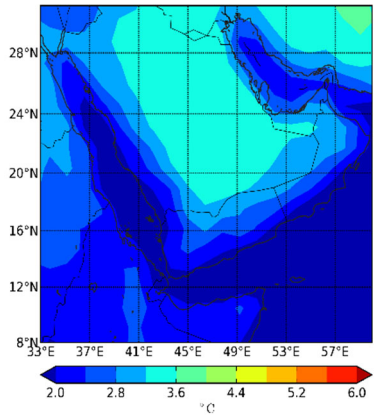

Fig. 1.3.2-c-2: CNRM-CM5 – Summer

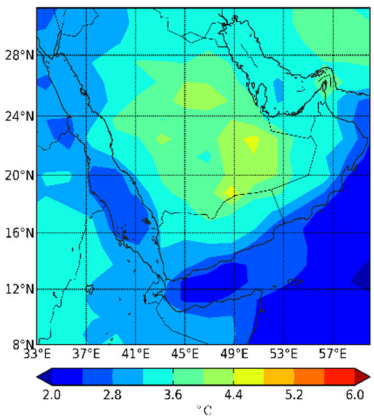

Fig. 1.3.2-d-1: CanESM2 – Winter

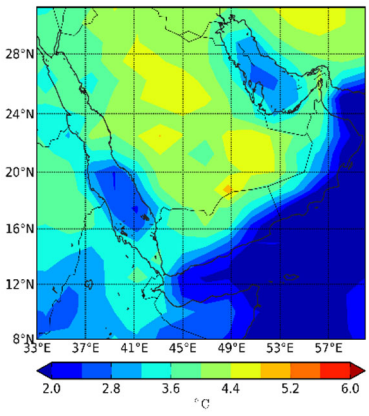

Fig. 1.3.2-d-2: CanESM2 – Summer

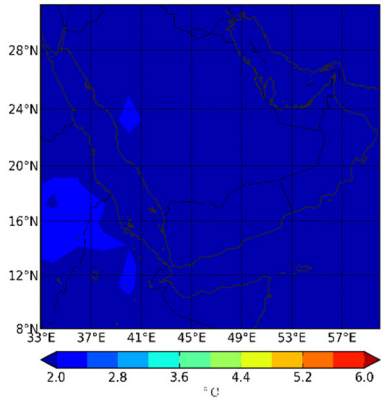

Fig. 1.3.2-e-1: HadGEM2-AO – Winter

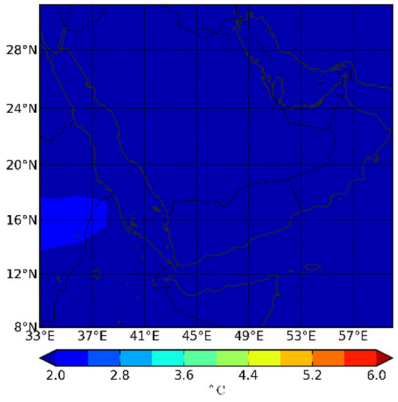

Fig. 1.3.2-e-2: HadGEM2-AO – Summer

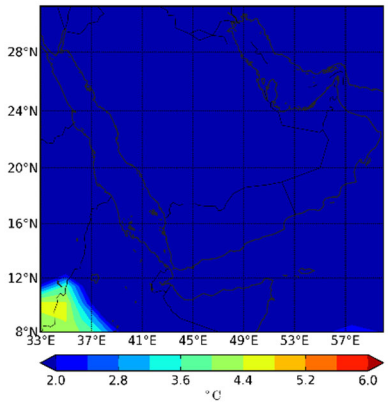

Fig. 1.3.2-f-1: IPSL-CM5A-MR – Winter

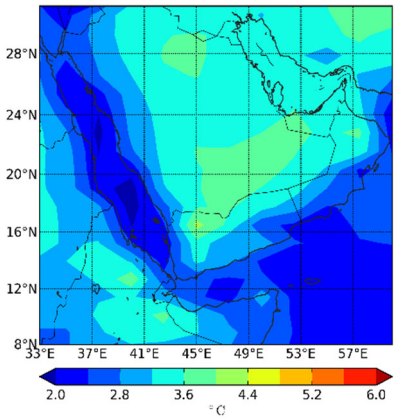

Fig. 1.3.2-f-2: IPSL-CM5A-MR – Summer

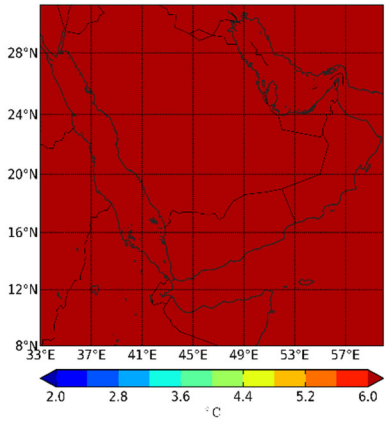

Fig. 1.3.2-g-1: BCC-CSM1-1 – Winter

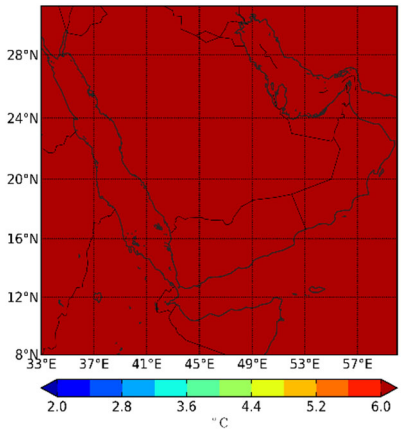

Fig. 1.3.2-g-2: BCC-CSM1-1 – Summer

Figure 1.3.2– Spatial distribution of seasonal averaged surface air temperature (°C) over Yemen and nearby regions for the 2070-2099 period relative to reference period for DJF and JJA seasons left and right columns respectively.

Table 1.3.2 – Changes in seasonal average tas obtained using CMIP5 models relative to 1976-2005 reference period.

Model Name	Δtas			
	2016-2045		2070-2099	
	DJF	JJA	DJF	JJA
INMCM4	0.6	0.6	1.5	1.5
MPI-ESM-MR	0.8	1.3	2.0	2.5
CNRM-CM5	1.5	1.4	2.5	2.5
CanESM2	1.5	1.7	2.8	3.0
HadGEM2-AO	1.4	1.6	3.0	3.2
IPSL-CM5A-MR	1.3	1.4	-8.6	3.0
BCC-CSM1-1	-9.1	1.1	-8.2	2.0

Quantitative analysis of CMIP5 simulations of seasonal averaged near the surface air temperature relative to 1976-2005 base period for the near future and by the end of 21st century table 1.3.1 shows, that INM, MPI, CNRM and CanESM2 projection of near the surface air temperature by the end of 21st century is better than the other models. Therefore, in this present study, only these selected four CMIP5 models will be used for further analysis.

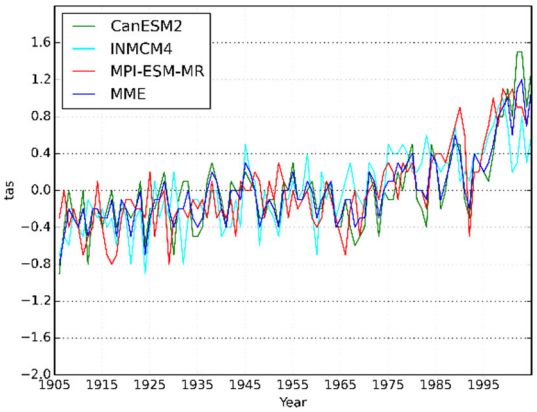

Fig. 1.3.3-a: RCP45 – period of 1906-2005

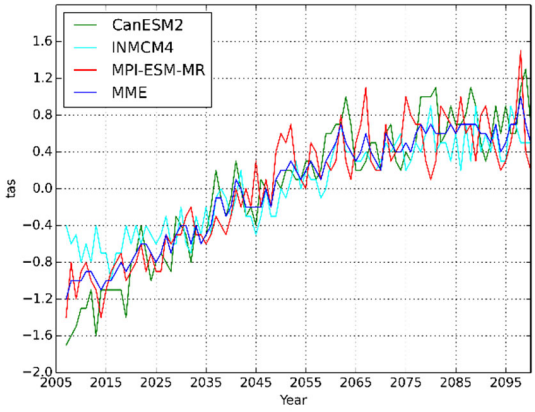

Fig. 1.3.3-b: RCP45 – period of 2005-2100

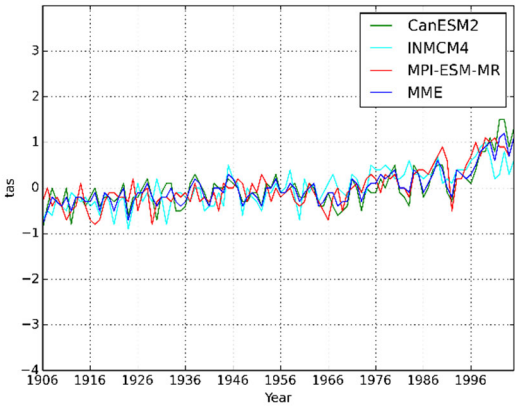

Fig. 1.3.3-a: RCP85 – period of 1906-2005

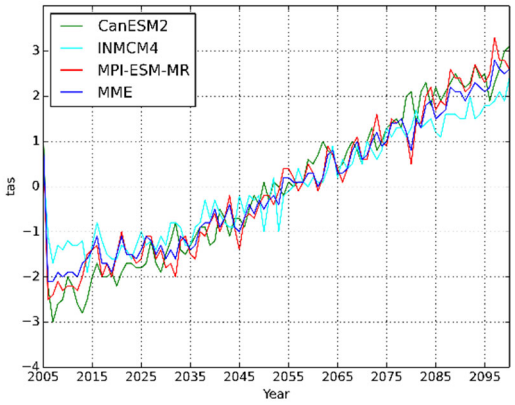

Fig. 1.3.3-b: RCP85 – period of 2005-2100

Figure 1.3.3. Chronological graphs of Yemen and Arabian Peninsula near the surface annual air temperature anomalies and Multi Models Ensemble (MME) over the period of 1906-2005 and 2006-2100 for rcp45 (a and b) and rcp85 (c and d).

Chronological graphs of CMIP5 models of averaged near the surface air temperature anomaly (Fig 1.3.1) over Arabian Peninsula depict increase in projected temperature by rcp85 throughout until the end of 21st century. RCP45 shows that the projected surface air temperature also increase up to the year 2065.

1.3.3. Projected climate changes by the end of near future period for scenario RCP45

Projection of climate changes in the Arabian Peninsula by the end of near future period for scenario RCP45 has been performed. Figure 1.3.2 shows spatial distribution of averaged near the surface air temperature for the near future period relative to recent-past period simulated by CMIP5 models as in Fig.1.3.3, except the MRI-CGCM model is excluded.

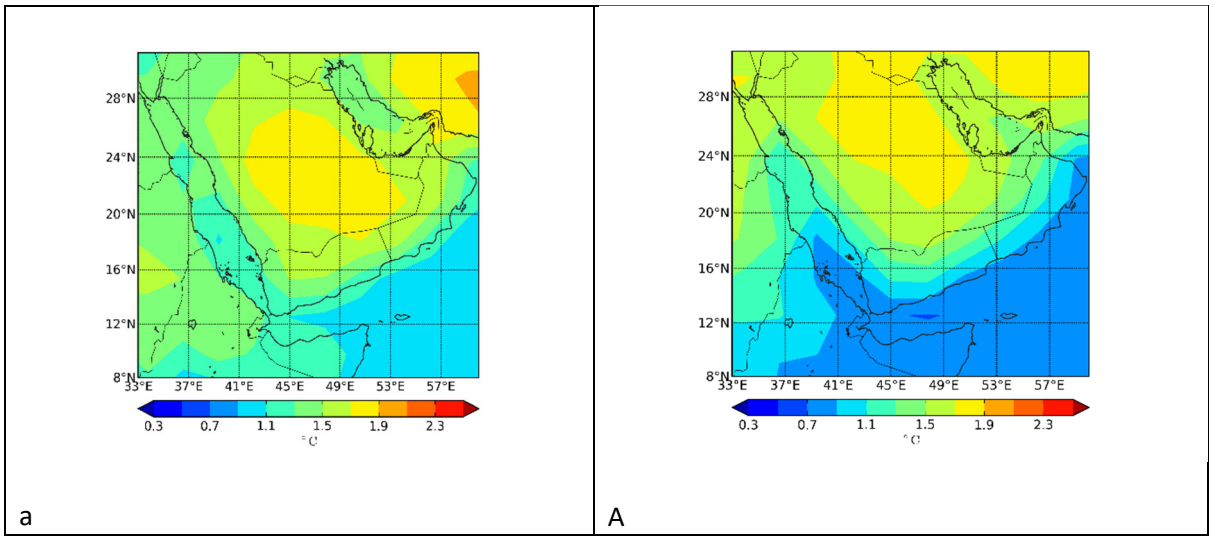

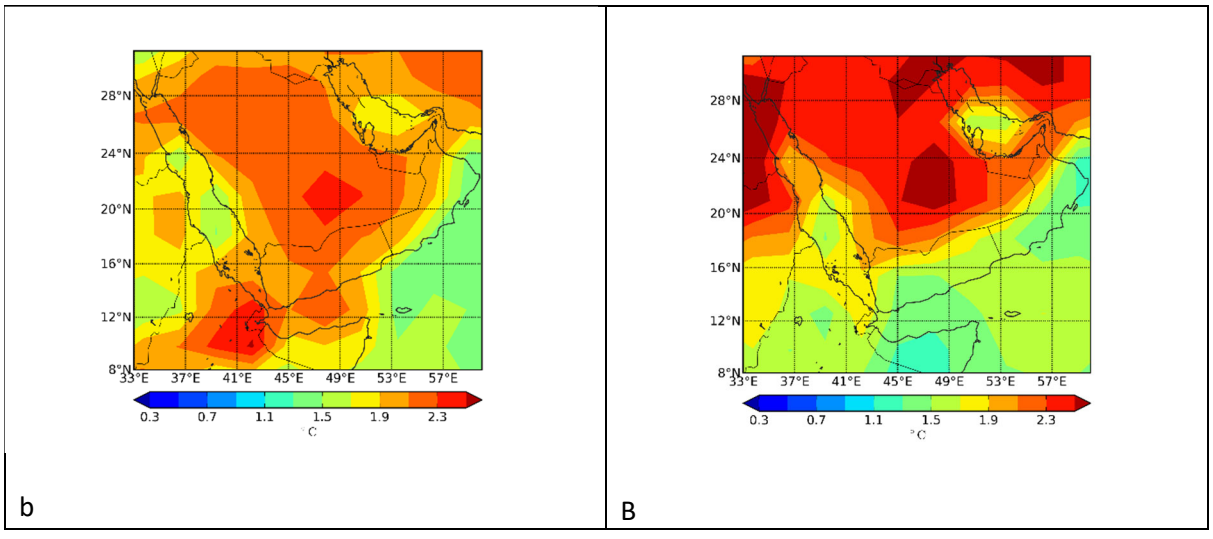

a

b

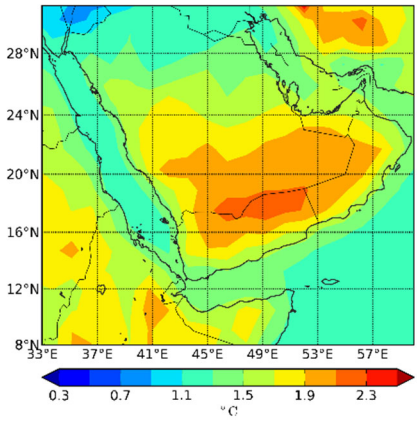
28°N
24°N
20°N
16°N
12°N
8°N
33°E 37°E 41°E 45°E 49°E 53°E 57°E
0.3 0.7 1.1 1.5 1.9 2.3
°C

c

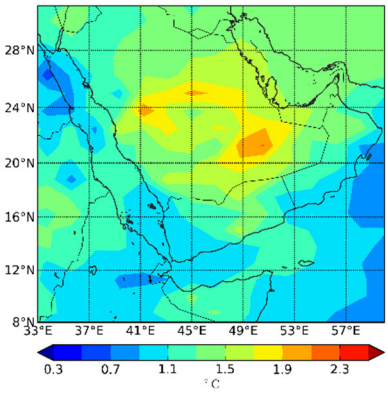
28°N
24°N
20°N
16°N
12°N
8°N
33°E 37°E 41°E 45°E 49°E 53°E 57°E
0.3 0.7 1.1 1.5 1.9 2.3
°C

d

A

b

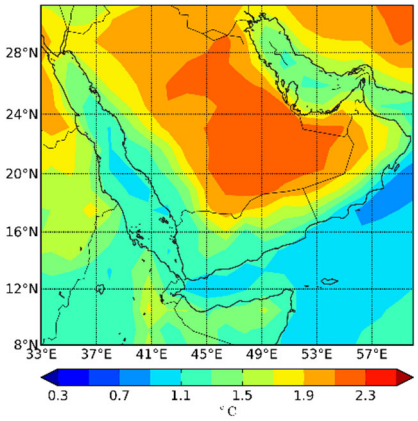
28°N
24°N
20°N
16°N
12°N
8°N
33°E 37°E 41°E 45°E 49°E 53°E 57°E
0.3 0.7 1.1 1.5 1.9 2.3
°C

c

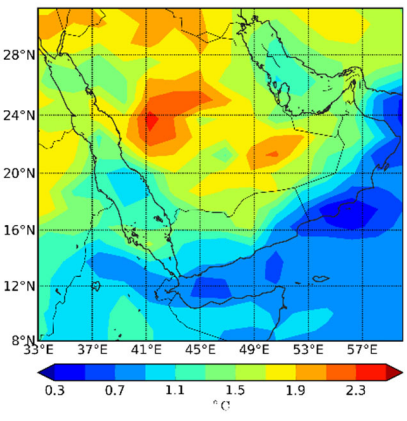
28°N
24°N
20°N
16°N
12°N
8°N
33°E 37°E 41°E 45°E 49°E 53°E 57°E
0.3 0.7 1.1 1.5 1.9 2.3
°C

d

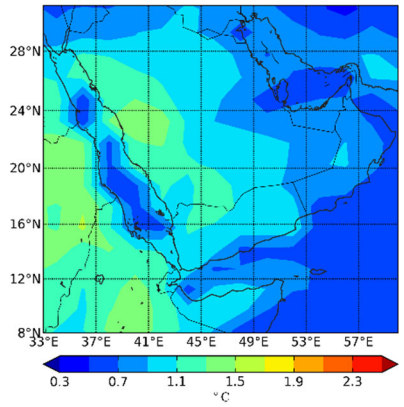
28°N
24°N
20°N
16°N
12°N
8°N
33°E 37°E 41°E 45°E 49°E 53°E 57°E
0.3 0.7 1.1 1.5 1.9 2.3
°C

e

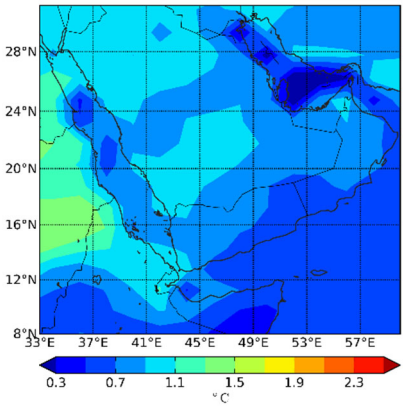
28°N
24°N
20°N
16°N
12°N
8°N
33°E 37°E 41°E 45°E 49°E 53°E 57°E
0.3 0.7 1.1 1.5 1.9 2.3
°C

e

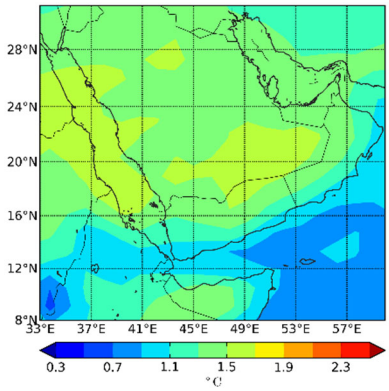
28°N
24°N
20°N
16°N
12°N
8°N
33°E 37°E 41°E 45°E 49°E 53°E 57°E
0.3 0.7 1.1 1.5 1.9 2.3
°C

f

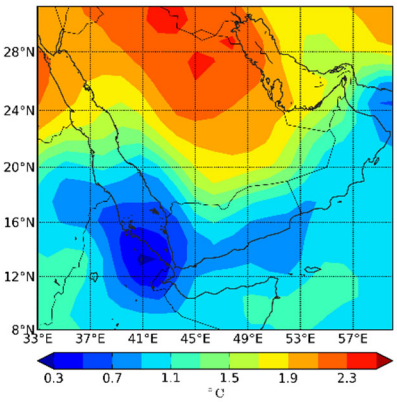
28°N
24°N
20°N
16°N
12°N
8°N
33°E 37°E 41°E 45°E 49°E 53°E 57°E
0.3 0.7 1.1 1.5 1.9 2.3
°C

f

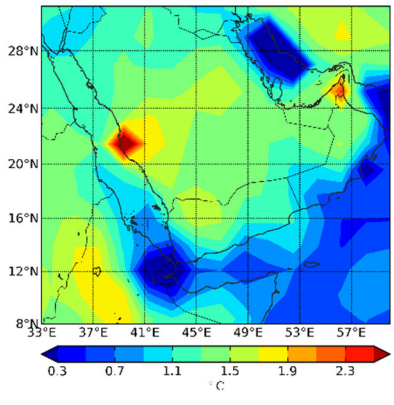
28°N
24°N
20°N
16°N
12°N
8°N
33°E 37°E 41°E 45°E 49°E 53°E 57°E
0.3 0.7 1.1 1.5 1.9 2.3
°C

g

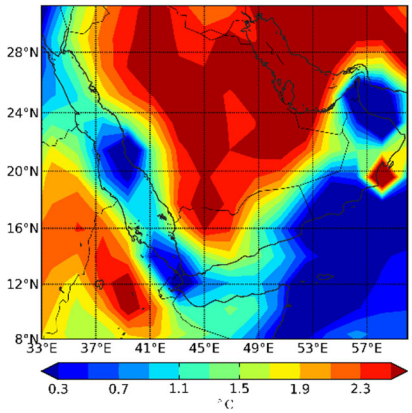
28°N
24°N
20°N
16°N
12°N
8°N
33°E 37°E 41°E 45°E 49°E 53°E 57°E
0.3 0.7 1.1 1.5 1.9 2.3
°C

g

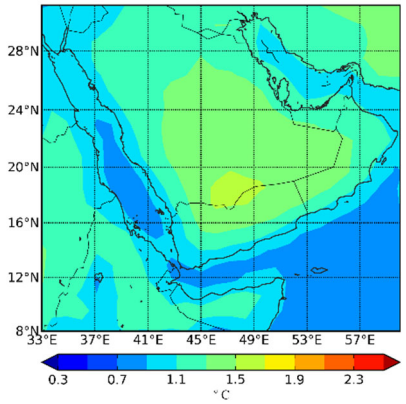

h

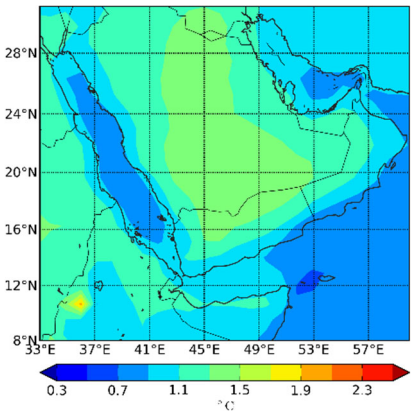

h

Figure 1.3.4– Spatial distribution of seasonal averaged surface air temperature (°C) over Yemen and the Arabian Peninsula for the near future period by different CMIP5 models relative to reference period for DJF and JJA seasons left and right columns respectively. Analysis of the spatial map indicate the projected warming of up to 1.9°C and 2.3°C for DJF - winter and JJA - summer seasons respectively over Yemen and Arabian Peninsula.

1.3.4. Projected climate changes by the end of 21 century for scenario RCP45

Figure 1.3.3 shows spatial maps of seasonal averaged near the surface air temperature for projected CMIP5 models (as in fig. 1.3.2), for scenario RCP45 by the end of 21st century against the base period of recent-past. Analysis of the results indicates a projected warming over the Peninsula with the largest and smallest increase in temperature during JJA and DJF seasons respectively.

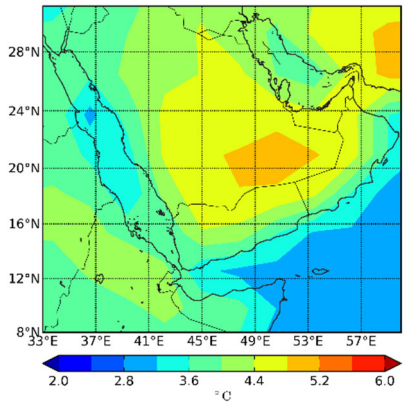

a

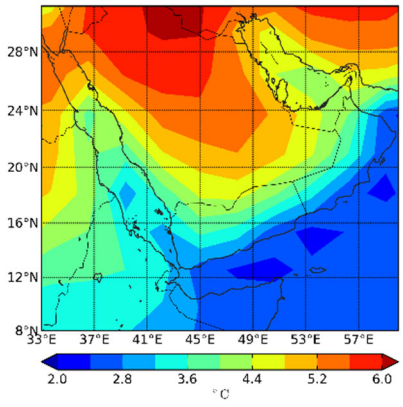

a

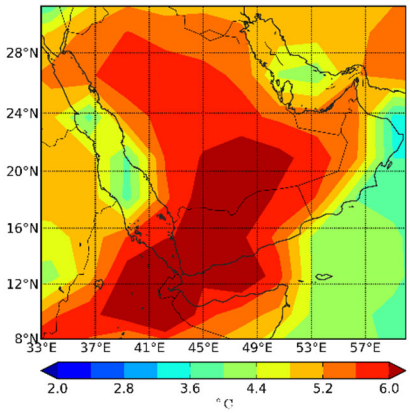
28°N
24°N
20°N
16°N
12°N
8°N
33°E 37°E 41°E 45°E 49°E 53°E 57°E
2.0 2.8 3.6 4.4 5.2 6.0
°C

b

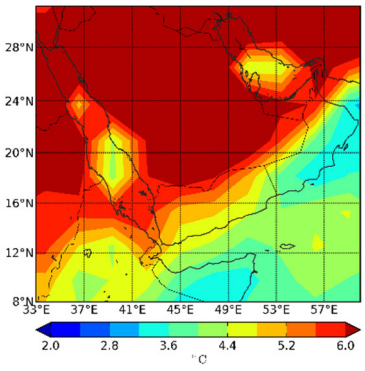
28°N
24°N
20°N
16°N
12°N
8°N
33°E 37°E 41°E 45°E 49°E 53°E 57°E
2.0 2.8 3.6 4.4 5.2 6.0
°C

b

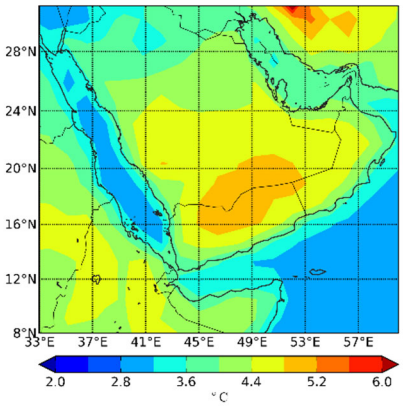
28°N
24°N
20°N
16°N
12°N
8°N
33°E 37°E 41°E 45°E 49°E 53°E 57°E
2.0 2.8 3.6 4.4 5.2 6.0
°C

c

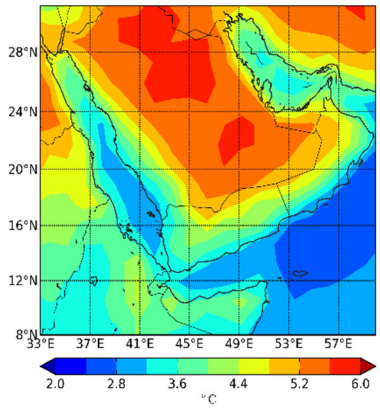
28°N
24°N
20°N
16°N
12°N
8°N
33°E 37°E 41°E 45°E 49°E 53°E 57°E
2.0 2.8 3.6 4.4 5.2 6.0
°C

c

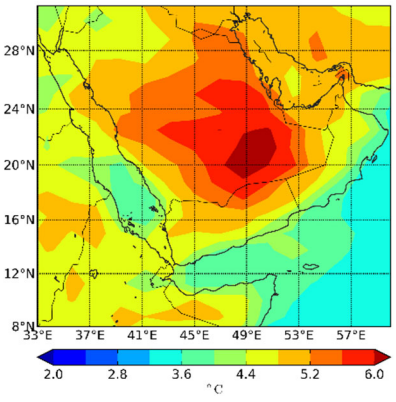
28°N
24°N
20°N
16°N
12°N
8°N
33°E 37°E 41°E 45°E 49°E 53°E 57°E
2.0 2.8 3.6 4.4 5.2 6.0
°C

d

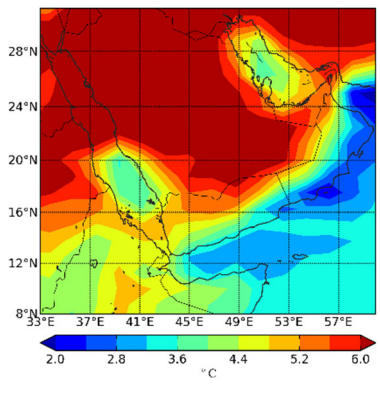
28°N
24°N
20°N
16°N
12°N
8°N
33°E 37°E 41°E 45°E 49°E 53°E 57°E
2.0 2.8 3.6 4.4 5.2 6.0
°C

d

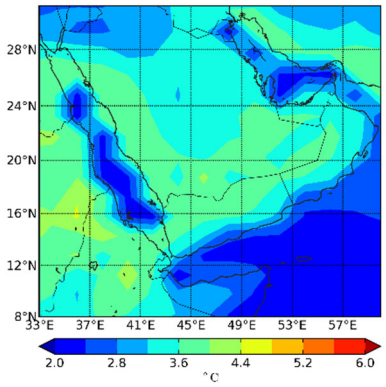
28°N
24°N
20°N
16°N
12°N
8°N
33°E 37°E 41°E 45°E 49°E 53°E 57°E
2.0 2.8 3.6 4.4 5.2 6.0
°C

e

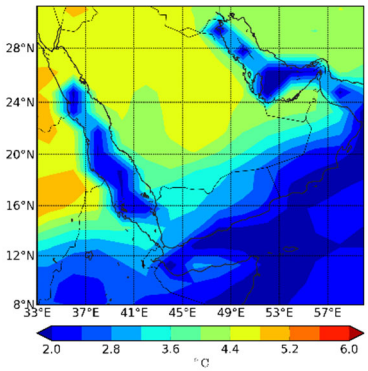
28°N
24°N
20°N
16°N
12°N
8°N
33°E 37°E 41°E 45°E 49°E 53°E 57°E
2.0 2.8 3.6 4.4 5.2 6.0
°C

e

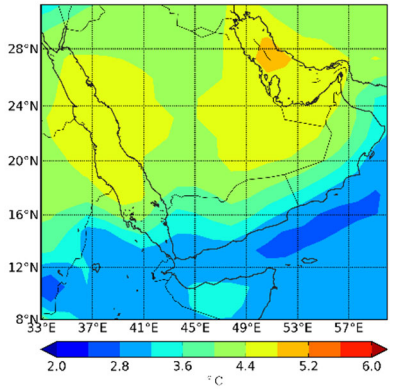
28°N
24°N
20°N
16°N
12°N
8°N
33°E 37°E 41°E 45°E 49°E 53°E 57°E
2.0 2.8 3.6 4.4 5.2 6.0
°C

f

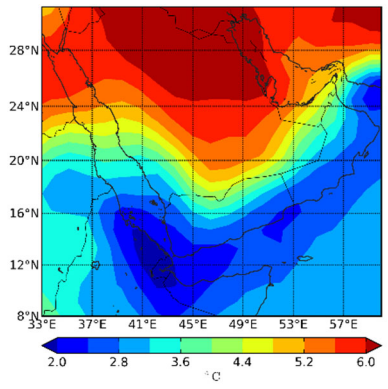
28°N
24°N
20°N
16°N
12°N
8°N
33°E 37°E 41°E 45°E 49°E 53°E 57°E
2.0 2.8 3.6 4.4 5.2 6.0
°C

f

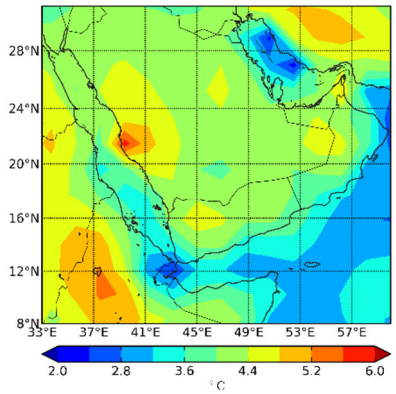
28°N
24°N
20°N
16°N
12°N
8°N
33°E 37°E 41°E 45°E 49°E 53°E 57°E
2.0 2.8 3.6 4.4 5.2 6.0
°C

g

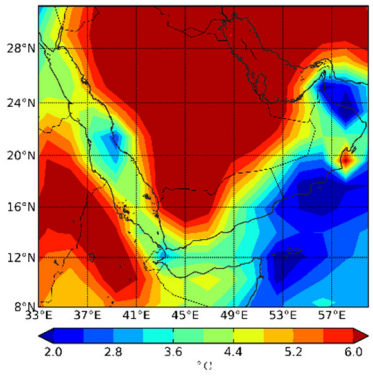
28°N
24°N
20°N
16°N
12°N
8°N
33°E 37°E 41°E 45°E 49°E 53°E 57°E
2.0 2.8 3.6 4.4 5.2 6.0
°C

g

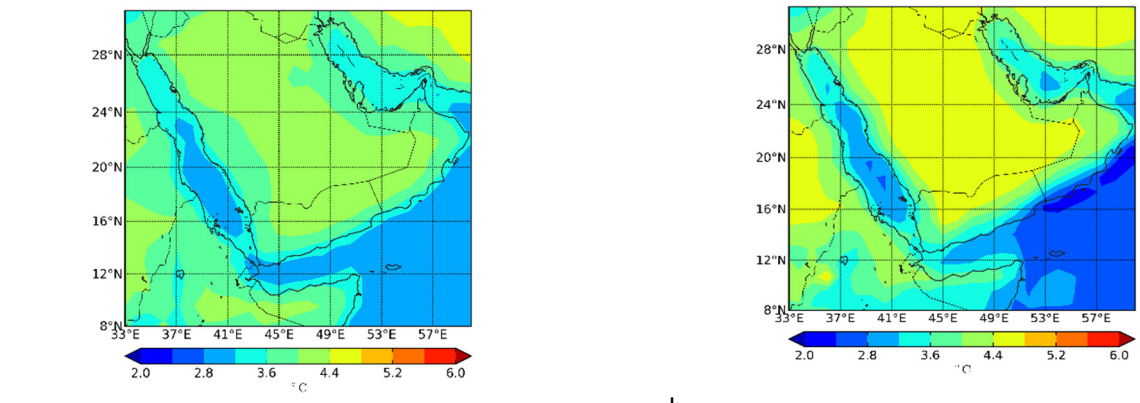

h h

Figure 1.3.5. Spatial distribution of seasonal averaged surface air temperature (°C) over Yemen and in the Arabian Peninsula for the 2070-2099 period relative to reference period for DJF and JJA seasons left and right columns respectively.

CMIP5 models show that, the projected average near the surface air temperature is varying from 2.0 to 6.0°C.

Table 1.3.4.1 – 1.3.4.5 displays results of projected monthly air temperature by CMIP5 models for three difference periods relative to base period and two RCP scenarios.

Table 1.3.4.1 – Changes in monthly average tas of rcp45 CMIP5 models for the 2016 – 2045 period relative to 1976 – 2005 reference period

Model Name	Δtas											
	2016-2045											
	Jan	Feb	Mar	Apr	May	June	July	Aug	Sept	Oct	Nov	Dec
INMCM4	0.3	0.5	0.9	0.6	0.6	0.6	0.6	0.7	0.4	0.6	0.9	0.6
MPI-ESM-MR	0.8	0.9	1.0	1.2	1.4	1.4	1.4	1.4	1.0	1.2	1.3	0.9
CNRM-CM5	1.7	1.5	1.4	1.5	1.4	1.3	1.4	1.4	1.4	1.7	1.6	1.3
CanESM2	1.3	1.6	1.4	1.7	1.7	1.8	1.7	1.7	1.8	1.9	1.9	1.8
HadGEM2-AO	1.4	1.2	1.6	1.2	1.7	1.6	1.6	1.8	1.6	1.5	1.6	1.4
IPSL-CM5A-MR	1.3	1.4	1.3	1.2	1.2	1.3	1.2	1.4	1.7	1.8	1.6	1.4
BCC-CSM1-1	1.4	1.1	0.7	1.0	1.3	1.1	1.2	1.0	1.1	0.9	1.0	1.1

Quantitative analysis of the projected monthly air temperature table 1.3.4.1 and table 1.3.4.2 over this area under study depicts a warming of about 2 K.

Table 1.3.4.2 – Changes in monthly average tas of rcp85 CMIP5 models for the 2016 – 2045 period relative to 1976 – 2005 reference period

Model Name	Δtas											
	2016-2045											
	Jan	Feb	Mar	Apr	May	June	July	Aug	Sept	Oct	Nov	Dec
INMCM4	0.7	0.9	1.2	1.0	0.9	0.8	0.9	0.9	0.7	0.9	0.5	0.9
MPI-ESM-MR	1.3	1.1	1.2	1.7	1.9	1.5	1.5	1.5	1.4	1.3	1.3	0.9
CNRM-CM5	1.6	1.5	1.6	1.7	1.6	1.4	1.5	1.5	1.7	1.7	1.7	1.5
CanESM2	1.8	1.8	1.7	1.5	1.6	1.8	2.0	1.9	2.0	2.2	2.1	2.2
HadGEM2-AO	1.3	1.0	1.3	0.9	1.2	1.3	1.2	1.4	1.3	1.1	1.4	1.2
IPSL-CM5A-MR	0.4	0.1	0.1	0.2	-0,2	-0,3	-0,3	0.7	1.2	1.5	1.0	0.7
BCC-CSM1-1	1.6	1.4	1.1	1.0	1.3	1.1	1.4	1.3	1.2	1.0	1.3	1.4

Table 1.3.4.3 – Changes in monthly average tas of rcp45 CMIP5 models for the 2046 – 2076 period relative to 1976 – 2005 reference period

Model Name	Δtas											
	2046—2075											
	Jan	Feb	Mar	Apr	May	June	July	Aug	Sept	Oct	Nov	Dec
INMCM4	0.9	1.4	1.1	1.4	1.2	1.2	1.1	1.3	1.2	1.5	1.4	1.1
MPI-ESM-MR	1.8	1.7	1.7	1.9	2.2	2.4	2.4	2.3	2.1	2.2	2.1	1.9
CNRM-CM5	2.0	2.0	2.2	2.1	2.2	2.0	2.2	2.2	2.1	2.4	2.3	2.0
CanESM2	2.5	2.4	2.1	2.3	2.4	2.5	2.6	2.7	2.8	2.9	2.7	2.7
HadGEM2-AO	2.6	2.2	2.3	2.5	2.7	2.7	2.6	2.8	2.7	2.5	2.6	2.5
IPSL-CM5A-MR	2.0	2.1	2.2	2.4	2.2	2.4	2.2	2.5	2.8	2.7	2.5	2.0
BCC-CSM1-1	2.1	1.6	1.5	1.7	2.0	1.7	1.8	1.7	1.8	1.8	1.9	1.8

Table 1.3.4.4 – Changes in monthly average tas of rcp85 CMIP5 models for the 2046 – 2076 period relative to 1976-2005 reference period

Model Name	Δtas											
	2046—2075											
	Jan	Feb	Mar	Apr	May	June	July	Aug	Sept	Oct	Nov	Dec
INMCM4	1.5	1.8	2.2	2.2	2.1	2.1	2.1	2.2	2.1	2.4	2.4	1.9
MPI-ESM-MR	2.8	2.7	2.7	3.0	3.5	3.1	3.1	3.1	3.0	3.0	3.1	2.8
CNRM-CM5	2.5	2.6	2.7	2.9	2.9	2.7	2.9	2.8	2.9	3.1	3.0	2.5

CanESM2	3.5	3.4	3.1	3.2	3.4	3.6	3.8	3.9	3.9	4.2	4.1	4.1
HadGEM2-AO	3.0	2.8	2.9	2.8	3.1	3.1	3.2	3.3	3.3	3.0	3.1	3.0
IPSL-CM5A-MR	2.0	1.5	1.4	1.4	1.1	1.2	2.1	2.3	2.7	3.0	2.5	2.2
BCC-CSM1-1	3.0	2.7	2.3	2.6	2.8	2.7	2.8	2.6	2.6	2.6	2.6	2.5

Table 1.3.4.4 – Changes in monthly average tas of rcp45 CMIP5 models for the 2071 – 2100 period relative to 1976 – 2005 reference period

Model Name	Δtas											
	2071—2100											
	Jan	Feb	Mar	Apr	May	June	July	Aug	Sept	Oct	Nov	Dec
INMCM4	1.1	1.5	1.6	1.6	1.6	1.5	1.5	1.5	1.5	1.6	1.6	1.6
MPI-ESM-MR	2.0	2.2	2.0	2.2	2.5	2.5	2.6	2.5	2.4	2.3	2.2	2.0
CNRM-CM5	2.6	2.5	2.4	2.7	2.6	2.5	2.5	2.5	2.6	2.8	2.8	2.5
CanESM2	2.8	2.7	2.6	2.7	2.7	2.9	3.0	3.1	3.1	3.2	3.2	3.1
HadGEM2-AO	3.1	2.9	3.1	2.9	3.3	3.1	3.1	3.2	3.2	2.9	2.9	3.0
IPSL-CM5A-MR	2.4	3.0	2.7	2.8	2.7	2.7	2.8	3.1	3.4	3.3	3.3	2.7
BCC-CSM1-1	2.1	2.1	1.7	2.0	2.2	1.8	2.0	1.9	2.1	1.8	2.0	2.2

Table 1.3.4.5 – Changes in monthly average tas of rcp85 CMIP5 models for the 2071 – 2100 period relative to 1976 – 2005 reference period

Model Name	Δtas											
	2071—2100											
	Jan	Feb	Mar	Apr	May	June	July	Aug	Sept	Oct	Nov	Dec
INMCM4	2.9	3.2	3.5	3.1	3.2	3.3	3.3	3.3	3.5	3.8	3.5	3.2
MPI-ESM-MR	4.0	4.0	4.0	4.7	5.2	4.9	4.9	4.9	4.7	4.7	4.7	4.3
CNRM-CM5	4.0	3.8	4.1	3.9	4.1	4.0	4.2	4.1	4.4	4.7	4.5	4.1
CanESM2	5.1	4.8	4.7	4.6	4.8	5.3	5.6	5.6	5.6	5.8	5.8	5.8
HadGEM2-AO	4.7	4.4	4.4	4.3	4.6	4.8	4.9	5.0	5.1	4.7	4.8	4.8
IPSL-CM5A-MR	3.3	2.5	2.9	2.8	2.6	2.5	3.4	3.6	4.0	4.4	4.0	3.5
BCC-CSM1-1	4.2	3.8	3.4	3.9	4.1	4.0	4.1	4.1	3.9	3.9	4.1	4.0

Monthly increase of air temperature up to 6 K in some months was projected by CMIP5 models over Yemen by the end of 21st century.

In this research, CMIP5 climate models data for different scenarios were verified against historical experiment of recent past. Verification process depicts that INM-CM4 model perform better than other climate models used in comparison analysis.

The projection of temperature of air near the surface was done on three different periods using RCP45 and RCP85. Results shows that, for near future period warming of up to 1.9°C and 2.3°C for DJF and JJA seasons respectively over Yemen and Arabian Peninsula. The projected

monthly near the surface air temperature is varying from 0.1 to 5.0°C, for the near, middle and end of 21st under RCP45 and RCP85 scenarios.

1.5. Applied research methods and the reasons for their use.

In this research, modern research technique of climatic changes in air temperature and precipitation data based on CMIP5 models and long-term observations includes the following main parts:

- Formation of a regional base in the long-term data monitoring stations, both in the Arabian Peninsula and adjacent territory;
- Analysis of the quality and uniformity of observations and reduction of short rows to the long-term period with the restoration passes observations;
- Identification of models for each time of observation and meteorological characteristics of each;
- Spatial generalization of the results of modeling of climate change on the territory;
- Obtaining climatic laws for stationary conditions on the Arabian Peninsula;
- Construction of territorial statistical models and study the dynamics of their coefficients.

Each part of the research methodology has its individual study. So regional database should include series of observations not only in the Arabian Peninsula, but also outside it due to the fact that these data can be used as a long-term series of analog to bring to long-term period of data on the peninsula, as well as for reliable spatial generalization of the results, especially at the borders of the peninsula. The second feature of the formation of the database - is the choice of effective climatic characteristics for analysis. In order to assess internal variability within the year and the impact of the individual months in the mean annual air temperature and the amount of annual precipitation, it is important to choose optimal month which is also in the research appears to be monthly increments. Data from this month are smoothed in order to determine meteorological extreme and individual synoptic processes. Analysis of the quality and uniformity of observations is the primary and one of the main parts of the methodology, as the reliability and quality of the data depends on the accuracy and reliability of the installed instruments. For an objective assessment of data quality statistical methods should be applied and objective assessment of uniformity based on statistical criteria. In this paper we applied two sets of criteria: first to assess the homogeneity of empirical distributions, which may be compromised by the presence of non-uniform extreme and second - to assess the homogeneity in time, which can be disrupted by changing the recording devices and other conditions of observation. Clearly, if the aim is to establish long-term changes in climate, the presence or

absence of one or more of the extreme in the multi-year time series should not influence the parameters of the model, as these extremes are due to inter-annual variability, rather than long-term changes in climate.

Therefore, if the extreme is not uniform, it can be excluded from a number of observations that should not affect the form and parameters of climatic time series model. The quality of the initial information applies to the reduction of a number of long-term periods for restoration of observations. This procedure is necessary for the following reasons:

- Determining the type and reliability of a time series model parameters depends on the duration and the uniformity of its observations, by assuming to missing data;
- Parameters of the models can be compared at different stations for the same time period.

For statistical modeling of time series were chosen the most simple model classes: stationary and non-stationary. At the same time determined by the unsteadiness of the main parameter - the average value of a set of observations. Also advantage stationary or non-stationary model should be determined by simple and clear indicators. One such indicator is the residual variance, or that could not be explained by the model. Thus, for a fixed model of residual variance of the natural variation of the time series, ie, climate assumed to be constant, and all natural inter-annual variability presented standard deviation. If the time series on non-stationary model is more consistent, its variance or standard deviation should be less than for the stationary model. This difference can be expressed as a percentage of estimates of statistical significance on statistical criteria. A feature of this technique is that, as a non-stationary model is considered not only a model of linear trend that has be used in modern empirical-statistical analysis, but also the model of step changes [104].

1.6. Installation climate modeling software

In this research the following tools for data processing and visualization were installed.

1. The Climate Data Operators (CDO)
2. The Grid Analysis and Display System (GrADS)
3. Python

The above mentioned utilities were covered under the title technical aspects of computer technology in meteorology, climate modeling and atmospheric sciences in general are the most used tools in modeling community. These tools were selected because in scientific research the most common data formats we are dealing with are Grid Regular Intermediate Binary (GRIB 1 &2) – the most used data format as per World Meteorological Organization (WMO) and

Network Common Data Format (NetCDF) – which is a set of software libraries and machine-independent data formats that support the creation, access, and sharing of array-oriented scientific data. These two data formats are used in most big numerical and climate modeling centers. Therefore, for the purpose of enhancing research capability by learning how to decode models data using the above mentioned tools is very actual task.

2. Formation of a regional database and analysis of the quality of the observed data

2.1. Selection of observation sites (gauged stations) and the formation of a regional database for Yemen area and nearby regions.

In this research, long time series of average monthly air temperature and total precipitation has been used for the purpose of climate changes modeling. Data base of long-term series of air temperature and precipitation are created using observational data received from Civil Aviation & Meteorology Authority Yemen Meteorological Service CAMA / YMS, while other data were downloaded from the following FTP Internet servers: The Royal Netherlands Meteorological Institute (http://www.knmi.nl) [105] and the Washington Climate Center (http://cdiac.ornl.gov) [106].

The Washington Climate Center server contains information of 6,000 stations measurements of air temperature and 7500 stations of observed precipitation around the world, beginning from 1980. The Royal Netherlands Meteorological Institute Internet servers have few stations, but information is constantly updated covering data up to the year 2014.
The spatial distribution criterion of choosing meteorological weather stations for the analysis was based on the following principles:

a) The chosen meteorological stations must be located in Yemen;

b) Choose a weather station on the territory of neighboring country in order to use them as analogues for the missing data and filling time series for stations in Yemen, as well as for the purposes of spatial interpolation of data from climate models for the stations located outside of the Republic of Yemen.

In this research, data of air temperature and precipitation from four meteorological stations located in Yemen has been used. Due to the lack of enough and quality observational data over this area under study, for the analysis of air temperature and precipitation, data from selected meteorological stations in the territory of neighbouring countries: Saudi Arabia, Oman, Djibouti and Eritrea have been used. Therefore, the total number of stations used is thirteen. Spatial distribution of meteorological stations used in this research is shown in Fig. 2.1.1, and their corresponding names and coordinates - in Table 2.1.1

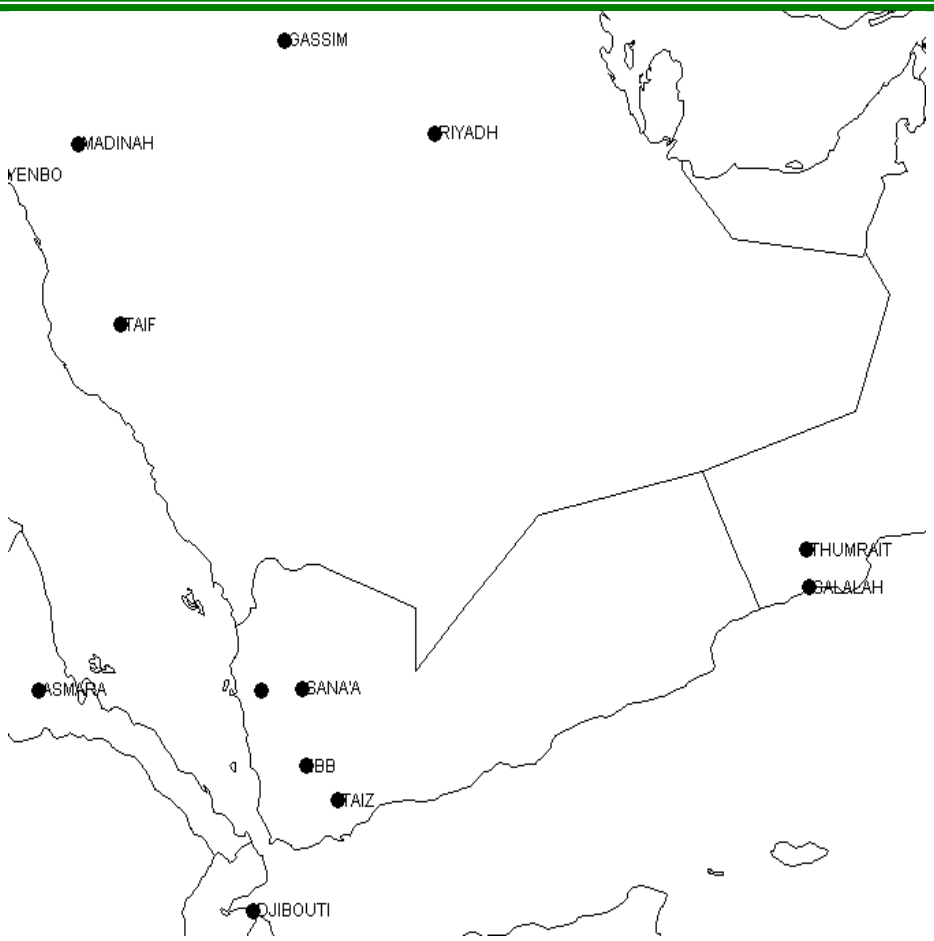

Figure 2.1.1. spatial distribution of meteorological stations used in this study

Table 2.1.1. Coordinates of meteorological stations located in Yemen and nearby countries.

Code	Stat.name	Latitude	Longitude
41404	SANA'A	15.31	44.11
41452	IBB	14	44.2
41466	TAIZ	13.41	44.8
41390	AL-MAHWET	15.27	43.3
63125	DJIBOUTI	11.55	43.15
63021	ASMARA	15.28	38.92
40405	GASSIM	26.3	43.77
40430	MADINAH	24.55	39.7
41316	SALALAH	17.03	54.08
41314	THUMRAIT	17.67	54.03
40438	RIYADH	24.72	46.73
41036	TAIF	21.48	40.55
40439	YENBO	24.02	38.22

For the analysis of monthly precipitation data four metrological stations located over Yemen were used and eleven other located in Saudi Arabia, Oman, Djibout and Sudan. List of all meteorological stations and their coordinates are presented in table 2.1.2.

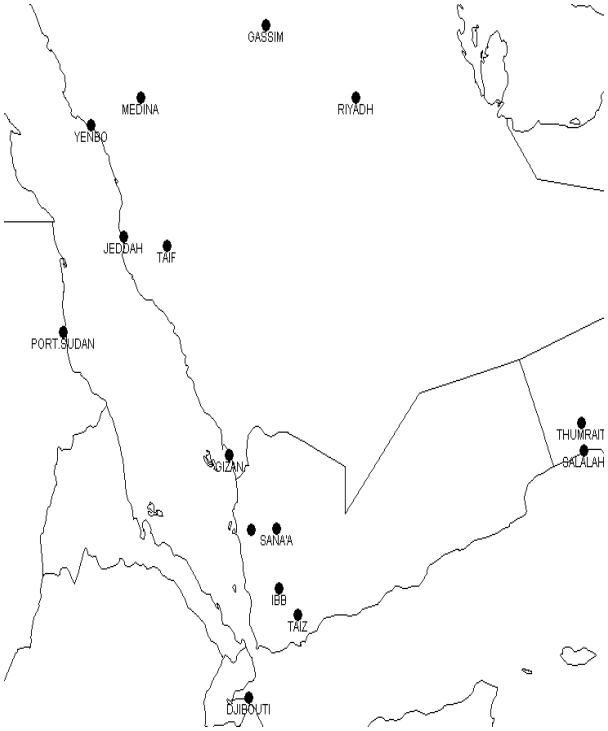

Figure 2.1.2. Spatial distribution of meteorological stations used in this study

Taple 2.1.2. Coordinates of meteorological stations located in Yemen and neighbouring countries

Code	Stat.name	Latitude	Longitude
41404	SANA'A	15.31	44.11
41452	IBB	14	44.2
41466	TAIZ	13.41	44.8
41390	AL-MAHWET	15.27	43.3
40405	GASSIM	26.3	43.77
41140	GIZAN	16.9	42.58
41024	JEDDAH	21.67	39.15
40430	MEDINA	24.7	39.7
40438	RIYADH	24.7	46.7
41316	SALALAH	17	54.1
41036	TAIF	21.48	40.55
41314	THUMRAIT	17.6	54
40439	YENBO	24.1	38.1
63125	DJIBOUTI	11.6	43.2
62641	PORT.SUDAN	19.60	37.20

Due to the fact that, further analysis and modeling of air temperature and precipitation were carried out separately for selected meteorological stations, two regional climate databases were established:

a. A database containing multi-year monthly mean time series of air temperatures for 13 stations;
b. A database containing multi-year monthly time series of rainfall for 15 stations.

For the formation of the regional database (DB), Hydrocalc software package was used.

2.2. Structure and information characteristics of regional climatic database.

The duration of period of observations, together with the quality of the data is one of the main conditions for the reliable statistical modeling results. Therefore, the longer original time series is and the fact that it include observations from recent years, the better the results.

Table 2.2.3 – Duration and period of observations of average air temperature at different weather stations in Yemen and nearby states.

№	Code	Station	Period of obs.	Duration of obs. (n)
1	41404	SANA'A	1983-2013	31
2	41452	IBB	1990-2013	24
3	41466	TAIZ	1983-2013	31
4	41390	AL-MAHWET	2006-2013	8
5	63125	DJIBOUTI	1911-1999	49
6	63021	ASMARA	1949-1991	43
7	40405	GASSIM	1967-2014	48
8	40430	MADINAH	1956-2014	59
9	41316	SALALAH	1942-2014	73
10	41314	THUMRAIT	1982-2014	33
11	40438	RIYADH	1941-2011	71
12	41036	TAIF	1961-2014	54
13	40439	YENBO	1967-2014	48

The periods of observations for the two formed data base in this study is different. Information's on the duration and period of observation of mean monthly air temperature is shown in table – 2.2.3, and precipitation table – 2.2.4 for all selected weather stations in Yemen and neighboring states.

Table 2.2.4 – Duration and period of observations of total monthly rainfall at different stations in Yemen and nearby countries.

№	Code	Station	Period of obs.	Number of Years (n)
1	41404	SANA'A	1983-2013	31
2	41452	IBB	1990-2013	24
3	41466	TAIZ	1983-2013	31
4	41390	AL-MAHWET	2006-2013	8
5	40405	GASSIM	1967-2014	48
6	41140	GIZAN	1967-2014	48
7	41024	JEDDAH	1951-2004	54
8	40430	MEDINA	1956-2014	59
9	40438	RIYADH	1941-2011	71
10	41316	SALALAH	1942-2014	73
11	41036	TAIF	1966-2014	49
12	41314	THUMRAIT	1980-2014	35
13	40439	YENBO	1967-2014	48
14	63125	DJIBOUTI	1901-2000	100
15	62641	PORT.SUDAN	1906-2014	109

Data given in table 2.2.3 and 2.2.4, shows that, the average number of observations for average air temperature is 44 years; weather stations located in Yemen have an average of 24 years. The average duration of observation of precipitation is 53 years, and meteorological stations located in Yemen have average duration of 24 years.

In general we can conclude that the information gathered allowed us to form two regional climatic databases. Although the average observation period is not big enough and contains a number of missing data, there also exist weather stations with the too long number of observations compared to other stations, as a results mean value was affected by the longer time series.

2.3. Methods of assessing the homogeneity and stationarity.

Analysis of homogeneity and stationarity of raw data in one hand allows us to check the reliability of the raw data and the presence data with of errors and large errors, on the other hand to make preliminary conclusions about the statistical significance of climate change for the separate intervals [107].

The first step in this part is to evaluate the uniformity of the empirical distributions of meteorological characteristics, which can be caused by extreme deviation of observed values from the maximum and minimum values. Evaluation of homogeneous series of meteorological observations carried out on the basis of genetic and statistical analysis of observed raw data. Genetic analysis is the process of identifying the physical reasons for the heterogeneity of the raw data. For the purpose of assessing the statistical significance of the homogeneity of the criteria outliers extreme values in the empirical distribution Smirnov-Grubbs criteria and Dixon [108, 109] are used.

There are three main reasons for the heterogeneity:

a) Outliers meteorological variables of specific weather formations, for example, weather conditions during typhoons;
b) Extreme event has a probability of occurrence of a rare event than that defined by the empirical formula when it is included in the general set of observations;
c) The outliers values caused by large measurement error.

Statistical criteria Dixon is calculated based on empirical data using the following formula

a) The maximum Dixon criterion of the data sample arranged in ascending order:

$$D1_n = (Y_n - Y_{n-1})/ (Y_n - Y_1) \qquad (2.3.1)$$

где $D1_n$ – Maximum criterion of arranged sample;
Y_n – Number of sample size.

$$D2_n = (Y_n - Y_{n-1})/ (Y_n - Y_2) \qquad (2.3.2)$$

$$D3_n = (Y_n - Y_{n-2})/ (Y_n - Y_2) \quad (2.3.3)$$

$$D4_n = (Y_n - Y_{n-2})/ (Y_n - Y_3) \quad (2.3.4)$$

$$D5_n = (Y_n - Y_{n-2})/ (Y_n - Y_1) \quad (2.3.5)$$

b) For a minimum member of the sample size aranged from smallest to largest (Y1):

$$D1_1 = (Y_1 - Y_2)/ (Y_1 - Y_n) \quad (2.3.6)$$

$$D2_1 = (Y_1 - Y_2)/ (Y_1 - Y_{n-1}) \quad (2.3.7)$$

$$D3_1 = (Y_1 - Y_3)/ (Y_1 - Y_{n-1}) \quad (2.3.8)$$

$$D4_1 = (Y_1 - Y_3)/ (Y_1 - Y_{n-2}) \quad (2.3.9)$$

$$D5_1 = (Y_1 - Y_3)/ (Y_1 - Y_n) \quad (2.3.10)$$

Where: $Y_1 < Y_2 < \ldots < Y_n$, and N – Number of observation

Statistical test Smirnov-Grubbs for the maximum term of the ranked sequence (Yn) is calculated as follows:

$$G_n = (Y_n - Y_{cp})/ \sigma \quad (2.3.11)$$

Where Y_{mean} , σ –mean value and standard deviation of data sample (Y_1):

$$G_1 = (Y_{mean} - Y_1)/ \sigma \quad (2.3.12)$$

The main idea of assessing homogeneity using these criteria is to compare the results of calculated value of empirical data from the data sets with the critical value obtained from table for a given sample size (n), significance level, the autocorrelation coefficient and asymmetry. The significance level is usually set to 5%, which corresponds to the adoption of the null

hypothesis of homogeneity with a probability of 95%. As a result, the homogeneity of the hypothesis can be accepted if the calculated value is less than the corresponding critical value.

Generally, asymmetric distribution of Pearson type 3 which takes into account internal relationship of a time series of criteria Dixon and Smirnov - Grubbs has the following features. Significant asymmetry in the analyzed samples leads to an increase in the critical values of the data sets defined for normal distribution if the maximum number is verified, and decrease the critical values of these statistics while checking the minimum number of members. The influence of autocorrelation is not as significant as asymmetry. At the same time, the more asymmetry data set is, the more the influence on autocorrelation they have. Therefore, using Dixon and Smirnov-Grubbs criteria based on normal distribution, can leads to significant fault on results. This is due to the fact that it is possible to take a minimum value belonging to nearest sample of data, but in reality, the data is not uniform with other members, in the sense that maximum or minimum data which obeys asymmetric distribution can be forced to undergo normal distribution.

The second step in the assessment of stationarity, is assessment of homogeneity in time for meteorological characteristics, measurement conditions which may have changed. For example, this might happens due to replacement of instruments. In assessing stationarity of data set, long time series is divided into parts, then means and variances are computed as well as their corresponding Student and Fisher criteria [110, 112, 113]. The analysis is carried out according to these criteria, after an assessment on the absence of outliers which normally affect the average values, and especially variances.

$$F = \sigma^2_j / \sigma^2_{j+1} . \qquad (2.3.13)$$

where F – Computed value by Fisher;

σ^2_j σ – Corresponding dispersion for two respectively sample size (j and j+1) with

$^2_{j1}$ – sample size n_1 and n_2, where $\sigma^2_j > \sigma^2_{j+1}$.

The stationarity hypothesis of dispersions taken at a given significance level α (%), is satisfied if the calculated value of the test empirical data is less than critical value ($F < F^*$) for a given degree of freedom and appropriate sample sizes (n1 and n2).

Critical value of Fisher criteria (F *) depends on significance level (%), coefficients of correlation (r (1)) and autocorrelation coefficient (R) of two equal numbers of samples space (nx = ny) tables [110].

When sample sizes n1 and n2 have greater than or equal to 25 numbers of observations, then the classic F-distribution for normally distributed independent random variables with the new degrees of freedom which depend on the autocorrelation and coefficient of asymmetry can be applied and are defined by:

$$n_{2F} = \frac{n_2 g}{1 + \frac{2r^2}{1-r^2}\left[1 - \frac{1 - r^{2n_2}}{n_2(1-r^2)}\right]} \qquad (2.3.14)$$

where g – Coefficient which takes into account the influence of asymmetry of raw data and can be obtained from special table;

r – autocorrelation coefficient between time series;

Estimated value of the statistic t-test to assess the steady-state mean values of two successive sub-samples is determined by the formula:

$$t = \frac{Ycp_I - Ycp_{II}}{\sqrt{n_1\sigma_I^2 + n_2\sigma_{II}^2}} \sqrt{\frac{n_1 n_2 (n_1 + n_2 + 2)}{n_1 + n_2}} \qquad (2.3.15)$$

Where Y_{meanI}. Y_{meanII}. σ^2_I. σ^2_{II} – means values and variances of two consecutive sample size; n_1 и n_2 – number of observations.

Student statistical critical value for the given equal number of observations can either be obtained from the table or calculated by using the following formula.

$$t'_\alpha = C_t \cdot t_\alpha . \qquad (2.17)$$

where t'_α – Student critical value obtained depending on availability of autocorrelation coefficient;

C_t – transition coefficient determined depending on the autocorrelation coefficients given in the table of [110];

t_α – critical statistics for Student random collection with the same number of degrees of freedom k = n1 + n2-2;

Evaluation of stationarity by using Student (test) is also carried out by comparing the calculated and the critical values of the data sets. If calculated is less than critical value for a given significance level, then the hypothesis of homogeneity (stationarity) has been verified.

2.4. Results of assessing of homogeneity and stationarity for each site and each climatic characteristic.

Analysis of homogeneity of empirical distributions of monthly air temperature and monthly rainfall amount precipitation was carried out using Dixon and Smirnov-Grubbs criteria for long term time series with period of observations of more than 20 years, and stationarity analysis was performed using Fisher and Student's criterion for long term time series of more than 40 years. Restrictions on the selected duration was caused by: short term time series of observations are likely associated with natural heterogeneity, influenced by the presence of extremes of rare frequency of occurrences than that calculated from series with few numbers of observations and to the natural cycles associated with oscillating periods of high and low air temperature and precipitation, which may be from one up to 2-3 decades. At the same time, the assessment of homogeneity and stationarity has been carried out for all stations located over Yemen and beyond.

Summarized results of assessment of uniformity of average maximum (Max.) and minimum (Min.) extreme temperatures using criteria Dixon (D) and Smirnov-Grubbs (SG) are shown in Table 2.4.1 for those stations classified as heterogeneous. In this table, "+" sign indicates that the homogeneity hypothesis is accepted, the sign "-" -is used when hypothesis has been rejected and if the calculated value of the data sample at significance level α from 3% – 5%, the hypothesis is accepted and placed in the table with "(+) ", and numerical value of the significance level corresponding to the calculated value is shown. If the statistics test of the calculated value have significance level ranged from 1 – 3%, the hypothesis of homogeneity is rejected and in the table is shown as "(-)", and also the numerical value of the significance level is indicated.

From the results in Tabl.2.4.1, the number of non-uniform extremes for average monthly air temperature is not so great. It can be noted that, the total number of tests based on two criteria (Dixon and Smirnov-Grubbs) for the two extremes (minimum and maximum) for 15 stations and 12 months is equal to 720, the total number heterogeneous cases is about 3% . If we consider only guaranteed conclusions about the non stationarity, by excluding those in brackets, their number will be 12, or 1.7%. If we analyze extremes (maximum and minimum) differently, then the number of heterogeneous cases of maximum temperature will be 0.3% (total case), and heterogeneous minima will be 3.0%.

Table 2.4.1. – Ranks of heterogeneous cases of average monthly temperature at different weather stations in Yemen and adjacent areas.

№	Code	Station	Max.		Min.		Max.		Min.	
			D	SG	D	SG	D	SG	D	SG
			January				February			
1	40438	RIYADH	(-)1.6	+	-	-	+	+	+	+
2	41256	SIB	+	(-)2.3	+	+	+	+	+	+
3	41452	IBB	+	+	+	+	+	+	-	(+)3.8
			March				April			
1	41467	SANA'A	+	+	+	+	+	+	-	(+)3.2
			May				June			
1	40405 GASSIM	GASSIM	+	-	+	-	+	+	+	+
2	40438	RIYADH	+	+	(-)1.4	+	+	+	+	+
3	41467	SANA'A	+	+	-	(-)2.1	+	+	(+)3.2	+
4	41452	IBB	+	+	+	+	+	+	(-)1.6	+
			September				October			
1	40405	GASSIM	+	+	-	+	+	+	+	+
2	40430	MEDINA	+	+	+-	-	+	+	(-)2.7	+
3	41314	THUMRAIT	+	(-)2.7	+	+	+	+	+	+
			November				December			
1	40405	GASSIM	+	-	+	-	+	+	+	+
2	40430	MEDINA	+	+	(-)2.5	+	+	+	+	+
3	41036	TAIF	+	+	+	+	(-)2.1	+	+	+

The analysis of long-term series containing heterogeneous extremes showed that the reasons for heterogeneous cases are mainly missing data and the total number of observations being not long enough, which leads to strengthened of statistical significance of extremes. Examples of long term time series containing heterogeneous extremes are shown in Figure 2.3.

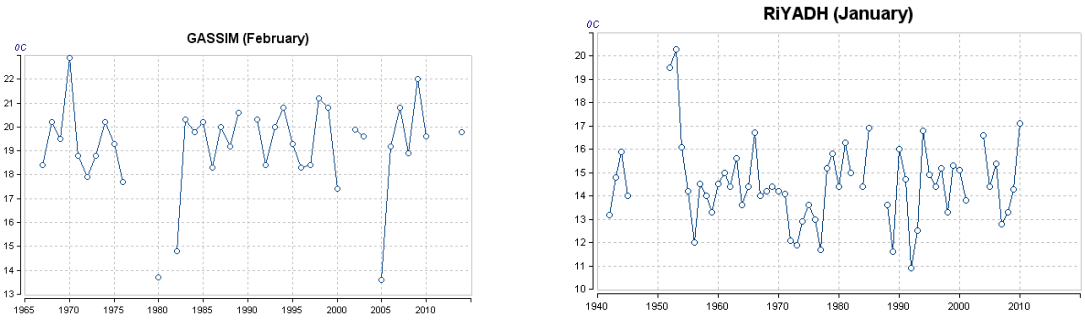

Figure 2.4.1 – Examples of heterogeneous extremes in average monthly air temperature

Results of the assessment of stationarity based on 15 stations using Fisher criterion (F) and Student (t-test) are given in table.2.4.2 for identification of non-stationary cases.

Table 2.4.2. – Ranks of heterogeneous cases of average monthly temperature at different weather stations in Yemen and adjacent areas.

№	Code	Station	F	St	F	St	F	St
			January		February		March	
1	41316	SALALAH		-				-
2	41466	TAIZ	-		-			
			April		May		June	
1	40405	GASSIM						(-)1.5
2	40438	RIYADH		-		-		-
3	41316	SALALAH		-		-		(-)3
			July		August		September	
1	40430	MEDINA		-		-		(-)1.4
2	40438	RIYADH		-		-		-
3	40439	YENBO		-		(-)1.3		
4	41316	SALALAH						(-)1.3
			October		November		December	
1	41036	TAIF		(-)1.4				
2	41316	SALALAH		-		-		(-)2.7

Results displayed in table 2.4.2 shows that, non stationary in terms of dispersions are just 2 cases from short term time series (2%) of the 96 series (8 weather stations with period of observations 40 years and more;

Non stationary on average are more than 15 cases (15.2%);

- non stationary cases in average more than variances, they occur not only at stations with heterogeneous extremes or missing data and generally they are characterized by non stationary climate, which is more evident during the warmer period of the year.

In any case, non-stationary air temperature is not caused by errors due to instruments, for example, change of measuring instruments, and therefore non-stationary data were excluded for further analysis. Examples of re-established non-stationary series are shown in Fig.2.4

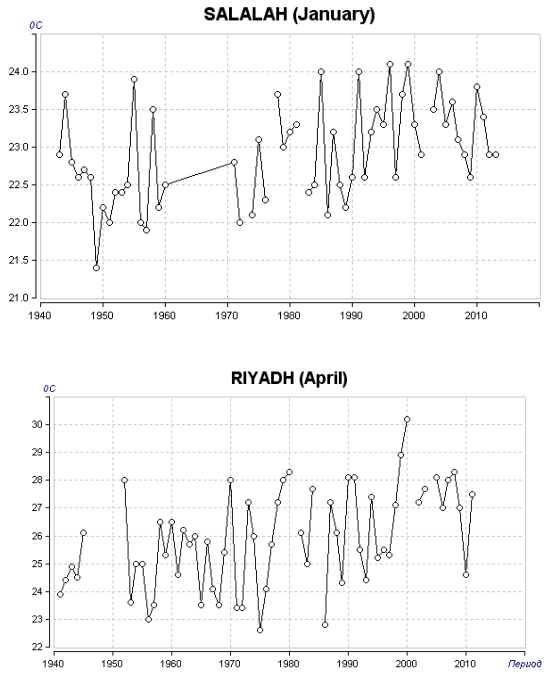

Figure 2.4.2 - Examples of non stationary observations cases

Likewise, assessment of homogeneity and stationarity of total monthly precipitation long-term time series was performed. Example of non-uniform set of extremes values for 44 stations in the Arabian Peninsula is shown in table 2.4.3.

Analysis of homogeneity empirical distribution was performed for monthly sums of precipitation and results are presented in table 2.4.3.

Table 2.4.3. – Ranks of heterogeneous cases of total monthly precipitation at different weather stations in Yemen and nearby areas.

№	Code	Station	Max.		Min.		Max.		Min.	
			D	SG	D	SG	D	SG	D	SG
			January				February			
1	40430	MEDINA					-		-	
			March				April			
2	41024	JEDDAH	(-)2.3		(-)1.8					
			May				June			
5	41140	JEDDAH					-			
9	41316	SALALAH	(-)1							
10	41466	TAIZ						-		-
11	41467	SANA'A					-		-	
			July				August			
1	40430	MEDINA	-							
2	40438	RIYADH					-		-	
7	41314	THUMRAIT					-		-	
9	41470	IBB						-		(-)2.8
			September				October			
6	40405	GASSIM					(-)1.6		(-)2.5	
8	40438	RIYADH					-		(-)2.5	
12	41314	THUMRAIT					-		-	
13	41467	SANA'A					-		-	
			November				December			
6	40438	RIYADH	(-)1.5		(-)1.5					
10	41316	SALALAH			(-)2.3		-		-	
11	41467	SANA'A								

Identified heterogeneous extremes were not excluded from the ranks of observations for subsequent gaps filling procedures and interpolation of time series, because these are the raw data and possibly interpolated values will not be perceived as a no stationary data. However,

the heterogeneity of the results obtained has been taken into account in the assessment of stationary of data.

From the results in table 2.4.3, the heterogonous cases of maximum extreme are 11 (3.3%) and heterogeneous minimum are 8 (2.4%). The reasons of these results are the same as explained in the case of air temperature.

Results of assessment of stationarity of the same precipitation stations 44 using Fisher test at 1% significance level are shown in table 2.4.4 .When Student's test was used, at the above stated significance level there no stationary values were detected.

Table 2.4.4 – No stationary variances of total monthly rainfall for meteorological stations in the Arabian Peninsula

Code	Station	Months											
		1	2	3	4	5	6	7	8	9	10	11	12
40430	MEDINA		-							-	-		-
40438	RIYADH							-				-	
40439	YENBO				-						-	-	-
41036	TAIF							-	-			-	
41314	THUMRAIT				-		-	-		-	-		-
41316	SALALAH			-	-	-					-	-	-

Results in table 2.4.3 shows that cases with non stationary have variance 25 (21%) out 120, which is large enough, if we are going to take into account the fact that for evaluation of homogeneous extreme these cases were only 2-3%. However, analysis of non-stationary time series showed that almost all cases of non-stationary of variance were due to the influence of one or more of the extreme, which can be homogeneous if assessed by criteria Dixon and Grubbs-Smirnova, but they appears to be heterogeneous when their variances are evaluated as the second moment of the distribution in the construction of the difference between extremes and average of square value. Heterogeneous monthly percentage cases are more from October to December. Stations Thumrait and Salalah have the highest number of months with non-stationary variance of precipitation (6 months).

In general, non- stationary data were kept for further analysis because these are actual data.

2.5. The technique for recovery permits observations and increasing of observed time Series

For the purpose of making models results time series being more reliable and to use them in a particular area, they must be:

a) Time series must have enough observations,
b) No gaps;
c) The period of observations must be the same.

For restoration of observations and interpolation of time series with few observations is based on the method of constructing the regression equations relationship of a time series and time series-analogues in nearby observation stations [112, 116, 117, 118].

2.6. Results of data recovery and the formation of the historical (long-term) time series for further modeling.

For the purpose of recovering data, and interpolating time series, the lowest value of correlation coefficients in this research was taken as R=0.8, and R=0.7 for mean monthly air temperature and total rainfall. The correlation coefficient for rainfall was taken to be smaller that of air temperature because rainfall is changing a lot in space. The minimum number of observation in filling the gaps was taken to be greater than 10 while the number of analogous was 3. The results of assessment of effectiveness of restoring gaps series of monthly air temperatures are given in table 2.6.1, where the numerator - number of years before restoration, the denominator - after interpolating to long-term period.

Table 2.6.1 - Assessment of effectiveness of restoring time series of air temperature to the long-term period of meteorological stations in Yemen and nearby countries

№	Code	Station name	Months					
			1	2	3	4	5	6
1	40405	Gassin	34/133	36/133	37/133	34/111	36/108	38/108
2	40430	MEDINA	50/111	52/110	53/92	54/77	51/80	54/95
3	40438	El-Riyadhi	55/87	55/106	61/108	58/71	58/79	58/105
4	40439	YENBO	28/111	31/101	29/107	33/71	30/63	31/63
5	41036	El-Taif	35/92	35/106	37/104	37/105	36/110	35/108
6	41314	Thumrat	25/69	21/92	23/69	24/69	25/98	23/82
7	41316	Salalah	52/130	49/105	54/70	54/72	55/95	55/71
8	41404	Sana'a	30/56	30/52	30/58	58/30	30/30	30/57
9	41452	Ibb	23/36	24/46	24/24	24/24	24/24	24/30
10	41466	Taiz	27/36	27/55	28/57	28/57	28/28	27/63
11	41390	Al-Mahwet	7/30	27/29	7/43	7/43	7/7	7/29
		Mean	**33/78**	**35/85**	**35/77**	**37/66**	**35/66**	**35/74**
			7	8	9	10	11	12
1	40405	GASSIM	35/93	34/107	34/107	32/98	34/94	33/105
2	40430	MEDINA	50/81	49/108	49/108	50/69	52/107	52/111
3	40438	El-Riyadh	58/98	55/83	55/83	56/110	56/107	60/109
4	40439	Yenbo	33/107	25/103	25/103	28/89	28/108	30/109
5	41036	El-Taif	35/103	34/99	34/99	30/106	32/110	31/100
6	41314	Thumrat	22/85	21/87	21/87	22/83	24/69	26/98
7	41316	Salalah	51/97	53/68	53/68	57/110	54/68	54/73
8	41480	Aden	93/127	95/125	95/125	93/128	95/129	95/128
8	41404	Sana'a	30/59	30/61	30/60	30/30	30/30	30/30
9	41452	Ibb	23/29	24/29	24/38	24/24	22/31	23/23
10	41466	Taiz	27/56	27/45	28/29	28/56	28/36	28/28
11	41390	Al-Mahwet	7/30	7/30	8/35	8/37	8/30	8/8
		Mean	**42/86**	**41/86**	**41/86**	**42/85**	**42/84**	**46/84**

Results of the procedure of restoration of data in the table above shows that the average period of observations of 33-46 years was increased to 66 (April) - 84-86 (August-February) years,

and recovered data in cold season was more effective than that in warm season, due to the greater uniformity of synoptic processes and better spatial temperature distribution during this period.

After the recovery process, verification of the long time series on the homogeneity on the extreme was carried out using Dixon and Smirnov-Grubbs criteria and stationary of means value and variances by Student's t test and Fisher. This was done because small heterogeneity and non-stationary in the data can lead to substantial heterogeneity in the recovered data and on the other hand there may be significant errors in the recovered data for individual years.

Results of homogeneity testing of the recovered time series for Yemeni are shown in table 2.6.2.

Table 2.6.2 - Assessment of homogeneity of restoring time series of air temperature in Yemen and nearby countries

№	Code	Stat name	Max		Min		Max		Min	
			D	SG	D	SG	D	SG	D	SG
			January				February			
1	41466	TAIZ	+	+	(-)2.6	(-)1.1	+	+	+	+
2	41390	AL-MAHWET	+	+	+	+	+	+	(-)1.1	(+)3.1
			June				August			
1	41404	SANA'A	+	+	+	+	-	+	(-)2.4	(+)4.3
2	41466	TAIZ	+	+	+	+	(+)3.7	+	+	+
3	41452	IBB	+	+	+	+	+	+	+	+
			September				October			
1	41404	SANA'A	+	+	-	-	+	+	+	+
2	41452	IBB	+	+	+	+	(-)2.5	(+)3.7	-	-
3	41390	AL-MAHWET	+	+	-	(+)3.3	+	+	+	+
			November				December			
1	41404	SANA'A	-	(-)1	+	+				
2	41390	AL-MAHWET	+	+	-	-				

Verification of homogeneity of extreme value of time series of air temperature guarantee that at $\alpha = 1\%$, heterogeneous cases was obtained 6 times out of which 2 cases contains heterogeneous maximum and 4 cases- heterogeneous minimum. All cases of heterogeneous extremes were excluded in the time series for further modeling. Even if they were observed they may also contain errors, and most important, the exclusion of the value in the long time

series practically should not affect the parameters of time series models and establishment of long term climate changes.

Analysis of stationarity of mean and variance table 2.6.3 of recovered long term time series based on Student and Fisher criteria indicates that, 5 cases were guaranteed non-stationary and with dispersion (10%) and 7 cases non-stationary with average (14%).

Table 2.6.3 – Results of heterogeneous cases of recovered data of mean monthly temperatures at different meteorological stations in Yemen.

№	Code	Stat.name	F	St	F	St	F	St
			January		February		March	
1	41404	SANA'A	+	(+)4.7	+	-	+	-
2	41466	TAIZ	+	+	(-)2.7	(-)2.9	+	-
3	41452	IBB	+	(+)3.7	+	-		
4	41390	AL-MAHWET	-	(+)3.4	+	+	+	(+)4.5
			April		May		June	
1	41404	SANA'A			+	(-)2.5	+	(+)4.7
2	41466	TAIZ			(-)1.7	+		
3	41452	IBB					(-)1.6	+
4	41390	AL-MAHWET			+	+		
			July		August		September	
1	41404	SANA'A	+	+	-	+	-	-
2	41466	TAIZ	+	(+)4	(+)3.3	+	-	+
3	41452	IBB	+	+	+	+	-	-
4	41390	AL-MAHWET	+	(-)1.5	(+)4.9	+	+	(-)1.6
			October		November		December	
1	41404	SANA'A	+	-				
2	41452	IBB	-	+	+	+		
3	41390	AL-MAHWET	+	(+)4.7	(-)1.1	+		

A detailed analysis of each restored time series showed that in most cases non-stationary variances and average values are influenced by the presence of heterogeneous extremes, which were excluded from the time series. In other cases, especially for the averages, non-stationary is caused by errors in the recovered data, which were also excluded from the time series of observations. As a result, the recovered time series of monthly air temperatures and monthly rainfall for subsequent modeling has been formed.

3. Statistical modeling of climate change in Yemen and neighboring regions

3.1. Statistical modeling techniques and basic models (random sample and two main non-stationary models: linear trend and step changes).

The following time series models were considered the following [119, 120, 121]:
- A model of a stationary sampling;

- Non-stationary model of monotonic changes as a trend,
- Non-stationary model of step changes, characterized by the transition from one steady state to another.

Direct modeling of time series consists of three main stages [137, 139]:

- Calculation of model parameters;
- Evaluation of the effectiveness of non-stationary models with respect to the stationary
- Evaluation of the statistical significance of non-stationary models with respect to the hundred-stationary.

Stationary model parameters are the mean value (Ycp) and standard deviation (σ), determined by a number of observations.

A stepwise changes model is similar to two (or more) stationary models for two (or more) time series, which characterized by constant over time mean and standard deviation for each of the series:

$$Y_{1cp} = \text{const1}, \quad Y_{2cp} = \text{const1},$$
$$\sigma_1 = \text{const1}, \quad \sigma_2 = \text{const2} \qquad (3.1)$$

Moment of stepwise changes (t_n) is determined visually or on the basis of additional information on the factors and the date of violation of stationarity (eg change in the index of atmospheric circulation), and can be determined by iteration when the minimum value of the sum of squared deviations from the mean value for each of the two parts of the temporary series:

$$SS = \sum_{1}^{n1} (Y_i - Y_{1cp})^2 + \sum_{n1+1}^{n} (Y_i - Y_{2cp})^2 = \min \qquad (3.2)$$

where n1, n2 - the volume of each of the two parts of the time series; SS - total sum of squared deviations.

The standard deviation of residuals stepwise changes model for a single-stage and two fixed intervals determined by the formula:

$$\sigma_{step} = \sqrt{\frac{\sigma_1{}^2 n_1 + \sigma^2{}_2 n_2}{(n_1 + n_2 - 1)}} \qquad (3.3)$$

where σ σ_{st} - standard deviation of the residuals of the model step changes; σ1, σ2 - standard deviations fixed intervals of time series; n1, n2 - the volumes of stationary segments.

Linear trend model is expressed by the following equation [115]:

$$Y(t) = b_1 t + b_0, \qquad (3.4)$$

where t - time; b1, b0 - the coefficients of the regression equation determined by mean square method:

$$b_1 = \frac{\sum_{i=1}^{n} (Y_i - Y_{cp})(t_i - t_{cp})}{\sum_{i=1}^{n} (t_i - t_{cp})^2}, \qquad (3.5)$$

$$b_0 = Y_{cp} - b_1 t_{cp} \qquad (3.6)$$

The statistical significance of the linear trend model is estimated by statistical significance coefficient b1 or correlation coefficient R according to (4), which is calculated by the formula:

$$R = \frac{\sum_{i=1}^{n} (Y_i - Y_{cp})(t_i - t_{cp})}{\sqrt{\sum_{i-1}^{n} (Y_i - Y_{cp})^2 \sum_{i=1}^{n} (t_i - t_{cp})^2}} \qquad (3.7)$$

The statistical significance of R is determined from the condition R≥R *, where R * - critical value of the correlation coefficient determined for a given number of degrees of freedom (ν) and a significance level (α) where ν = n-2, n- volume number, α = 5% [108].

For linear trend model standard deviation of residuals calculated by the formula:

$$\sigma_\varepsilon = \sigma_y \sqrt{1 - R^2} \qquad (3.8)$$

where σy - standard deviation of the original series (model of a stationary medium); σε - standard deviation of the residuals with respect to model the linear trend; R - correlation coefficient equation linear trend.

To quantify the differences between the trend model and model of step changes on the model of a stationary average relative deviations are calculated by the formulas:

$$\Delta_{tr} = \left(\frac{\sigma_y - \sigma_\varepsilon}{\sigma_y} \right) * 100\% \quad , \qquad (3.9)$$

$$\Delta st = \left(\frac{\sigma_y - \sigma_{cmyn}}{\sigma_y} \right) * 100\% \quad , \qquad (3.10)$$

where Δtr, Δst - relative deviations or variations (%) trend model and the model of step changes in the model fixed sample; σy, σε, σstup - standard deviations residues, respectively models of random sampling, the linear trend and step changes.

$$F_{TP} = \frac{\sigma^2{}_Y}{\sigma^2{}_\varepsilon} \quad , \qquad (3.11)$$

$$F_{CTУП} = \frac{\sigma^2{}_Y}{\sigma^2{}_{cmyn}} \qquad (3.12)$$

The numerator will always be the variance of the original series of observations, as it is greatest, or at least equal to the residual dispersion competing models. If the calculated statistic value is larger than the Fisher critical, then the variance of the two models to have statistically significant difference from the model and the corresponding (or step changes in the trend) is statistically more effective than the model of stationary sample.

3.2. Results of simulation of climate change in long-term time series of monthly air temperature.

The parameters of time series models and their performance characteristics were calculated and compared with stations data of air temperature on the territory of Yemen, and neighboring territories.

Modeling results time series for 4 stations in Yemen and for all 12 months are shown in Table 3.2.1.

Table 3.2.1 - Models time series and their characteristics for the average monthly air temperature at weather stations in Yemen.

WMO	Δ_{tr}%	Δ_{step}%	F_{tr}	F_{step}	Fst	St st	Tstep.	Tin.	Tfin.	N	Rтр
January											
41390	3.2	9.4	1.07	1.22	1.68	-2.16	2003	1984	2013	29	-0.25
41404	7.9	9.6	1.18	1.22	1.26	2.06	1998	1983	2013	31	0.39
41452	5.4	**10.1**	1.12	1.24	1.08	2.21	1999	1975	2013	33	0.32
41466	0.3	6.3	1.01	1.14	20.48	1.49	1990	1971	2013	35	0.08
February											
41390	2.4	2.3	1.05	1.05	1.34	-1.04	2004	1984	2014	28	-0.22
41404	5.9	**17**	1.13	1.45	4.76	2.13	1994	1983	2014	32	0.34
41452	8	**18.8**	1.18	1.52	1.38	2.84	1994	1970	2013	37	0.39
41466	0.9	**12**	1.02	1.29	7.25	1.68	1994	1983	2013	31	0.13
March											
41390	9.6	**14.1**	1.22	1.36	3.29	2.15	2000	1987	2014	26	0.43
41404	**15.3**	**19.8**	1.39	1.55	5.64	-3.57	1981	1950	2013	58	-0.53
41452	6.8	0	1.15	1			1981	1990	2005	16	0.36
41466	0.1	3.5	1	1.07	1.54	1.12	1995	1983	2013	30	0.05

WMO	$\Delta_{tr}\%$	$\Delta_{step}\%$	F_{tr}	F_{step}	F_{st}	St st	$T_{step.}$	$T_{in.}$	$T_{fin.}$	N	R_{TP}
April											
41390	**13.5**	**12.5**	1.34	1.31	1.38	4.08	2003	1957	2014	58	0.5
41404	6.6	**10.9**	1.15	1.26	1.01	2.12	1998	1983	2013	31	0.36
41452	5.7	0	1.12	1	2.21	1.57	1998	1990	2005	16	0.33
41466	0	6.7	1	1.15	1.33	-1.62	2002	1983	2013	29	0.02
May											
41390	0	1.6	1	1.03	1.87	-0.85	2003	1983	2013	29	0
41404	3.1	5.6	1.07	1.12	1.59	1.66	1999	1983	2013	31	0.25
41452	0.1	6	1	1.13	1.55	1.33	1999	1989	2013	25	0.05
41466	1.2	5	1.02	1.11	1.3	1.25	1994	1983	2013	31	0.15
June											
41390	**12**	**13.5**	1.29	1.34	2.75	2.8	2003	1983	2014	32	0.47
41404	1	3.7	1.02	1.08	2	1.07	1990	1980	2013	34	0.14
41452	0.9	1.4	1.02	1.03	2.55	-0.78	2004	1988	2014	27	-0.14
41466	5.6	**12.7**	1.12	1.31	1.68	-2.27	2003	1983	2013	29	-0.33
July											
41390	0	1.1	1	1.02	1.4	-0.7	1994	1983	2013	30	-0.01
41404	1.6	3.2	1.03	1.07	1.74	1.54	1987	1968	2013	46	0.18
41452	0.1	5	1	1.11	3.51	1.29	1996	1983	2013	29	0.05
41466	3.7	**11.5**	1.08	1.28	1.52	-3.68	2003	1958	2013	56	-0.27

WMO	$\Delta_{tr}\%$	$\Delta_{step}\%$	F_{tr}	F_{step}	Fst	St st	Tstep.	Tin.	Tfin.	N	Rтр
August											
41390	10	**11.1**	1.23	1.26	1.01	-2.31	2003	1983	2013	30	-0.44
41404	2.3	3.3	1.05	1.07	1.32	-1.32	2003	1983	2013	31	-0.22
41452	5	9.9	1.11	1.23	1.06	-2.11	2003	1983	2013	29	-0.31
41466	**24.5**	**19.1**	1.75	1.53	1.99	-3.07	2003	1983	2013	30	-0.66
September											
41390	5.2	0	1.11	1			0	1994	2013	18	-0.32
41404	0.4	3	1.01	1.06	2.03	-1.22	2000	1983	2013	31	-0.09
41452	**14.3**	3.7	1.36	1.08	2.59	1.23	1999	1967	2013	26	0.52
40466	2.4	5.6	1.01	1.02	1.07	0.16	1908	1983	1919	45	-0.09
October											
41390	5.9	8.2	1.13	1.19	2.75	1.75	2003	1990	2014	25	0.34
41404	0.3	1.6	1.01	1.03	1.06	-1.01	2003	1983	2013	31	-0.08
41452	0	0.9	1	1.02	1.73	0.73	2001	1980	2014	33	0.03
41466	0.7	3.7	1.01	1.08	1.06	-1.33	2002	1982	2013	31	-0.12
November											
41390	0.9	6.4	1.02	1.14	1.26	-1.58	2000	1985	2012	27	-0.14
41404	0	0.7	1	1.01	1.66	0.65	2002	1983	2013	31	0
41452	0.7	6.2	1.01	1.14	1.48	1.44	1998	1987	2014	27	0.12
41466	4.7	9.9	1.1	1.23	2.4	-2.13	2002	1983	2013	28	-0.3

WMO	$\Delta_{tr}\%$	$\Delta_{step}\%$	F_{tr}	F_{step}	Fst	St st	Tstep.	Tin.	Tfin.	N	Rтр
December											
41404	2.1	3.8	1.04	1.08	2.49	1.27	1994	1983	2013	30	0.2
41452	**15.5**	0	1.4	1	2.9	1.01	1994	1990	2004	14	0.53
41466	6.8	**20.8**	1.15	1.59	1.91	-2.7	2000	1983	2013	29	-0.36

From Table 3.2.1 shows the most significant non-stationary models for different months and different stations:

- February - stepwise change model for weather stations: Sana'a (Δstep = 17%), Ibb (Δstep = 18.8%), Taiz (Δstep = 12%)
- March - for the weather station Al-Mahwet (Δstep= 14.1%), Sana'a (Δstep = 15.3% = 19.8% Δtr);
- April for the weather station Al-Mahwet (Δstep = 12.5% = 13.3% Δtr);
- June for the weather station Al-Mahwet (Δstep = 13.5%, Δtr = 12%) and Taiz (Δstep = 15.3%);
- August for the weather station Taiz (Δstep = 19.1%% Δtr = 24.5%););
- September for the weather station Ibb (Δtr = 14.3%);
- December for the weather station Ibb (Δtr = 15.5%), Taiz (Δstep = 20.8%)

Of all the 20 effective non-stationary models (14 models stepwise changes and trend models 6), which makes a total of 16 non-stationary series, or one-third of all (33.3%) is statistically significant only one non-stationary model for the weather station Taiz and August temperatures (Δtr = 24.5 %)), and December (Δstep = 20.8%).

The time series for some non-stationary models at Δ> 15% are shown in figure 3.2.1.

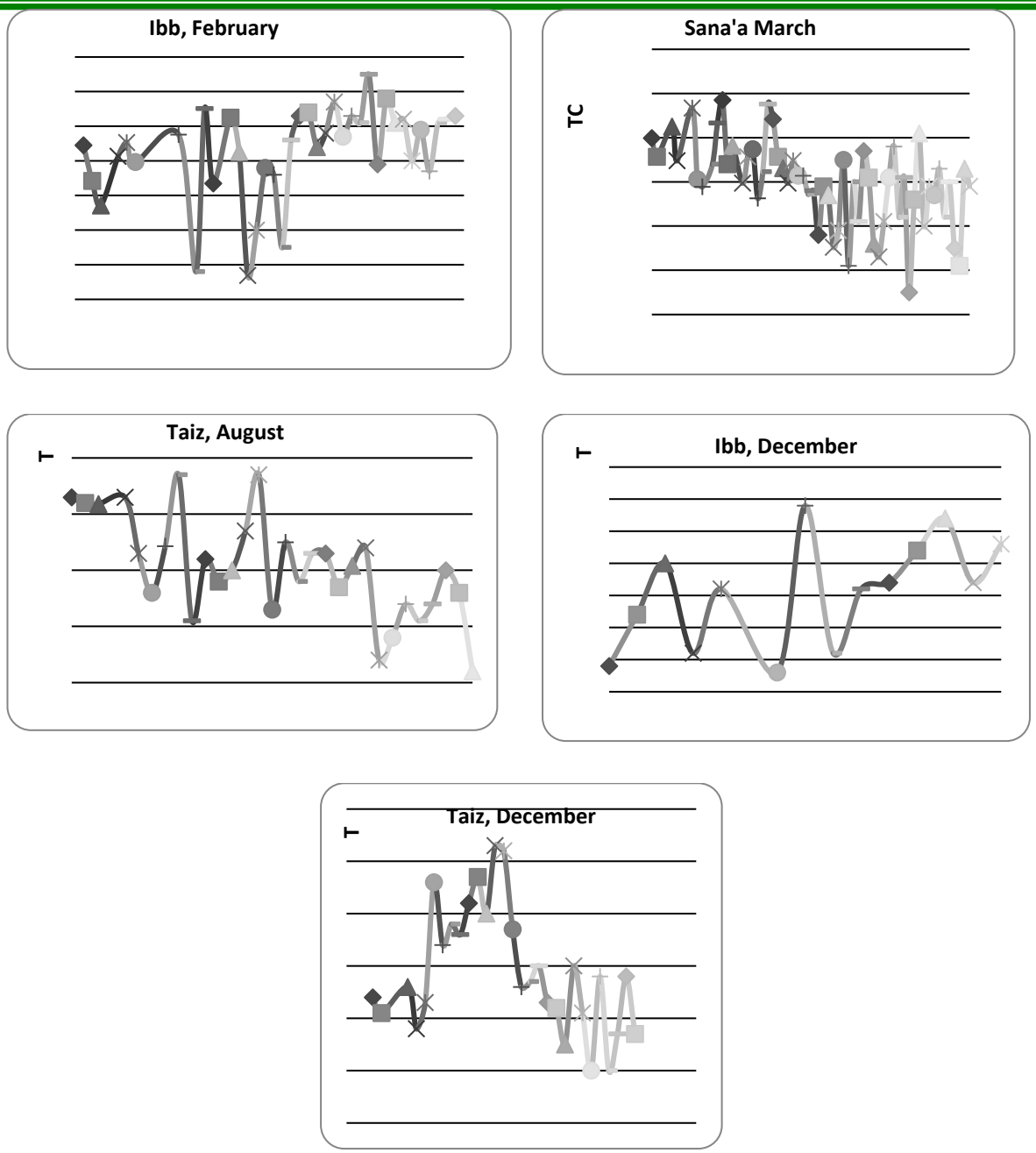

Figure 3.2.1. Non-stationary time series of long-term temperature air temperature at meteorological stations in Yemen

From the analysis of non-stationary time series graphs that in two cases out of five has been an increase in temperature: Weather Station Ibb (December and February), and in three cases - the temperature drop: Weather Station Taiz (August and December) and weather station Sa-na'a (march).

A detailed analysis of the graphs showed the following:

- The temperature at Sana'a weather stations in March was recovered for the period from 1950. to 1982, which causes non-stationary observed data are shown in Figure 3.2.2);
- On the station Ibb observations are available only since 1990, so non-stationarity can be caused by short duration of observations and errors in the recovered data (observed data are also shown in Figure 3.2.2).
- At the meteorological station Taiz observed data are available since 1983, and the model reflect the situation of observed data of poor quality (Figure 3.2.2).

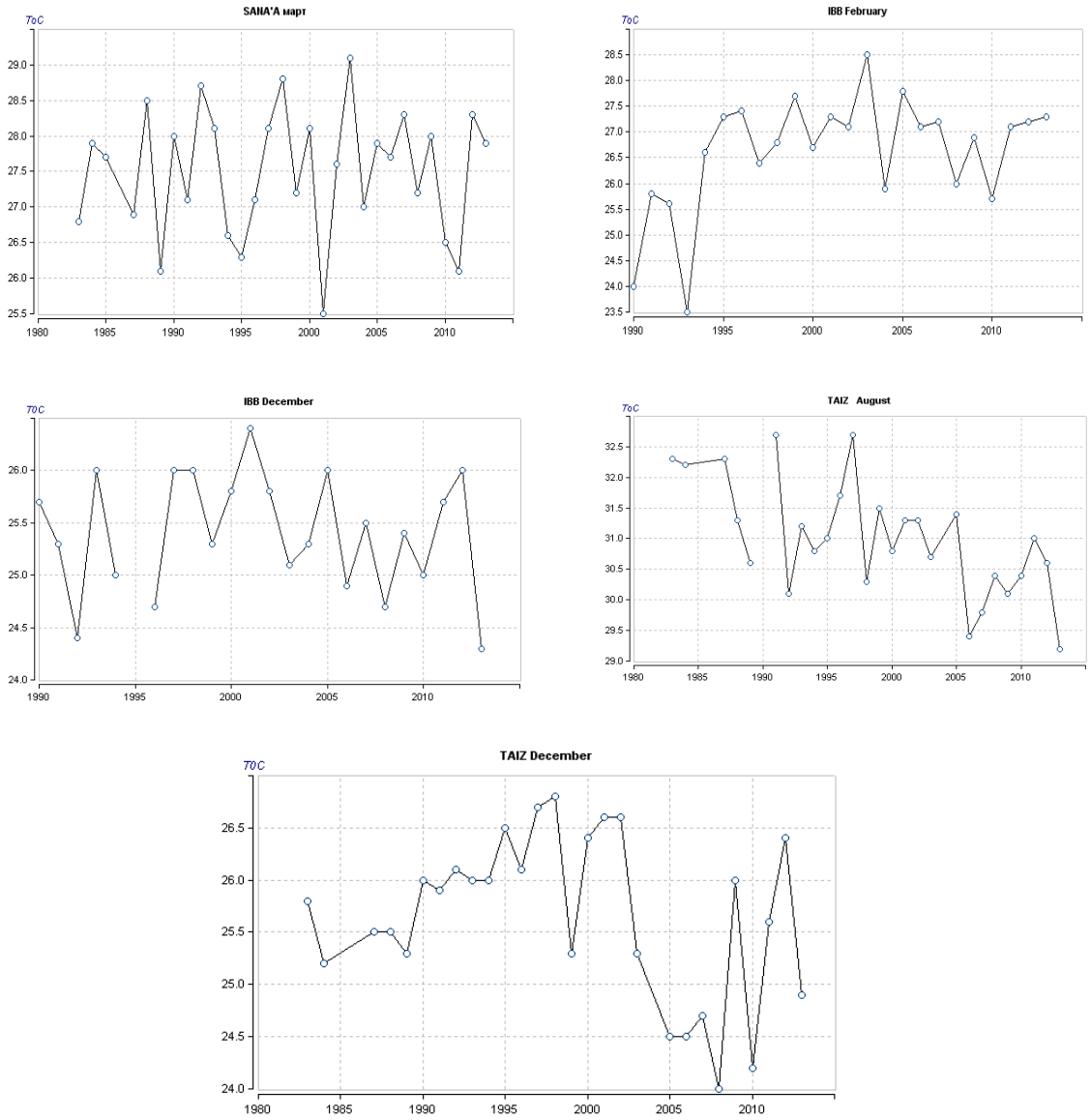

Figure 3.2.2. Observational data on weather stations in the Republic of Yemen.

As a result, the analysis of time series models in Yemen the following conclusions:

- The vast majority of the time series of observations at meteorological stations 4 Republic of Yemen are stationary;
- Individual non-stationary cases, such as at the meteorological station Taiz, are caused by insufficient length of observation and possible measurements errors.

For the purpose assessing changes in climate, the study area was selected and data from different weather stations was examined including surrounding countries represented in a regional database. For these stations also recovering of time series was performed.

And if non-stationary case has been depicted, then assessment was done by excluding after recovered data have been excluded, extremes of data for the first part of time series 1950-1960's. As a result, the following time-dependent model temperature model was obtained.

Table 3.2.2. - Effective time-dependent stationary models and their characteristics (air temperature in the surrounding areas).

WMO	Δ_{tr}%	Δ_{step}%	F_{tr}	F_{step}	F_{st}	St_{st}	T_{step}	T_{in}	T_{fin}	N	R_{tr}
January											
41452	5.4	**10.1**	1.12	1.24	1.08	2.21	1999	1975	2013	33	0.32
41316	**14.7**	**14**	1.37	1.35	3.27	4.42	1914	1881	2011	130	0.52
February											
41404	5.9	**17**	1.13	1.45	4.76	2.13	1994	1983	2014	32	0.34
41452	8	**18.8**	1.18	1.52	1.38	2.84	1994	1970	2013	37	0.39
March											
41316	**16.6**	**19.6**	1.44	1.55	3.95	4.27	1985	1941	2011	60	0.55
41404	**15.3**	**19.8**	1.39	1.55	5.64	-3.57	1981	1950	2013	58	-0.53
41390	0.2	**16.3**	1	5.24	2.98	-1.39	1987	1983	2014	56	-0.06
April											
40405	7	**10.5**	1.16	1.25	1.29	5.07	1999	1901	2011	111	0.37

WMO	Δ_{tr}%	Δ_{step}%	F_{tr}	F_{step}	Fst	St st	Tstep	Tin	Tfin	N	Rtr
January											
41452	5.4	**10.1**	1.12	1.24	1.08	2.21	1999	1975	2013	33	0.32
41316	**14.7**	**14**	1.37	1.35	3.27	4.42	1914	1881	2011	130	0.52
40438	**10**	**13.3**	1.24	1.33	1.4	4.41	1999	1938	2011	71	0.44
40439	**13.7**	**12.6**	1.34	1.31	1.38	3.09	1978	1967	2011	45	0.5
41316	**29.9**	**26.4**	2.03	1.84	3.1	5.45	1984	1937	2010	71	0.71
41404	6.6	**10.9**	1.15	1.26	1.01	2.12	1998	1983	2013	31	0.36
May											
40438	**25.2**	**25.2**	1.79	1.79	2.4	4.85	1973	1923	2011	79	0.66
40439	6	**15.2**	1.13	1.39	1.7	4.13	1987	1944	2010	63	0.34
41314	**14.2**	**16.1**	1.36	1.42	1.99	4.73	1948	1906	2010	94	0.51
June											
40405	**25.6**	**30.4**	1.81	2.07	2.61	5.28	1996	1962	2011	50	0.67
40438	**18.6**	**24.3**	1.51	1.75	2.16	5.91	1994	1941	2011	71	0.58
40439	**14.2**	**13.1**	1.36	1.32	1.49	3.2	1994	1967	2011	45	0.51
July											
40405	**17.8**	**23.8**	1.48	1.72	2.39	4.63	1996	1962	2011	50	0.57
40430	**13.1**	**12.9**	1.32	1.32	2.53	3.69	1986	1951	2011	61	0.49
40438	**30.4**	**26.6**	2.07	1.86	8.09	4.82	1978	1941	2011	71	0.72
40439	**15.4**	**25.2**	1.4	1.79	2.24	5.65	1995	1950	2011	62	0.53
August											
40405	**18.6**	**30.6**	1.51	2.08	2.49	6.61	1998	1951	2010	60	0.58
40430	**24.1**	**25.7**	1.74	1.81	2.55	6.42	1995	1941	2010	70	0.65
40438	**41.7**	**30.7**	2.95	2.08	3.42	5.73	1985	1938	2010	67	0.81
40439	**29.3**	**29.6**	2	2.02	2.42	6.4	1995	1947	2010	64	0.71
41036	**20.2**	**24**	1.57	1.73	4.05	4.2	1983	1951	2010	60	0.6
September											
40405	0.1	**10.2**	1	1.24	7.93	2	1915	1904	2010	105	0.04
41452	**14.3**	3.7	1.36	1.08	2.59	1.23	1999	1967	2013	26	0.52
40430	**13.5**	**16.4**	1.34	1.43	1.73	3.73	1996	1963	2010	48	0.5

WMO	$\Delta_{tr}\%$	$\Delta_{step}\%$	F_{tr}	F_{step}	Fst	St st	Tstep	Tin	Tfin	N	Rtr
January											
41452	5.4	**10.1**	1.12	1.24	1.08	2.21	1999	1975	2013	33	0.32
41316	**14.7**	**14**	1.37	1.35	3.27	4.42	1914	1881	2011	130	0.52
40438	**39.4**	**28.3**	2.73	1.94	4.47	5.56	1965	1941	2010	70	0.8
40439	**28.1**	**39.6**	1.93	2.75	9.22	4.72	1979	1931	2010	62	0.69
41314	9.1	**13.7**	1.21	1.34	1.56	3.57	1987	1953	2010	58	0.42
November											
40430	**10.3**	**12.9**	1.24	1.32	1.13	3.31	1986	1956	2010	55	0.44
40438	**21.9**	**22.9**	1.64	1.68	1.71	4.99	1985	1941	2010	68	0.62
40439	**38.8**	**34.7**	2.67	2.35	4.28	4.1	1986	1961	2010	50	0.79
41036	7.5	**10.9**	1.17	1.26	2.14	3.3	1985	1951	2010	58	0.38
41316	**22.3**	**22**	1.66	1.65	2.8	5.09	1985	1943	2008	66	0.63
November											
41314	7.6	**12.4**	1.17	1.3	1.33	3.35	1993	1961	2010	50	0.38
41316	**22.9**	**19.5**	1.68	1.54	1.87	4.86	1986	1942	2010	67	0.64
December											
41452	**15.5**	0	1.4	1	2.9	1.01	1994	1990	2004	14	0.53

From table 3.2.2, for the winter months non-stationary cases were absent, and the largest number of them depicted in July and August and they sum up to 40-45% of all cases. At the same time, the average for the territory Δstep following: for May Δstep = 12.5% for June Δstep = 10.5% for July Δstep = 15.2% for August - Δstep = 18.0% for September Δstep = 10.6%. In comparison, for the winter months: Δstep = 4.8% for December Δstep = 3.3% for January Δstep = 4.2% for February. In almost all cases non-stationary cases were caused by stepwise increase in temperature and in most cases, this date refers to the 1980 - 1990 years. Linear trend model is less efficient than step changes and averages Δtr% for the warm half of the year are as follows: 9.6% - for May, 6.9% for June, 11.4% for July, 12.5% for August and 7.7% in September.

Figure 3.3 shows the spatial distribution of temperature deviations Δstep for May, June, July and August, with the greatest difference from the stationary model, where the territory of a non-stationary model for effective Δstep> 10% is represented by the colors red shades, and inefficient non-stationary models of blue shades.

It can be seen from Figure 3.2.3, the non-stationary model is dominant in the summer months almost the entire territory except in the south. The biggest difference from the stationary model takes place in August, with almost the entire area shows tendency to 20-30% with the exception of coastal southern regions. In May in the same area, stationary model is depicted in the west of the Peninsula in the Red Sea, and in the summer months, gradually shifting from west the south.

Figure 3.2.4 shows the spatial distribution of deviations Δstep for April and autumn months, in which the percentage of non-stationarity is less.

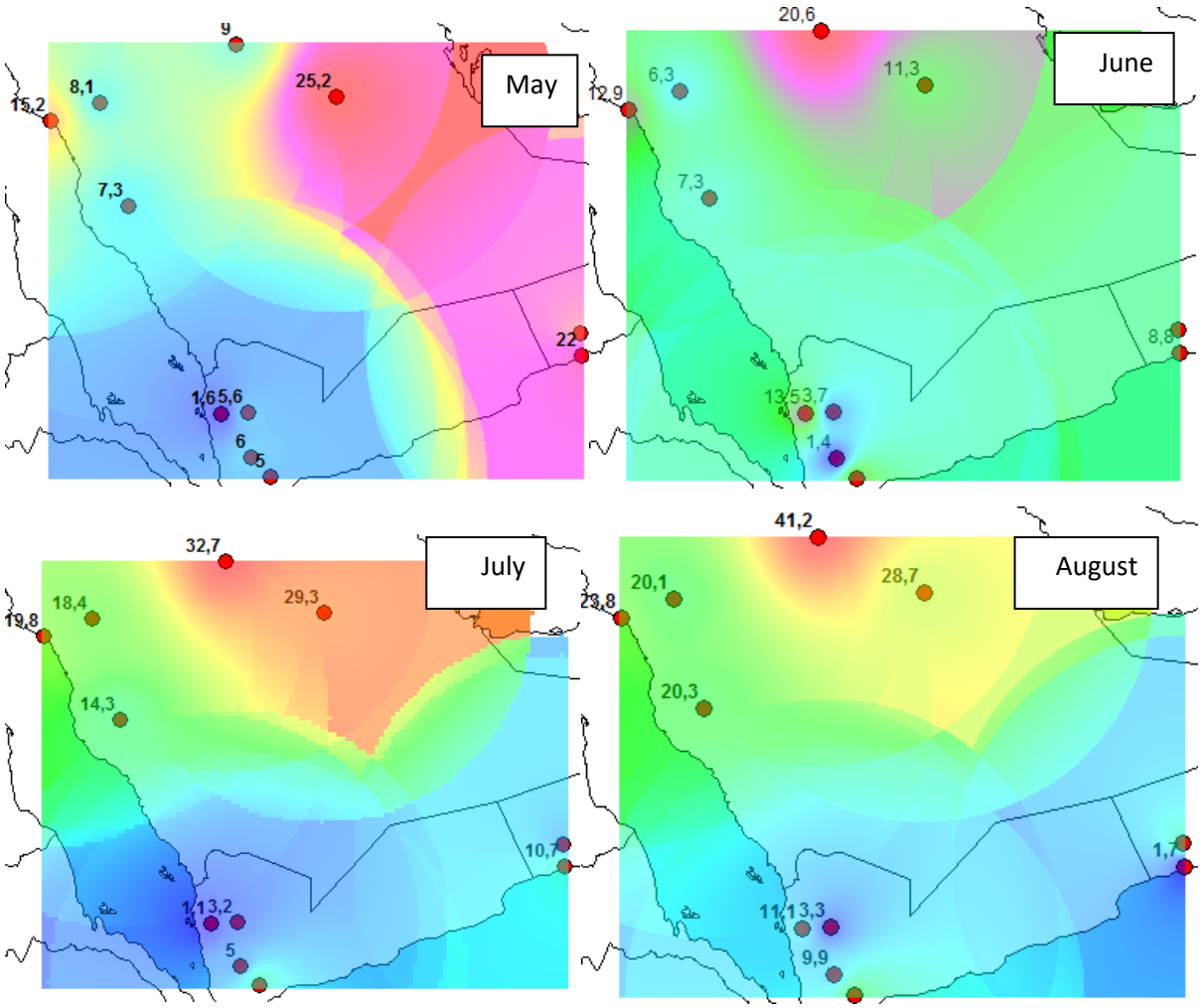

Figure 3.2.3 – Spatial deviation of non-stationary model from $\Delta_{step\ in}$ % for May, June, July and August monthly mean.

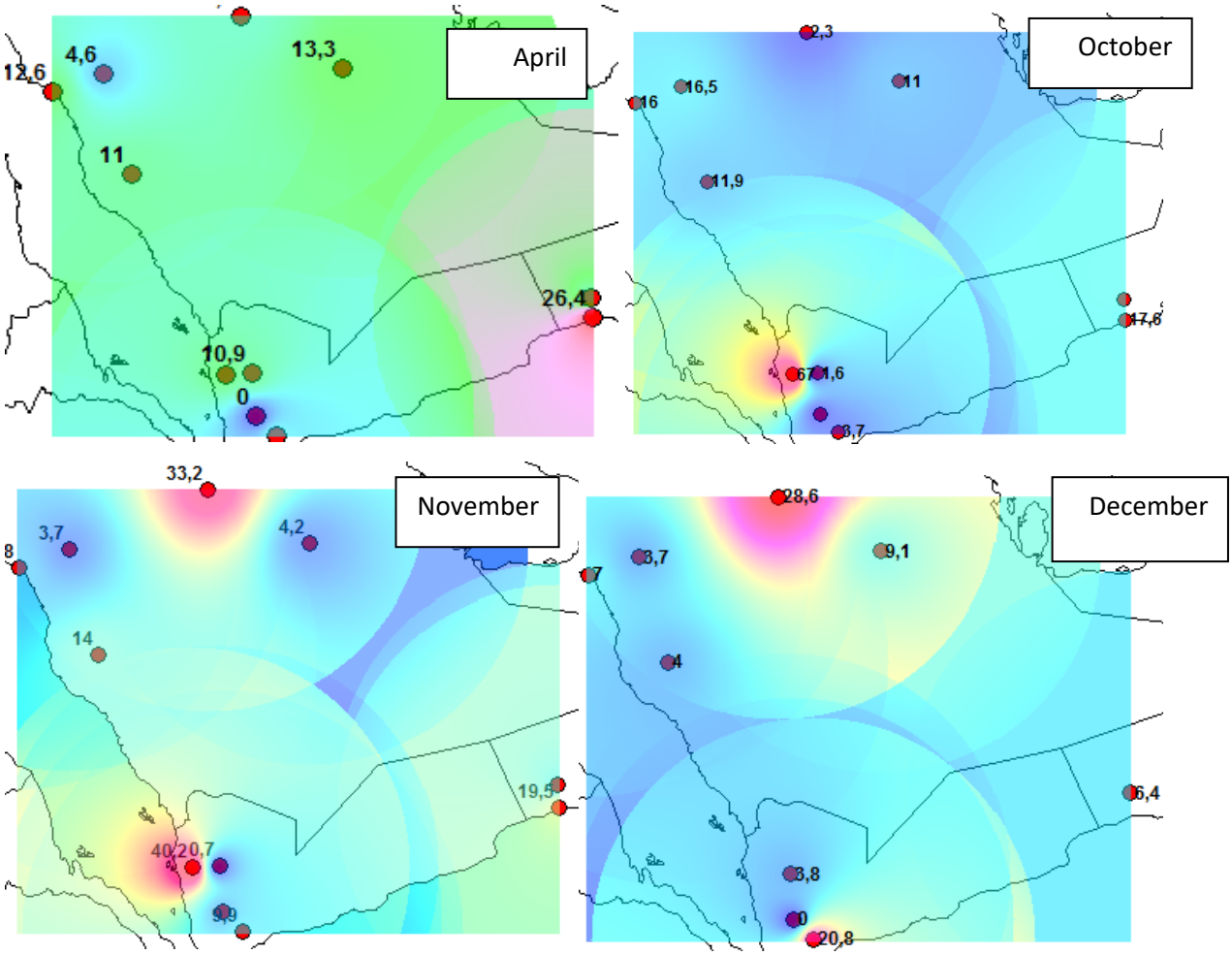

Figure 3.2.4 – Spatial deviation of non-stationary model from Δstep (%) for April, September, October and November.

Figure 3.2.4 shows that in the autumn non-stationary mode is gradually decreased and shifted to the southwest, ie, in coastal areas. In April, on the contrary, it extends from the south to the central regions.

In general, there is annual variation of the dynamics of spatial non-stationarity in the entire Arabian Peninsula. If during the winter almost the entire Peninsula have stationary temperature, in March non-stationarity can be depicted in the individual stations in the south; in April - in the south and center of the peninsula;

In May - almost the entire Peninsula except the western part; in June - the only stationary cases are depicted south and south-west; in September stationary shifted to the eastern part of the Peninsula.

In October additional stationary cases appears in southwest; In November stationary cases are apparent in most parts of the Peninsula, except for some of the south and west areas.
In winter time-dependent model on the peninsula is almost absent and manifested only in one southern station - Salalah. Since the spring, is spread and offset unsteadiness of coastal areas in the southern, central, and southern coastal areas by June become stationary.

In August, almost the entire area of the Arabian Peninsula is represented by non-stationary models, except for the southern regions and individual stations in the Red Sea coastal developments. At the beginning of the fall, non-stationarity shifted towards the south, and moved to the center of the Peninsula is occupied by stationary models.
The main conclusion from the analysis of spatio-temporal dynamics of non-stationary model is to ensure that the time-dependent models can be used in the warm season, and are more common in the inner parts of the Peninsula, and in the cold season temperature is usually stationary except for the coastal areas of the south and west of the peninsula.

Examples of some non-stationary time series are shown in Figure 3.5, the graphs which it follows that a step increase in temperature takes place since the mid-1980s.

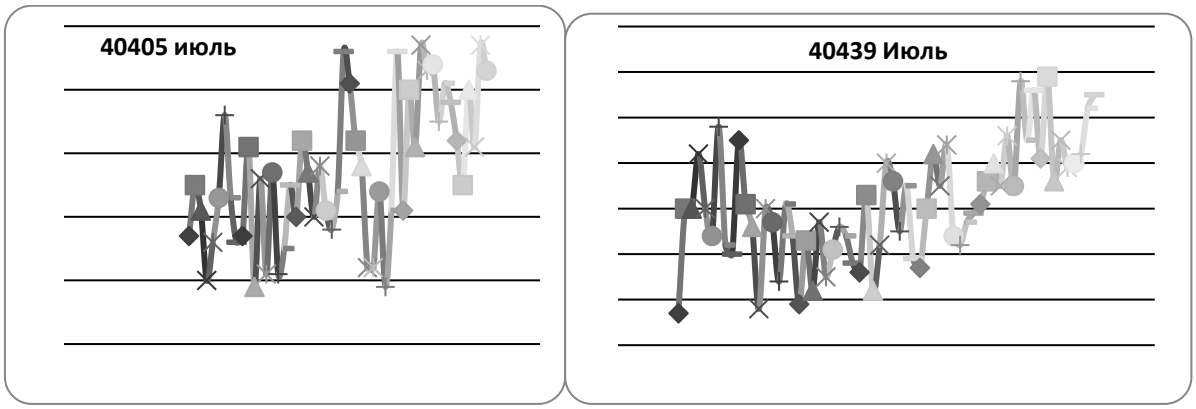

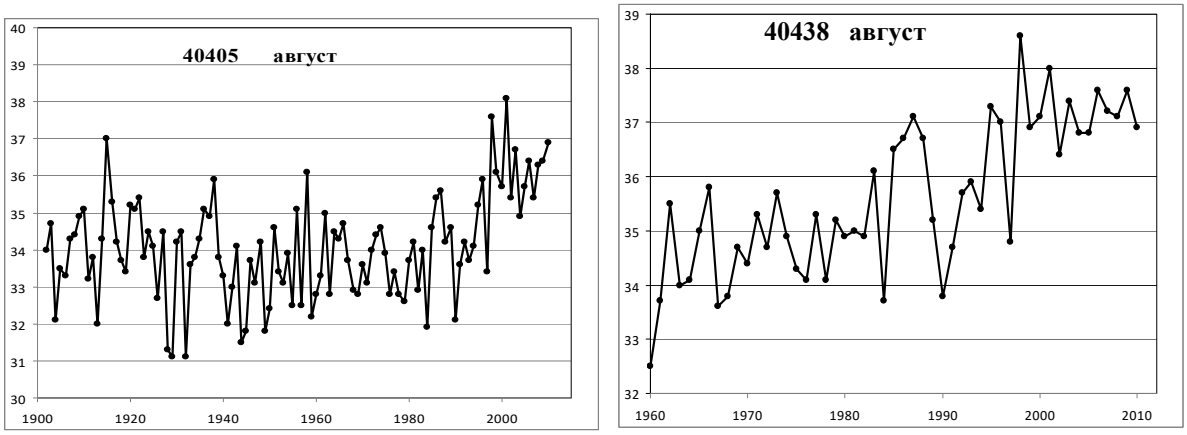

Figure 3.2.5 - Examples of non-stationary time series of monthly air temperatures at stations Yemen and surrounding areas.

In general, results of time series of monthly air temperature are displayed in Table 3.2.3, from which it follows that:

- Time-dependent models have intra-annual distribution and the largest percentage is 60% of the time series in July and August, while in the winter months non stationary model is completely not existing;
- The most effective non-stationary model is the model of stepwise changes, which differs from the stationary model by 15-18% (with maximum up to 30-32%), while the efficiency of the linear trend model reaches 11-12% (with maximum 30-33%).

Table 3.2.3 - Average values Δstep and area Δtr (%) and the percentage of effective non-stationary models (% n) for the average monthly air temperature in Yemen and adjacent areas.

Characteristic	Months											
	1	2	3	4	5	6	7	8	9	10	11	12
Δ_{step}	3.3	4.2	6.1	7.4	12.5	10.5	15.2	18.0	10.6	9.5	6.2	4.8
%н	4.3	0	4.2	17.4	58.3	29.2	58.3	62.5	34.8	29.2	16.7	0
Δ_{tr}	1.2	1.8	2.9	5.8	9.6	6.9	11.4	12.5	7.7	6.4	2.6	1.8
%н	0	0	4.2	13.0	41.7	25.0	41.7	50.0	26.1	20.8	8.3	0

4. Spatial patterns of climatic characteristics in Yemen and neighboring area

4.1. Methods for determining of spatial patterns

After in the previous chapter have been selected types of model for each time series and their performance were researched under this study area, it is possible for spatial generalization of climatic characteristics for practical purposes. Procedure for determining the climatic characteristics and their generalizations on the territory consists of two main parts [140]:

- Identification of the main calculated climatic characteristics in the form of standards, standard deviations, and quintiles of rare occurrence in the observation points;
- Construction of spatial interpolation model of climatic norms and other indicators of climate distribution (variance, quintiles of rare occurrences).

The most common characteristic to estimated climate is climatic norm, which is defined as the average over many years [132, 133]. If the series is stationary, then the norm and standard deviation can be determined over a long period of observation, the longer the number, the less random error of the mean and variance of time series [108, 134, 114]. WMO proposed to determine the climatic norm for the last conventionally fixed period of 1961 - 1990 years. [132, 141]. In addition to the rules and standard deviations in applied climatology for construction and other design of] practical interest climatic characteristics of rare events, which occur, for example, 1 in 100 years or 1 in 200 years [136]. Moreover, these climatic characteristics can be maximum (rare greatest temperature) and minimum (rare lowest temperature). These climatic characteristics of rare repeatability are called design characteristics [112].

Determination of the design characteristics in the presence of a sufficient duration of observations carried out by applying the analytical distribution function of annual probabilities - curves density. In this theory, it follows that the longer the time series, the less random error parameters and quintiles of the distribution.

Empirical annual probability density Pm of climatic characteristics determined by the formula:

$$P_m = \frac{m}{n+1} 100\% \quad , \qquad (4.1)$$

Where m – number of member of climate characteristics, in decreasing order; n - total number of terms.

For smoothing and extrapolation of the empirical distribution curves of annual probabilities three-parameter of distribution are usually used: Kritsky-Menkelya in any respect C_s/C_v and Pearson type III distribution (binomial curve) at $C_s/C_v \geq 2$, as well as the log-normal distribution with $C_s \geq 3C_v + C_v^3$ and other distributions.

Estimates of the parameters of analytical distribution curves: long-term average $\overline{Q}$, the coefficient of variation (Cv) and the ratio to the coefficient of variation Cs / Cv, established in rows of observations considered climatic characteristics of the method of approximate maximum and method of moments.

For the next step - spatial interpolation was performed in the MapInfo GIS method of triangles and its improved version - the method of polygons [127, 128]. The aim of the method of polygons is that the territory on which data is averaged is divided into a number of polygons corresponding to the number of stations located within it. Within each polygon one station is removed. As the weights, averaging coefficients proportional to the area of corresponding polygons are used.

The next type of spatial generalization is the construction of spatial statistical models based on the method given in [121, 122] and representing yea- relationship between the field of climate characteristics of a given year and long-term climate field. The average long-term climatic or field formed on the basis of historical averages climatic characteristics at each station represented at the geographical space. This field is characterized by climatic geography of climate change on the territory in question and is always there, but every year the boundaries and parameters vary depending on the joint influence of climatic factors and the advection of the year.

4.2. Spatial variability of the design characteristics (mean, standard deviation, quintiles) of monthly air temperature in Yemen and neighboring area

Climatic norm or long-term average air temperature is one of the main design climatic characteristics. Climate normals of air temperatures were calculated for the period recommended by WMO (1961-1990) [132] and for all the available period, including both the observed data and reconstructed missing observations, averaging about 100 years. In addition

to that also determined the variability of the time series, standard deviation (σ) and normalized to the average value - the coefficient of variation (Cv), as well as the calculated temperature limits repeatability 1 in 100 years, which corresponds to 1.0% to ensure maximum and 99% for minimum temperatures and 1 in 200 years, which corresponds to the provision of 0.5% and 99.5% [133,112], respectively, for the largest and smallest values. Example of calculation for temperatures in January, which is the most stationary month was shown in chapter 3, is shown in Table 4.2.1.

Table 4.2.1 - Parameters of distributions (normal and variability) and frequency of occurrence values of 100 and 200 years for the average monthly temperature in January at the meteorological stations in the Arabian Peninsula.

№	Code	Normal		Variability				1 in 100 years				1 in 200 years			
		WM0	Weight	WM0		Weight		WM0		Weight		WM0		Weight	
				Cv	Σ	Cv	σ	1.0%	99%	1.0%	99%	0.5%	99.5%	0.5%	99.5%
1	40356	7.1	7.2	0.21	1.5	0.20	1.4	10.3	3.3	10.7	3.7	10.6	2.8	11.1	3.3
2	40373	11.5	11.6	0.14	1.6	0.14	1.5	15.0	7.3	15.3	7.6	15.3	6.8	15.7	7.2
3	40375	10.8	10.4	0.19	2.0	0.20	2.1	16.3	6.6	15.5	5.7	17.1	6.3	16.0	5.2
4	40394	10.2	9.99	0.14	1.4	0.15	1.5	13.1	6.2	13.1	6.1	13.3	5.6	13.4	5.7
5	40400	18.4	18.7	0.1	1.8	0.11	2.0	22.9	15.2	23.7	13.8	23.5	15.0	24.5	13.2
6	40405	12.2	12.4	0.11	1.3	0.11	1.4	14.6	8.3	15.5	8.6	14.7	7.8	15.8	8.1
7	40416	15.2	15.8	0.1	1.5	0.1	1.6	18.5	11.7	18.9	12.5	18.9	11.3	19.2	12.1
8	40430	17.6	17.8	0.08	1.4	0.08	1.4	20.1	13.4	21.1	14.3	20.2	12.8	21.5	13.9
9	40438	14.0	14.5	0.12	1.7	0.12	1.7	17.3	9.4	18.4	10.6	17.5	8.8	18.8	10.2
10	40439	19.7	20.2	0.08	1.6	0.07	1.4	23.0	15.5	23.5	16.5	23.2	14.9	23.8	16.1
11	40580	12.5	12.4	0.16	2	0.15	1.9	16.1	6.8	16.2	7.2	16.3	6.0	16.5	6.5
12	40581	12.8	12.7	0.19	2.4	0.16	2.0	16.1	4.9	16.2	6.4	16.2	3.5	16.4	5.5
13	40582	12.5	12.6	0.13	1.6	0.12	1.5	15.7	7.9	15.9	8.7	15.9	7.2	16.1	8.2
14	40583	12.7	12.8	0.14	1.8	0.14	1.8	16.4	7.8	16.5	8.0	16.6	7.1	16.8	7.4

№	Code	Normal		Variability				1 in 100 years				1 in 200 years			
		WM0	Weight	WM0		Weight		WM0		Weight		WM0		Weight	
				Cv	Σ	Cv	σ	1.0%	99%	1.0%	99%	0.5%	99.5%	0.5%	99.5%
15	40584	13.3	13.5	0.14	1.8	0.11	1.5	16.7	8.1	16.8	9.5	16.9	7.4	17.1	9.0
16	41020	23.2	23.1	0.06	1.4	0.06	1.4	25.7	18.7	26.2	19.3	25.8	18.0	26.5	18.8
17	41036	15.3	15.2	0.07	1.1	0.09	1.4	18.2	13.0	18.7	12.3	18.6	12.8	19.2	12.0
18	41140	25.8	25.9	0.02	0.5	0.02	0.5	27.3	24.6	27.3	24.8	27.5	24.5	27.5	24.7
19	41150	17.1	16.9	0.08	1.4	0.07	1.2	19.4	12.9	19.6	13.8	19.5	12.3	19.8	13.4
20	41170	17.3	17.2	0.07	1.2	0.08	1.4	20.0	14.2	20.0	13.6	20.3	13.8	20.2	13.1
21	41256	22.1	22.0	0.03	0.6	0.05	1.1	23.4	19.9	24.3	18.7	23.5	19.5	24.4	18.2
22	41314	18.9	18.8	0.07	1.3	0.07	1.3	22.0	15.8	21.9	16.0	22.3	15.4	22.2	15.7
23	41316	22.7	22.5	0.04	0.9	0.04	0.9	24.6	20.6	24.8	20.1	24.8	20.4	25.0	19.8
24	41480	25.5	25.3	0.03	0.8	0.03	0.7	27.1	23.9	27.1	23.7	27.3	23.7	27.3	23.6
Cp.		16.2	16.2		1.44		1.44	19.2	12.3	19.5	12.6	19.4	11.8	19.9	12.1

Results in the table above shows that the rate of temperature in January in the Arabian Peninsula vary from 7 ° C in the north (40356) to almost 26 ° C on the south coast of the Red Sea and Gulf of Aden (41140 - Jizan, 41480 - Aden), and if we consider temperature rare frequency of occurrences in 100 and 200 years, their lowest values may be about 3 ° C in the north, with the largest - about 27.5 ° C in the south-west. The spatial distribution of norms and standard deviation for the of air temperatures in January is shown in Figure 4.2.

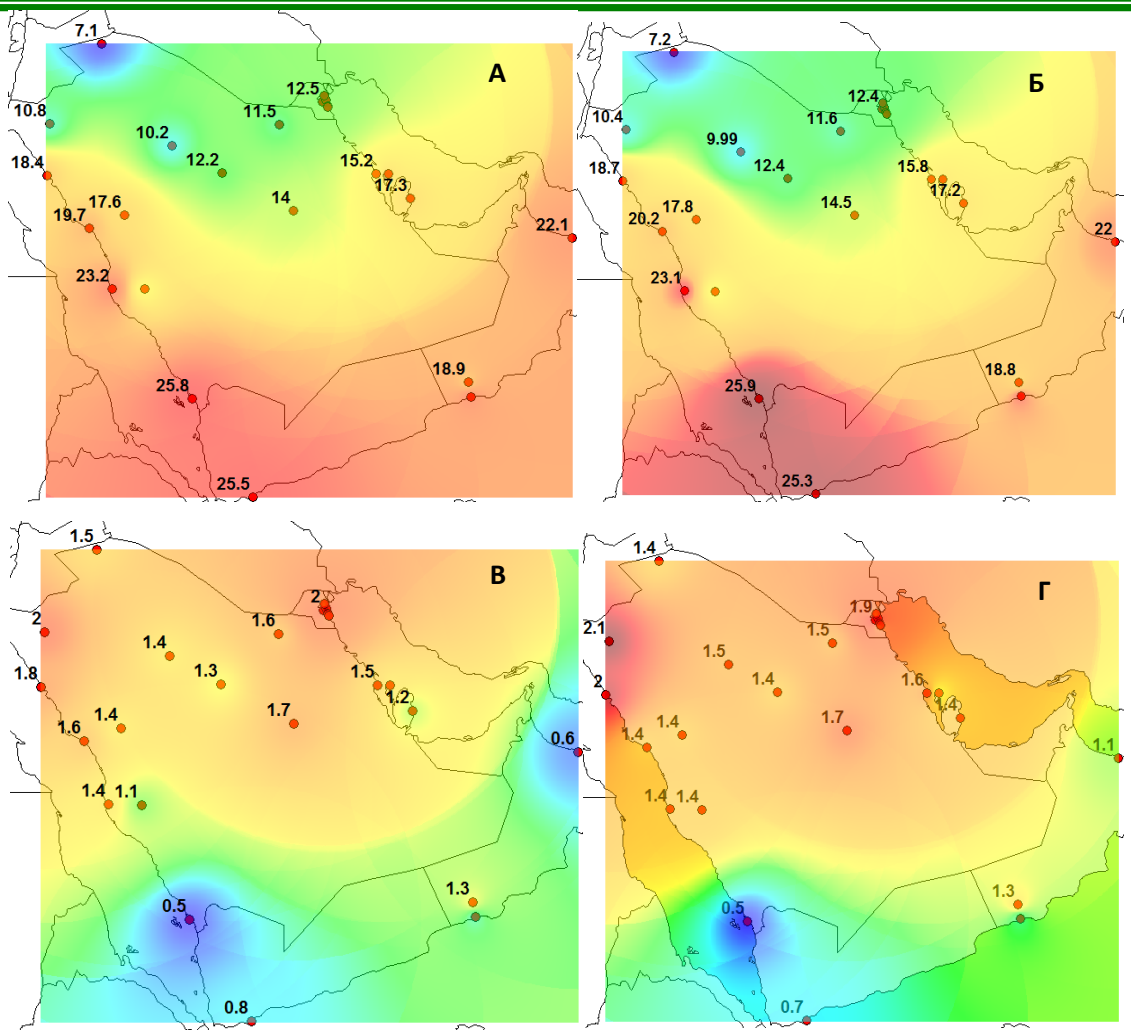

Figure 4.2.1 - Spatial variability of the parameters of the temperature distribution in January in the Arabian Peninsula (A, B - normal temperature for a period of WMO and the entire observation period, C, D - standard deviation for the period of the WMO and the entire observation period).

From the analysis and comparison of the spatial distributions of the parameters shown in Figure 4.2, the following results were obtained:

- General spatial structure changes remains almost the same as in the period of the WMO and the entire observation period and temperature norm characterizes the decrease from south to north, and the standard deviation to the contrary - they increase from south to north;
- For the entire period of observation the most effective, south-west area of the Arabian Peninsula have the highest temperatures up to 25-26 °C and the lowest - 7-9 ° C in the north-west;

- the same way to the standard deviation on spatial maxima and minima are also more pronounced in the compilation of data for the entire period than in a shorter period of WMO and more consistent spatial climate laws.

The calculated values of the average January temperature of rare event at 0.3-0.5 ° C, for both the calculated maximum and minimum obtained for the entire period of observations are systematically more than those obtained in the period of WMO. All these features must be considered in the preparation of the calculated climatic characteristics for construction and other types of design.

Evaluation of the stability of climatic norms for example temperature in January is shown in Table 4.2.2, which shows the average values for 4 consecutive 30-year time period, as well as the total change in the rate for the entire period, the difference between the maximum and the minimum of its value.

Results of the assessment of the stability of climatic norms for example temperature in January are shown in Table 4.2.2, which shows that the average values for 4 consecutive 30-year time period, as well as the total change of norms for the entire period, as the difference between the maximum and its minimum value.

Table 4.2.2. - Climatic norms for January temperature (° C) obtained for different periods.

Station code	Climatic norms				Changes in norms
	1901-1930	1931-1960	1961-1990	1982-2011	
40356	6.9	7.5	7.2	7.2	0.6
40373	11.3	11.5	11.5	11.8	0.5
40375	9.9	10.1	10.8	10.7	**0.9**
40394	9.5	9.8	10.2	10.2	**0.7**
40400	18.7	18.5	18.4	19.1	**0.7**
40405	11.7	12.5	12.2	12.6	**0.9**
40416	16.1	16.2	15.2	15.2	**1.0**
40430	18.1	17.6	17.6	17.8	0.5
40438	15.2	14.6	13.9	14.5	**1.3**
40439	19.9	20.3	19.7	20.8	**0.9**
40580	12.0	11.9	12.5	12.9	**1.0**

40581	12.6	12.5	12.8	12.5	0.3
40582	12.0	12.6	12.5	13.0	**1.0**
40583	12.3	12.7	12.8	13.1	**0.8**
40584	13.2	13.4	13.3	13.4	0.2
41020	22.6	22.9	23.2	23.1	0.6
41036	15.0	14.9	15.3	15.3	0.4
41140	26.1	25.9	25.8	25.9	0.3
41150	16.6	17.0	17.1	16.9	0.5
41170	16.7	16.6	17.3	17.4	**0.7**
41256		21.4	22.1	22.5	**0.9**
41314		18.6	18.8	18.7	0.2
41316	22.0	22.7	22.7	23.2	**1.2**
41480	24.6	25.6	25.5	25.7	**1.1**

The random error of the climatic norm (σ_{mean}) is given by:

$$\sigma_{mean} = \frac{\sigma}{\sqrt{n}}, \qquad (4.2.1)$$

where: σ –standard deviation of time series, *n* – observation (*n*=30), thus when σ=1-2°C, σ_{mean}= 0.2-0.4°C.

In table 4.2.2, bright color highlights values that clearly exceed twice its average random error, ie, changes constitute a 0.5-0.6 ° C and can therefore be considered significant. Analysis of the results of 24 stations shows that the tendency stated above, when their changes of norms is more random, 14 and graphs of changes of their norms are shown in Figure 4.2.2. From the graphs it follows that changes of mean values takes place not in all stations but occurs either in the ground or areas of high temperatures (weather station 41256 Sib, 41316 Salalah) or low (weather station 40375 Tabuk, Hail 40394), in the coastal and north areas. We can therefore assume that the central part of the Arabian Peninsula has a more stable rate of January temperatures than the other areas.

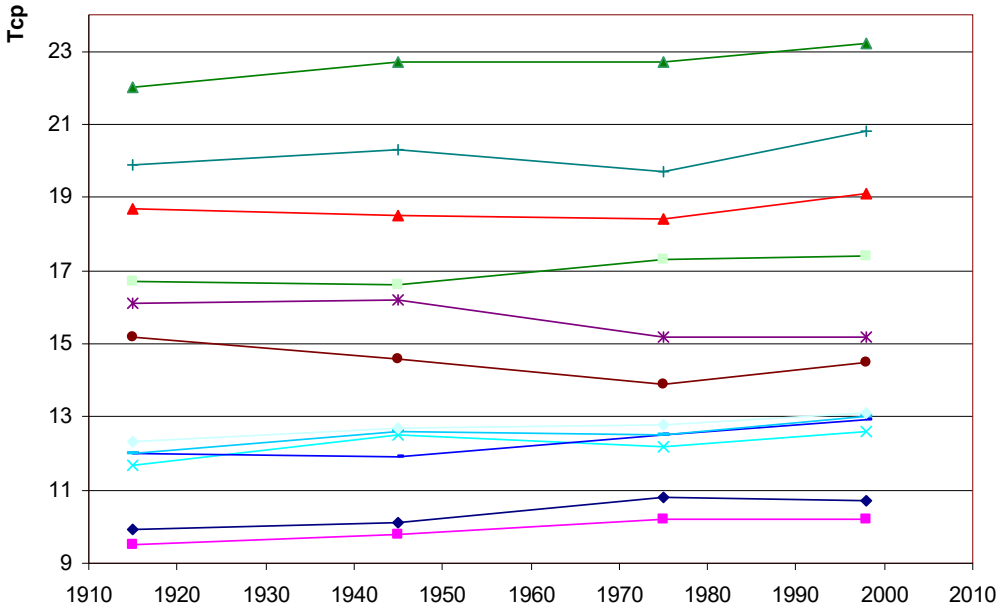

Figure 4.2.2 - Significant changes in climatic norms of January temperature at weather stations in the Arabian Peninsula.

Similar calculations were performed for temperatures in July, the month with highest and the least fixed temperature in the year, results are presented in Table 4.3.

Similar procedures were done for July maximum and minimum temperatures and the least stationary month, results are shown in table 4.2.3.

Table 4.2.3 - Parameters of normal and variability distribution and values of rare events which occurs 1 in 100 and 200 years for average monthly temperatures in July at the meteorological stations of the Arabian Peninsula.

№	Code	Norms for the period		Variability				1 in 100 years				1 in 200 years			
		WMO	Weights	WMO		Weights		WMO		Weights		WMO		Weights	
				Cv	σ	Cv	σ	1.0%	99%	1.0%	99%	0.5%	99.5%	0.5%	99.5%
1	40356	28.4	28.4	0.05	1.4	0.05	1.4	32.2	26.1	32.4	26.2	32.7	26.0	33.0	26.1
2	40373	36.1	36.0	0.02	0.7	0.03	1.1	38.3	34.6	39.1	33.9	38.5	34.4	39.5	33.7
3	40375	30.8	30.8	0.03	0.9	0.04	1.2	32.4	28.2	33.4	28.0	32.5	27.9	33.7	27.6
4	40394	31.9	32.7	0.04	1.3	0.7	2.3	36.3	29.8	39.5	29.3	37.0	29.7	40.5	29.2
5	40400	28.9	29.3	0.02	0.6	0.03	0.9	30.5	27.6	31.3	27.8	30.7	27.4	31.6	27.6
6	40405	34.3	34.3	0.03	1.0	0.04	1.4	36.8	32.7	37.2	31.2	37.1	32.5	37.5	30.9
7	40416	35.5	35.7	0.02	0.7	0.02	0.7	37.5	33.7	37.9	33.8	37.8	33.6	38.1	33.6
8	40430	35.8	35.6	0.03	1.1	0.04	1.4	38.0	33.6	39.0	33.0	38.2	33.3	39.4	32.8
9	40438	35.2	34.8	0.03	1.0	0.04	1.4	37.1	31.7	38.9	31.6	37.2	31.2	39.4	31.3
10	40439	31.4	31.6	0.03	0.9	0.04	1.3	33.9	29.4	35.1	29.0	34.1	29.2	35.5	28.8
11	40580	36.5	36.8	0.02	0.7	0.03	1.1	38.4	35.3	40.2	34.8	38.6	35.2	40.7	34.6
12	40581	37.0	37.1	0.03	1.1	0.03	1.1	39.9	35.4	39.9	35.3	40.4	35.3	40.3	35.1
13	40582	37.3	37.4	0.02	0.7	0.03	1.1	40.1	36.2	40.2	34.6	40.5	36.1	40.5	43.3
14	40583	36.6	36.3	0.03	1.1	0.04	1.4	38.1	32.5	39.4	33.4	38.1	31.8	39.7	33.0
15	40584	35.9	36.1	0.03	1.1	0.03	1.1	37.7	32.7	38.8	33.2	37.8	32.2	39.0	32.8
16	41020	32.1	32.0	0.02	0.6	0.04	1.3	33.7	31.0	34.5	28.8	33.9	30.9	34.7	28.3
17	41036	28.5	28.1	0.03	0.8	0.04	1.1	30.5	26.1	30.5	24.8	30.6	25.8	30.7	24.3
18	41140	33.3	33.4	0.02	0.6	0.02	0.6	34.8	31.1	34.7	31.1	34.9	30.8	34.8	30.7
19	41150	34.0	33.7	0.01	0.3	0.03	1.0	35.3	33.2	36.0	31.9	35.5	33.2	36.2	31.7
20	41170	35.4	35.4	0.02	0.7	0.02	0.7	37.4	34.6	37.3	33.5	37.8	34.6	37.5	33.3
21	41256	27.6	27.6	0.03	0.8	0.03	0.8	30.0	25.5	29.6	25.2	30.3	25.3	29.7	24.9
22	41314	29.7	30.1	0.04	1.2	0.04	1.2	33.8	27.8	33.1	27.4	34.4	27.7	33.4	27.2
23	41316	26.4	25.8	0.04	1.0	0.04	1.0	29.4	24.4	28.1	23.0	29.8	24.2	28.3	22.6
24	41480	32.4	31.7	0.02	0.6	0.03	0.9	34.5	30.9	33.8	29.5	34.8	30.8	34.0	29.2
ср		32.9	32.9		0.87		1.15	35.3	31.0	35.8	30.5	35.6	30.8	36.2	30.5

From the table above, the norm temperature change on the peninsula in July from 26-27 ° C at meteorological stations 41316 (Salalah), 41170 (Doha), 40400 (Al Wajh), located on the coast to 37°C weather station 40581 (Chuvalo) , 40582 (Kuwait), located in the desert. The spatial

temperature gradient norm is 2 times lower than in the winter and is about 10 °C. Temperatures of rare events, 1 in 100 and 200 years, can reach temperature of more than 40 °C. July temperature variability ranges from 0.3 ° C in Bahrain and can reach to 1.4 ° C in the north of the Peninsula. And for the shorter period of the WMO average on the territory, variability is lower than 0.9 °C for the entire period of observation that is equal to 1.1 °C. Here it may be noted that in January the natural variation of the temperature is even higher, averaging 1.4 ° C over the period both WMO and the entire observation period. Spatial distribution norms of temperatures in July and standard deviation are shown in Fig.4.2.3.

Overall territorial patterns of temperatures norms lie in the fact that the lowest values observed in the south-east and north-west, and the maximum - in the central part of the peninsula, and especially near the Persian Gulf. Natural variability the smallest in the south of the peninsula, while the highest - in the central and northern parts.

On the average on territory of the norms for the period of the WMO and the entire observation period are almost identical and constitute 32.9 ° C. The greatest differences at individual stations reach 0.7 ° C in one or another direction. The temperature for the period of WMO is higher than for the overall period mainly at the coastal stations, and below - within the peninsula, in general, this is not a consistent pattern. Results on the evaluation of stability of climatic norms are given in Table 4.2.4 in July.

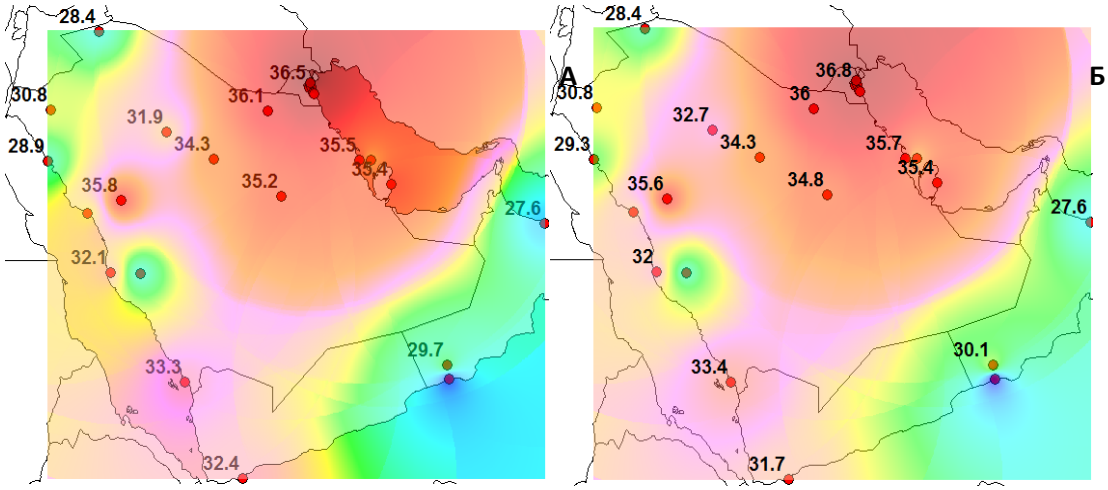

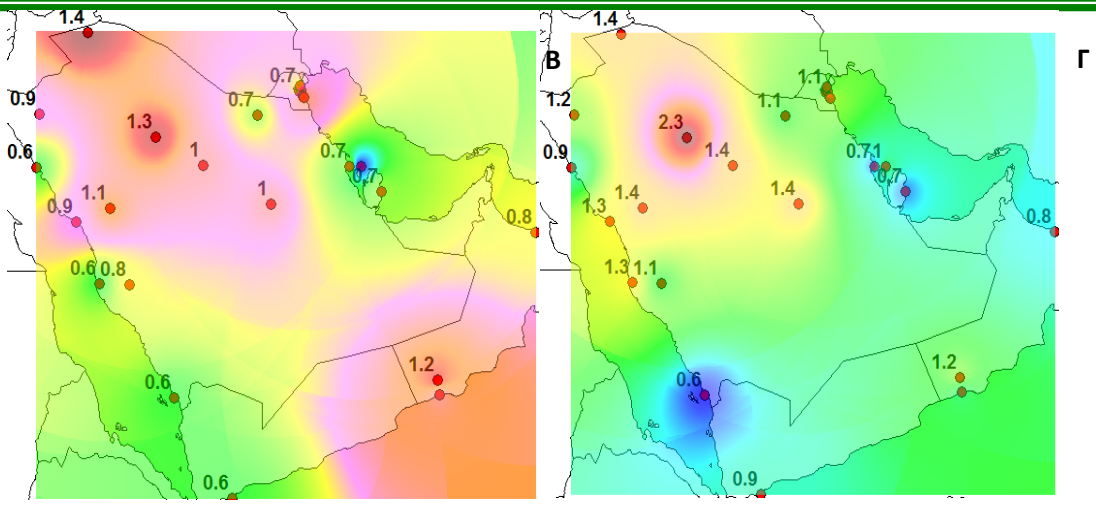

Figure 4.2.3 - Spatial variability of the parameters of the July temperature distribution in the Arabian Peninsula (A, B - normal temperature for a period of WMO and the entire observation period, C, D - standard deviation for the period of WMO and the entire observation period).

Table 4.2.4 - Climate July norms temperature (° C) obtained for different periods

Station code	Climatic norms				Changes in norms
	1901-1930	1931-1960	1961-1990	1982-2011	
40356	27.8	28.0	28.4	29.4	**+1.6**
40373	35.4	35.6	36.1	36.7	**+1.3**
40375	30.5	30.6	30.8	31.3	**+0.8**
40394	34.0	32.8	31.9	32.4	**-1.6**
40400	29.2	29.2	28.9	29.7	**+0.8**
40405	33.9	33.8	34.3	35.1	**+1.3**
40416		35.8	35.5	36.1	0.6
40430	33.7	34.8	35.8	36.4	**+2.7**
40438	33.5	33.9	35.2	36.4	**+2.9**
40439	31.3	31.1	31.4	32.8	**+1.7**
40580	37.0	36.6	36.5	37.3	**+0.8**
40581	36.5	36.9	37.0	37.9	**+1.4**
40582	37.2	36.6	37.7	38.7	**+2.1**
40583	36.1	35.7	36.6	37.1	**+1.4**
40584	36.6	36.3	35.9	35.7	**-0.9**
41020		31.0	32.1	32.7	**+1.7**
41036	27.4	27.6	28.5	28.8	**+1.4**

Station code	Climatic norms				Changes in norms
	1901-1930	1931-1960	1961-1990	1982-2011	
41140		33.3	33.3	33.5	0.2
41150	33.0	33.5	34.0	34.5	**+1.5**
41170	35.1	35.0	35.4	36.0	**+1.0**
41256	27.7	27.7	27.6	27.2	-0.5
41314	30.5	30.6	29.7	29.6	**-1.0**
41316	25.1	25.7	26.4	26.1	**+1.3**
41480	31.2	31.7	32.4	32.6	**+1.4**

If we assume that the maximum random error of the mean value is about the same as in January, the significant changes in norms of the random errors of its calculation will be nearly the same in all weather stations and in the majority of cases July temperatures norms is rising ("-" sign in the Table 4.4 indicates a decrease in the norm, "+" - its magnification). And the greatest increase in norms to 3.1 ° C occurs in the center of the peninsula and the Persian Gulf, where temperatures are already very high.

Unlike norms, standard deviations for the entire WMO period of observation period in the average by 0.9 ° C and 1.2 ° C (Table 4.3) that leads to a difference in the calculated temperature of rarely occurring events of 0.3-0.6 ° C and calculated maxima for the entire period of observation is always greater than the period of WMO and lows behave differently and differ by only 0.3 ° C.

Similar investigations of spatial and temporal changes in climatic norms of air temperature, their variability and calculated values of rare events were performed for other months of the year. Figure 4.2.4 shows the spatial patterns of norms temperatures obtained for the entire observation period for all months. The analysis of results shows that winter highest temperatures occur in southern costal of the Arabian Peninsula, especially in the south-west. Since the spring areas of maximum temperatures begin to shift from the southwest to the center and east of the Peninsula, and by August - September reached the Gulf coast, and then, starting in October again shifted to the southwest, reaching their peak in January - February.

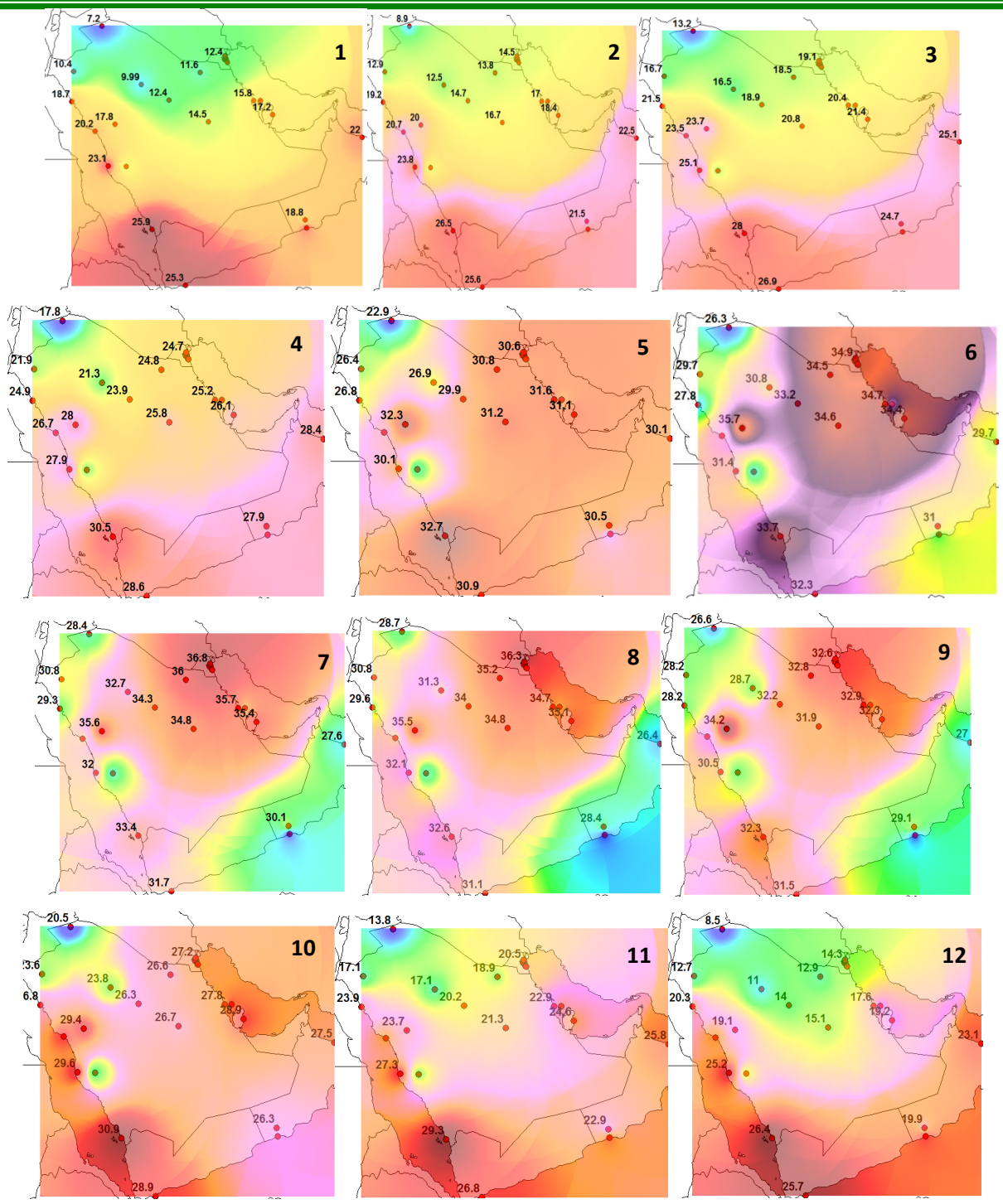

Figure 4.2.4 - Spatial variability average temperatures norms in the Arabian Peninsula during the entire observation period (the number in the figure corresponds to the number of calendar months).

Spatial-temporal analysis of natural variation found that:

- Variability of long-term fluctuations in air temperature in the cold season is smallest in the south and the largest in the center and north, and changes in the across the country 4 times: from about 0.5 ° C to 2.0 ° C, and a little more;

- Variability of long-term fluctuations in air temperature in the warm season also shows the same tendency, smallest in the southwest, and the largest in the center and north, but changes in the territory less than in winter (approximately 2 times and not 4): from 0.6 ° C to 1.3 ° C.
- Between climatic normal (Tmean) and the calculated temperature of rare events which occurs 1 in 100 years (T1%) (quantile of the distribution) for temperatures in January, the following territorial dependence of the form% = TP: b1Tsr + b0:

$$\text{All period } T1_{1\%} = 0.897\ T1_{mean} + 4.9 \quad R=0.99 \qquad (4.17)$$

$$\text{WMO period } T1_{1\%} = 0.883\ T1_{mean} + 4.9 \quad R=0.99 \qquad (4.18)$$

$$\text{All period } T1_{99\%} = 1.138\ T1_{mean} - 5.9 \quad R=0.99 \qquad (4.19)$$

$$\text{WMO period } T1_{99\%} = 1.171\ T1_{mean} - 6.6 \quad R=0.98 \qquad (4.20)$$

For the remaining months and frequency of occurrences of 1 in 100 years (P = provision of 1% for maximum values and 99% - for a minimum) and 1 in 200 years (P = supply of 0.5% for the maximum values, and 99.5% - for minimum), spatial coefficients b1 and b0 dependency and correlation coefficients R are given in Table 4.2.5.

Table 4.2.5 – Spatial coefficients equations to determine the climatic characteristics for calculated temperatures in the Arabian Peninsula.

Mon	Prob.once in	Maximum (P=1%, 0.5%)						Minimum (P=99%, 99.5%)					
		All Period			Period WMO			All Period			Period WMO		
		b1	b0	R	b1	b0	R	b1	b0	R	b1	b0	R
1	100	0.897	4.9	0.99	0.883	4.9	0.99	1.138	-5.9	0.99	1.172	-6.6	0.98
	200	0.889	5.4	0.99	0.876	5.2	0.98	1.155	-6.6	0.99	1.195	-7.5	0.98
2	100	0.905	5.5	0.96	0.840	6.5	0.97	1.096	-5.4	0.98	1.194	-7.1	0.99
	200	0.896	6.0	0.94	0.830	7.0	0.96	1.108	-6.0	0.98	1.022	-4.8	0.92
3	100	0.799	7.6	0.98	0.874	5.5	0.99	1.150	-6.2	0.98	1.158	-6.4	0.99
	200	0.775	8.5	0.97	0.863	6.0	0.98	1.169	-6.9	0.98	1.178	-7.1	0.98
4	100	0.795	8.6	0.95	0.713	10.1	0.88	1.143	-6.9	0.96	1.093	-5.1	0.96
	200	0.772	9.5	0.94	0.661	11.7	0.82	1.158	-7.6	0.94	1.090	-5.3	0.95

Mon	Prob.once in	Maximum (P=1%, 0.5%)						Minimum (P=99%, 99.5%)					
		All Period			Period WMO			All Period			Period WMO		
		b1	b0	R	b1	b0	R	b1	b0	R	b1	b0	R
5	100	0.994	3.3	0.93	0.989	-2.5	0.97	0.963	-2.1	0.90	0.935	-1.0	0.92
	200	0.986	3.9	0.92	0.984	2.8	0.96	0.950	-2.0	0.87	0.975	-2.6	0.91
6	100	1.074	0.7	0.93	0.915	4.8	0.96	0.869	1.3	0.92	0.908	0.8	0.96
	200	1.078	0.9	0.91	0.898	5.6	0.95	0.858	1.4	0.91	0.880	1.4	0.94
7	100	1.036	1.7	0.96	0.925	4.8	0.97	1.022	-3.2	0.99	1.003	-2.1	0.97
	200	1.043	1.8	0.94	0.914	5.4	0.96	1.180	-8.4	0.91	0.996	-2.0	0.96
8	100	1.125	-0.8	0.96	0.970	3.3	0.96	0.943	-1.2	0.94	1.002	-2.4	0.96
	200	1.148	-1.2	0.96	0.956	4.0	0.94	0.945	-1.6	0.92	0.999	-2.5	0.95
9	100	0.964	4.3	0.91	0.910	5.0	0.95	0.903	0.05	0.93	0.942	-0.6	0.95
	200	0.950	5.1	0.89	0.896	5.6	0.94	0.873	0.7	0.90	0.925	-0.3	0.93
10	100	0.927	4.9	0.91	0.949	3.7	0.95	1.047	-4.4	0.87	1.097	-5.5	0.94
	200	0.934	4.9	0.90	0.941	4.2	0.93	1.076	-5.6	0.87	1.117	-6.4	0.92
11	100	0.894	5.5	0.94	0.926	3.9	0.97	1.170	-6.7	0.99	1.307	-10.	0.99
	200	0.887	6.1	0.92	0.879	5.3	0.98	1.191	-7.5	0.98	1.342	-11.	0.98
12	100	0.817	7.0	0.98	0.852	5.6	0.98	1.196	-6.9	0.99	1.164	-6.2	0.99
	200	0.801	7.7	0.97	0.840	6.2	0.97	1.217	-7.6	0.99	1.186	-7.0	0.99

Table 4.2.5 indicates that the spatial relationship between the mean temperature values and the rarely events is very close and in most cases the correlation coefficients greater than 0.9. Moreover, in the months of cold period, the correlation coefficient is above and often reaches values of 0.99.

The resulting spatial dependence are of great practical importance for climate applications, as in one hand they allow us to obtain estimates of climatic characteristics of rare events in the 100 and 200 years for the considered stations, and on the other hand, based on spatial interpolation norms (Figure 4.5), and these spatial dependence using regression equation, climatic characteristic at any point can be obtained in the Arabian Peninsula, where observations are missing.

4.4. Spatial variability of the design characteristics (mean, standard deviation, quintiles) of annual temperature and parameters of seasonal function and other characteristics (maxima and minima) on the intra-annual scale in Yemen and nearby area.

The average annual temperature, results from chapter 3, are the most non-stationary characteristic of the, but at the same time climatic norms calculated over a period of WMO and the entire observation period (Table 4.3.1) are virtually identical in spatial, average values in both cases is 25.4 °C. Between norms for the entire period of observation (Y) and the period of WMO (X) exists linear relationship with a correlation coefficient R = 0.996 and with coefficients b1 = 0.996, i.e., hardly differs from one line or a bisector of the right angle, and b0 = 0.14, i.e. almost close to 0.

Table 4.3.1 Parameters of normal and variability distributions and frequency of 100 and 200 years for the average annual temperature at the meteorological stations of the Arabian Peninsula.

№	Code	Norms		Variability				1 in 100				1 in 200			
		WMO	Weight	WMO		Weight		WMO		Weight		WMO		Weight	
				Cv	σ	Cv	σ	1.0%	99%	1.0%	99%	0.5%	99.5%	0.5%	99.5%
1	40356	18.5	18.4	0.03	0.5	0.04	0.7	19.9	16.8	20.5	16.6	20.0	16.5	20.7	16.5
2	40373	24.7	24.8	0.03	0.7	0.03	0.7	25.9	22.6	26.5	22.9	26.0	22.3	26.7	22.7
3	40375	21.7	21.8	0.03	0.6	0.08	1.7	22.9	19.5	23.1	20.3	23.0	19.8	23.2	20.1
4	40394	21.9	21.9	0.02	0.4	0.03	0.6	23.5	21.0	24.0	20.3	23.7	20.9	24.3	20.2
5	40400	24.5	24.7	0.02	0.5	0.02	0.5	25.8	23.5	26.0	23.4	25.9	23.4	26.1	23.3
6	40405	23.6	23.9	0.03	0.7	0.03	0.7	25.2	22.2	25.8	21.9	25.4	22.1	26.0	21.7
7	40416	26.0	26.5	0.02	0.5	0.03	0.8	27.5	24.7	28.4	24.8	27.7	24.5	28.6	24.6
8	40430	27.9	28.1	0.02	0.5	0.02	0.5	28.9	26.2	29.7	26.2	29.0	26.0	29.8	26.0
9	40438	25.6	25.7	0.03	0.7	0.04	1.0	27.3	23.9	28.6	23.6	27.1	23.7	28.9	23.4
10	40439	26.5	27.0	0.02	0.5	0.04	1.1	27.9	25.1	29.7	25.2	28.1	25.0	30.1	25.0
11	40580	25.3	25.3	0.02	0.5	0.03	0.7	26.6	24.0	27.1	23.7	26.8	23.9	27.3	23.6
12	40581	26.0	25.9	0.02	0.5	0.03	0.7	27.5	24.7	27.9	24.4	27.6	24.5	28.2	24.2
13	40582	25.7	25.6	0.02	0.5	0.03	0.8	26.9	24.3	27.4	24.1	27.0	24.1	27.6	24.0
14	40583	25.7	25.5	0.02	0.5	0.03	0.7	27.2	24.3	27.7	23.7	27.3	24.1	28.0	23.5

№	Code	Norms		Variability				1 in 100				1 in 200			
		WMO	Weight	WMO		Weight		WMO		Weight		WMO		Weight	
				Cv	σ	Cv	σ	1.0%	99%	1.0%	99%	0.5%	99.5%	0.5%	99.5%
15	40584	25.4	25.3	0.02	0.5	0.03	0.7	26.8	24.3	26.9	23.6	27.0	24.2	27.1	23.4
16	41020	28.0	28.2	0.01	0.3	0.02	0.5	29.0	27.1	29.7	27.2	29.1	27.0	29.8	27.1
17	41036	22.3	22.5	0.02	0.4	0.02	0.4	23.4	21.3	24.0	21.2	23.5	21.1	24.2	21.1
18	41140	30.1	30.2	0.01	0.3	0.01	0.3	30.7	29.5	31.0	29.4	30.9	29.5	31.1	29.4
19	41150	26.5	26.2	0.02	0.5	0.02	0.5	27.8	25.5	28.0	24.9	27.9	25.4	28.2	24.8
20	41170	27.1	26.7	0.02	0.5	0.04	1.1	28.2	25.8	29.3	24.3	28.3	25.6	29.5	24.0
21	41256	26.3	26.3	0.01	0.3	0.01	0.3	27.0	25.5	27.1	25.6	27.1	25.4	27.2	25.5
22	41314	25.7	25.7	0.02	0.5	0.02	0.5	26.8	24.7	26.9	24.3	26.9	24.6	27.0	24.2
23	41316	25.7	25.9	0.01	0.2	0.02	0.5	26.8	25.1	27.2	25.0	27.0	25.0	27.3	25.1
24	41480	28.9	28.7	0.01	0.03	0.02	0.6	29.6	28.2	29.9	27.8	29.6	28.2	30.0	27.6
Cp.		25.4	25.4		0.46		0.69	26.6	24.2	27.2	23.9	26.7	24.0	27.4	23.8

Between the other parameters of Table 4.3.1, for the period defined by WMO and the entire observation period, the following territorial relationship:

$$\sigma \text{ (weight)} = 0.909\ \sigma \text{ (WMO)} + 0.27 \quad R=0.46 \qquad (4.21)$$

$$T100max \text{ (weight)} = 1.03\ T100max \text{ (WMO)} - 0.21 \quad R=0.98 \qquad (4.22)$$

$$T100min \text{ (weight)} = 0.970\ T100min \text{ (WMO)} + 0.49 \quad R=0.99 \qquad (4.23)$$

$$T200max \text{ (weight)} = 1.02\ T200max \text{ (WMO)} - 0.20 \quad R=0.98 \qquad (4.24)$$

$$T200min \text{ (weight)} = 0.969\ T200min \text{ (WMO)} + 0.49 \quad R=0.99\ , \qquad (4.25)$$

where σ (weight), σ (WMO) – standard deviations for the entire observation period and the period of the WMO; T100max, T100min - the calculated values of mean annual temperature repeatedly 1 in 100 years for a maximum of (provision of 1%) and minimum (security 99%); T200max, T200min - the calculated values of mean annual temperature repeatedly 1 in 200 years for a maximum of (provision 0.5%) and minimum (99.5% availability).

From the analysis of regional average values for each parameter (Table 4.6) and received regional dependencies (4.21) - (4.25), we can conclude that the standard deviation for the entire observation period was 1.5 times more than in the period of the WMO. The calculated values of the maxima of rare events obtained on the entire observation period by an average of 0.3-0.4 ° C higher than those obtained for the period of WMO, at the same time lows 0.4-0.6 °C below. This fact should be taken into account in building design and use the estimated values of annual temperatures obtained for the entire observation period, as they give more collect values of calculated climatic characteristics.

The spatial distribution of norms and standard deviations of the average annual temperature in the Arabian Peninsula is shown in Fig.4.6 from which it follows that the norms temperature distribution obtained by averaging the data for different periods do not differ and tend to decrease from the south to the north-west. At the same time, the spatial distribution of mean-square deviations differs significantly over. If during the period of the WMO observed at least one significant variability in the southwest and almost homogeneous field standard deviations of all the central and northern parts of the peninsula, over the entire period of observation field in the northern part of the peninsula is already heterogeneous, and more homogeneous in the southern part of the peninsula with small variation.

The calculated values of norms and variability of the basic parameters for the coefficients of the seasonal changes in temperature are given in Table. 4.3.2.

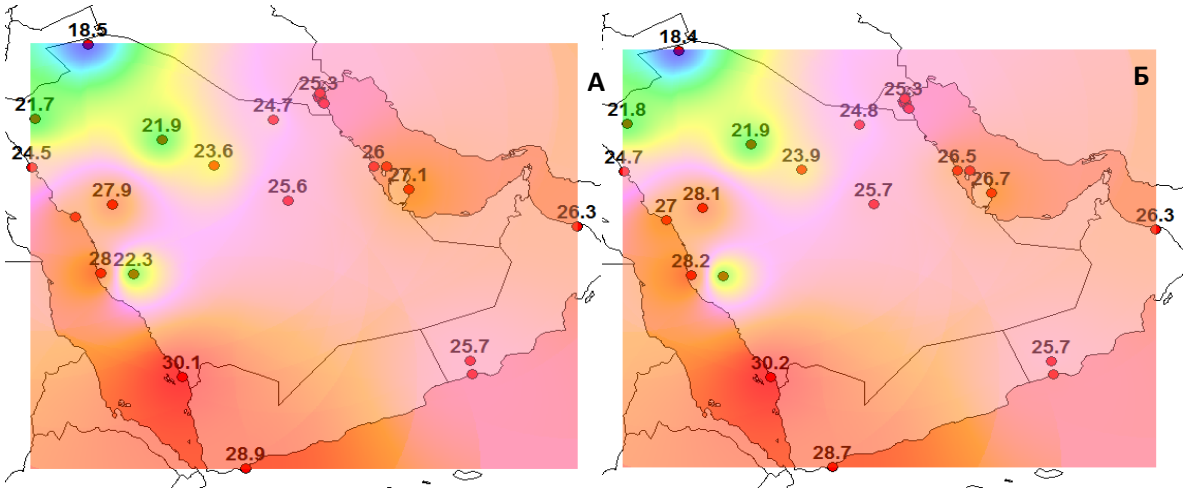

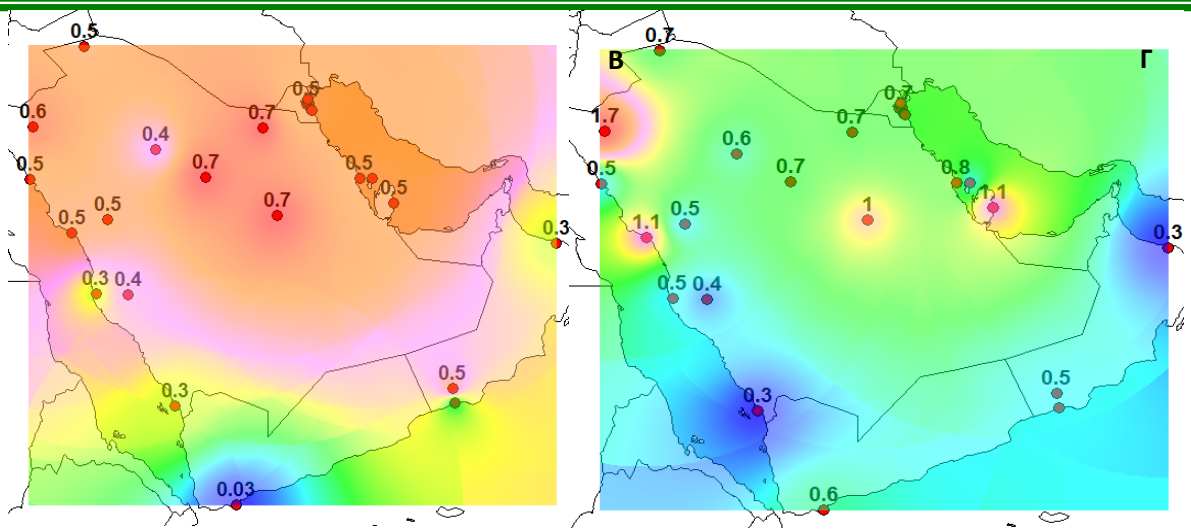

Figure 4.3.1 - Spatial variability parameters of the distribution of average annual temperatures in the Arabian Peninsula (A, B - normal temperature for a period of WMO and the entire observation period, C, D - standard deviation for the period of the WMO and the entire observation period).

Table 4.3.2 - The rate variability parameters and function of seasonal changes in weather stations of the Arabian Peninsula.

№	Code	B1						B0				Se			
		mean		variability											
		WMO	Weight	WMO		weight		normal		σ		normal		Σ	
				Cv	σ	Cv	σ	WMO	Weight	WMO	Weight	WMO	Weight	WMO	Weight
1	40356	0.9	1.0	0.05	0.04	0.07	0.07	-0.01	-0.07	0.7	1.4	1.18	1.18	0.27	0.3
2	40373	0.9	0.9	0.06	0.05	0.06	0.05	0.2	-0.04	1.4	1.4	1.2	1.2	0.3	0.3
3	40375	0.9	1.0	0.05	0.04	0.1	0.1	0.2	-0.09	1.1	1.7	0.99	1.2	0.26	0.4
4	40394	1.0	0.9	0.06	0.06	0.06	0.05	0.5	0.05	1.3	1.3	1.1	1.1	0.3	0.3
5	40400	1.0	1.0	0.07	0.07	0.1	0.1	-0.4	0.003	2.0	2.5	0.81	0.88	0.3	0.32
6	40405	1.0	1.0	0.06	0.06	0.06	0.06	-0.14	-0.08	1.7	1.8	1.1	1.2	0.3	0.4
7	40416	0.9	0.9	0.06	0.05	0.05	0.4	-0.36	-0.22	2.0	1.7	0.8	1.0	0.2	0.4
8	40430	1.0	0.9	0.06	0.06	0.07	0.06	-0.04	-0.14	0.2	2.2	0.8	1.0	0.2	0.3
9	40438	1.0	1.0	0.06	0.06	0.8	0.08	-0.74	-0.35	1.8	2.0	1.0	1.1	0.3	0.33
10	40439	0.9	0.9	0.09	0.08	0.1	0.09	-0.11	0.12	2.5	3.4	0.8	0.9	0.2	0.3
11	40580	0.9	1.0	0.05	0.04	0.05	0.05	0.34	0.01	1.7	1.3	1.0	1.0	0.3	0.3
12	40581	1.0	0.9	0.06	0.06	0.06	0.05	0.04	0.03	1.8	1.7	1.0	1.1	0.44	0.33
13	40582	1.0	1.0	0.05	0.05	0.05	0.05	0.03	0.04	1.4	1.2	0.9	0.9	0.27	0.3
14	40583	1.0	1.0	0.05	0.05	0.06	0.06	-0.17	-0.03	1.8	1.7	1.2	1.2	0.4	0.4
15	40584	0.9	1.0	0.06	0.05	0.06	0.06	0.05	0.005	1.8	1.8	0.9	1.1	0.27	0.33
16	41020	0.9	1.0	0.1	0.09	0.1	0.1	0.7	0.005	3.0	2.6	0.7	0.9	0.3	0.4
17	41036	1.0	1.0	0.05	0.05	0.06	0.06	-0.08	-0.02	1.2	1.8	0.8	0.9	0.2	0.4

№	Code	B1						B0				Se			
		mean		variability											
		WMO	Weight	WMO		weight		normal		σ		normal		Σ	
				Cv	σ	Cv	σ	WMO	Weight	WMO	Weight	WMO	Weight	WMO	Weight
18	41140	1.0	1.0	0.06	0.06	0.07	0.07	-0.23	-0.01	2.0	2.1	0.5	0.5	0.2	0.2
19	41150	1.0	1.0	0.06	0.06	0.06	0.06	0.06	-0.04	1.9	1.5	0.7	0.6	0.3	0.2
20	41170	0.9	0.9	0.06	0.05	0.06	0.05	0.4	0.07	1.5	1.6	0.7	0.9	0.2	0.3
21	41256	1.0	1.0	0.08	0.08	0.1	0.1	-0.49	-0.04	2.4	3.2	0.5	0.6	0.2	0.2
22	41314	1.0	0.9	0.1	0.1	0.1	0.09	-0.21	-0.01	2.6	4.2	1.0	0.9	0.3	0.3
23	41316	1.0	1.0	0.1	0.1	0.1	0.1	-0.25	0.007	3.2	2.7	0.6	0.6	0.2	0.2
24	41480	1.0	1.0	0.05	0.05	0.08	0.08	-1.22	-0.04	1.7	2.3	0.6	0.4	0.2	0.1
Mean.		1.0	1.0	0.1	0.1	0.1	0.1	-0.08	-0.04	1.8	2.0	0.9	0.9	0.3	0.3

From table 4.3.2, it can be seen that the mean values of the spatial coefficients B1 are equal to 1, i.e. are both stationary in time and unbiased. Spatial average coefficient values B0 have slight negative bias to the time and area in two different cases, at the same time the parameter Se is stationary over time and equal to the average 0.9 ° C.

Spatial distribution of coefficients B1, B0 and Se parameter in Figure 4.3.2, for the entire observation period. The figure shows that the spatial distribution of B1 and B0 are practically homogeneous, and some of their local minimum occurs for B1 in the north, in the Gulf and in the south, and the coefficient B0 - in the central part of the peninsula. Distribution parameter Se has spatial patterns of growth from the south to the north of the peninsula, ie intensity macro synoptic processes in the north and center of the peninsula, which correspond to the continental climate, more than in the south and in coastal areas.

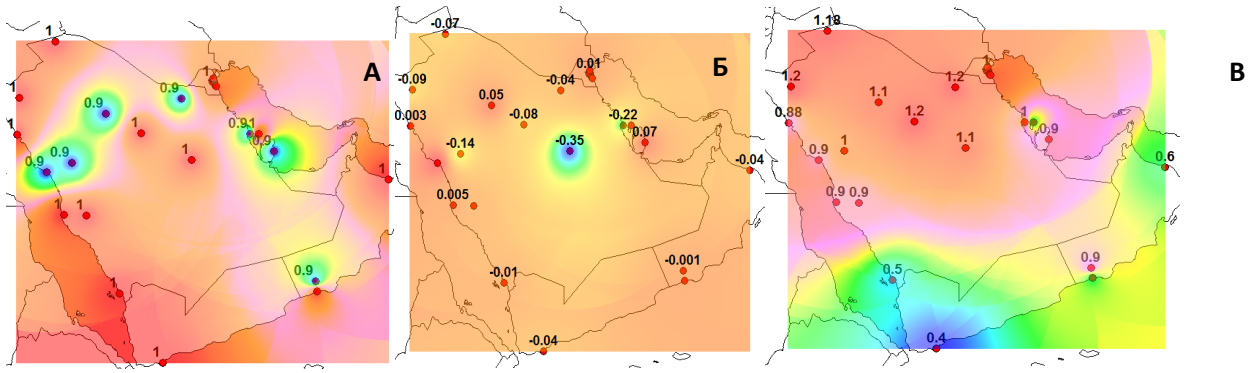

Figure 4.3.2- Spatial variability of coefficients intra-annual fluctuations norms, where A - the coefficient B1, B - coefficient B0, B - Se parameter for the entire observation period.

Between the parameters of the distribution, the following territorial relationship:

Se_{mean} (weight)= 0.987 Se_{mean} (BMO) +0.07 R=0.89 (4.26)

Se_{mean} (weight)= 0.267 σ_{Se} (weight) +0.055 R=0.80 (4.27)

Se_{cp} (WMO)= 0.202 σ_{Se} (WMO) +0.092 R=0.66 (4.28)

Where Se - average value Se, σ Se - standard deviation parameter Se.

Formula (4.26) - (4.28) shows that the norms of Se parameter for the entire period and the period of the WMO are closely related and have standards displacement and also exist a linear relationship between norms and standard deviation, but for the entire observation period, this dependence is more effective than in the period WMO.

4.5. Spatial variability of the design characteristics (mean, standard deviation, quintiles) of precipitation (monthly, seasonal, annual Yemen and neighboring area.

In accordance with the findings in chapter 3, rainfall is almost stationary climatic characteristics and therefore it's better to determine the climatic norm and quantile probability distribution of rare events through the ranks given to the long-term time series. Example of calculation of parameters and quantiles for precipitation in January is shown in Table 4.4.1.

Table 4.4.1. - Parameters of normal and variability distributions and rare events in 100 and 200 years for precipitation in January at the meteorological stations in the Arabian Peninsula.

№	Code	Norms		Variability				1 in 100 years				1 in 200 years			
		WMO	Weight	WMO		Weight		WMO		Weight		WMO		Weight	
				Cv	Σ	Cv	σ	1.0%	99%	1.0%	99%	0.5%	99.5%	0.5%	99.5%
1	40375	4.9	8.9	1.2	5.9	1.0	8.9	26.2	0	42.9	0.0	30.6	0	49.9	0.0
2	40400	2.7	5.3	1.8	4.9	1.5	7.9	23.6	0	38.3	0.0	28.8	0	45.7	0.0
3	40416	11.4	31.3	1.2	13.7	1.1	34.4	64.7	0	153	0	76.1	0	177	0
4	40430	10.2	13.9	1.6	16.3	1.2	16.7	74.8	0	78.6	0	89.5	0	92.3	0

№	Code	Norms		Variability				1 in 100 years				1 in 200 years			
		WMO	Weight	WMO		Weight		WMO		Weight		WMO		Weight	
				Cv	Σ	Cv	σ	1.0%	99%	1.0%	99%	0.5%	99.5%	0.5%	99.5%
5	40438	18.3	20.5	1.4	25.6	1.0	20.5	86.9	0	93.1	0	120	0	106	0
6	40439	14.1	16.6	1.2	17.0	1.1	18.3	83.2	0.5	86.1	2.2	89.4	0.5	101	2.1
7	40582	26.4	33.0	0.7	18.5	0.7	23.1	79.6	0	130	11.9	87.4	0	150	11.8
8	41024	15.3	25.5	1.5	22.9	1.3	33.1	108	0	157	0	129	0	186	0
9	41114	14.9	22.7	1.2	17.8	1.0	22.7	83.8	0	112	1.8	98.6	0	131	1.8
10	41140	17.3	28.5	1.3	22.5	1.2	34.2	109	1.0	167	4.9	130	1.0	198	4.9
11	41150	17.9	17.3	1.3	23.3	1.3	22.5	111	0	104	0	132	0	123	0
12	41168	11.8	25.2	1.7	20.0	1.2	30.2	96.5	0	142	0	117	0	168	0
13	41256	19.1	24.5	1.3	24.8	1.2	29.4	117	0	140	0	139	0	164	0
14	41258	34.8	75.3	1.1	38.2	1.1	82.8	177	0	379	0	206	0	441	0
15	41268	35.0	37.9	1.5	52.5	1.5	56.8	252	0	288	2.1	301	0	348	2.1
16	41314	1.2	1.9	1.2	1.4	1.7	3.2	6.6	0	17.0	0.5	7.7	0	21.6	0.5
17	41316	0.7	1.2	3.2	2.2	2.2	2.6	11.1	0	13.4	0	14.5	0	16.9	0
18	41443	9.4	7.5	0.5	4.7	0.6	4.3	22.0	0	19.8	0	23.5	0	21.5	0
19	41466	7.1	5.8	1.2	8.5	1.3	7.5	40.0	0	34.4	0	46.7	0	40.4	0
20	41467	5.0	6.9	1.7	8.5	1.2	8.3	40.7	0	39.6	0	49.0	0	46.3	0
21	41468	11.6	17.3	1.4	16.2	1.5	26.0	77.5	0	130	0	92.2	0	157	0
22	41469	24.7	30.4	1.2	29.6	1.2	36.4	136	0	167	1.9	160	0	197	1.8
23	41470	12.2	26.1	1.9	23.1	1.4	36.5	113	0.1	177	0	139	0.1	211	0
24	41471	9.9	12.9	2.1	20.7	1.3	16.7	101	0.03	79.6	0	126	0.03	93.9	0
25	41472	10.1	15.4	0.8	8.0	1.0	15.4	40.0	0	74.1	2.6	45.1	0	86.7	2.6
26	41474	6.6	14.6	1.0	6.6	0.8	11.7	29.9	0	57.5	0	34.0	0	64.9	0

№	Code	Norms		Variability				1 in 100 years				1 in 200 years			
		WMO	Weight	WMO		Weight		WMO		Weight		WMO		Weight	
				Cv	Σ	Cv	σ	1.0%	99%	1.0%	99%	0.5%	99.5%	0.5%	99.5%
27	41476	15.5	18.8	1.4	21.7	1.1	20.6	99.0	0	99.4	1.2	118	0	117	1.2
28	41478	21.3	34.2	1.2	25.5	0.9	31.0	110	0	122	0.1	126	0	132	0.1
29	41479	4.4	10.4	2.4	10.5	1.6	16.6	52.7	0	79.5	0	67.1	0	95.1	0
30	41480	10.4	8.2	1.2	12.5	1.4	11.5	57.8	0.6	54.1	0	68.2	0.6	64.5	0
31	41485	4.2	7.2	0.7	2.9	1.1	7.9	12.7	0	45.1	4.4	13.8	0	57.3	4.4
32	42801	26.4	31.1	0.7	18.4	0.5	15.5	79.5	0	75.3	0	87.3	0	81.1	0
33	40250	13.5	14.5	0.9	12.1	0.8	11.6	55.4	0	54.7	0	62.8	0	61.7	0
34	40310	7.1	10.9	1.2	8.5	0.9	9.8	39.1	0.6	42.9	0	46.0	0.3	48.6	0
35	40608	63.5	74.3	0.6	38.1	0.6	44.6	181	3.6	243	24.1	199	0.8	275	23.8
36	40621	68.0	81.5	1.0	68.0	0.8	65.2	355	21.4	349	28.6	419	21.4	408	28.6
37	40642	20.1	19.5	0.6	12.1	0.7	13.6	56.3	0	60.4	0	61.5	0	66.8	0
38	40650	28.3	28.2	0.6	17.0	0.7	19.7	76.7	3.5	96.8	0	84.3	2.4	108	0
Mean		16.7	22.6	1.3	18.5	1.1	23.0	86.5	0.8	112	2.3	102	0.7	130	2.2

From the table it can be noted that the average rainfall across the Peninsula for the entire observation period longer than the period of WMO, as well as standard deviations and quantiles, probabilities 1% and 0.5%. At the same time 99% quantile probability and 99.5% obtained for the entire observation period is higher than for the period of WMO. The following spatial relationship between parameters and quantiles for the period of WMO and for the entire period of observations:

$$P_{mean}\,(\text{weight}) = 1.194 P_{mean}(\text{BMO}) + 2.8 \quad R=0.92 \qquad (4.29)$$

$$\sigma\,(\text{weight}) = 1.113\sigma\,(\text{WMO}) + 2.6 \quad R=0.88 \qquad (4.30)$$

$$P_{1\%}\,(\text{weight}) = 1.135 P_{1\%}(\text{WMO}) + 13.4 \quad R=0.90 \qquad (4.31)$$

$$P._{0.5\%}\,(\text{weight}) = 1.123P_{0.5\%}(\text{WMO}) + 16.1 \quad R=0.89 \qquad (4.32)$$

Where: P_{mean}, $P_{1\%}$, $P_{0.5\%}$ - rainfall and maximum rainfall probability of 1 in 100 and 200 years.

Formula (4.29) - (4.32) are important for practical, because they allow the determination of the parameters and calculated of climatic characteristics of precipitation in the WMO long-term period. Effective spatial relationship between the minimum rainfall for the entire period and the period of WMO cannot be computed because more than half of the minimum estimated rainfall weather stations have 0 mm and the rest as high as 20-30 mm.

Thus, normal precipitation significantly vary in area: almost 1 mm to 70-80 mm. Spatial distribution of rainfall norms and standard deviations are shown in January Fig.4.4.1.

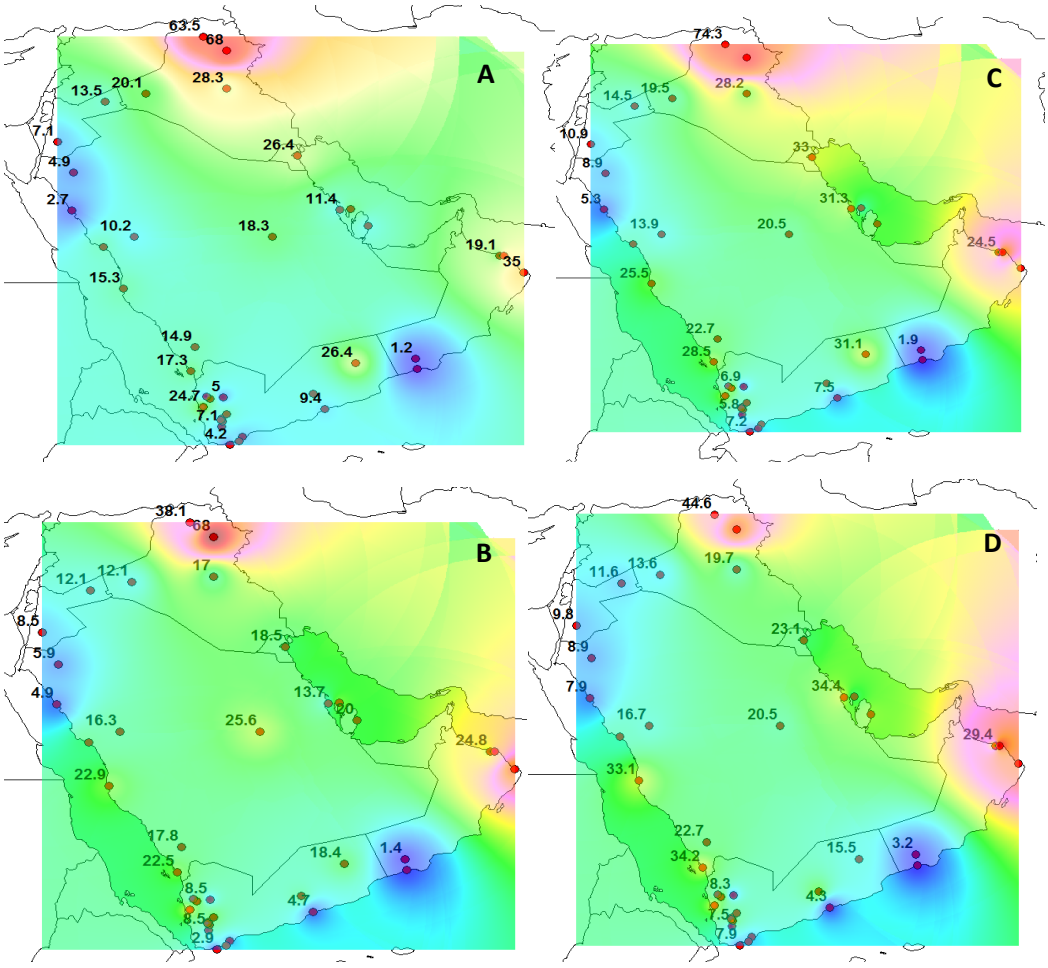

Figure 4.4.1 - Spatial distribution of January rainfall norms and standard deviations in the Arabian Peninsula (A, B - rainfall during the period of the WMO and the entire observation period, C, D - standard deviation for the period of the WMO and the entire observation period).

From the figure above, January rainfall and their standard deviations have a tendency to increase from south to north. This trend is more vivid for the parameters obtained for the period of WMO and for the entire period of observation depict maximum near the Persian Gulf.

Another example of determining climatic characteristics is given in Tabl.4.4.2 for August, which is the month with the highest precipitation in the year for the Arabian Peninsula.

Table 4.4.2 - Parameters of norms and variability distributions and probability of once in 100 and 200 years for precipitation in August at the meteorological stations in the Arabian Peninsula.

№	Station name	Norms		Variability				1 in 100 years				1 in 200 years			
		WMO	Weight	WMO		Weight		WMO		Weight		WMO		Weight	
				Cv	σ	Cv	σ	1.0%	99%	1.0%	99%	0.5%	99.5%	0.5%	99.5%
1	40394	0.4	0.6	2.3	0.9	2.3	1.4	4.8	0	6.8	0	6.1	0	8.7	0
2	41024	3.9	2.5	2.6	10.1	3.0	7.5	50.1	0	38.2	0	64.4	0	49.9	0
3	41114	41.9	49.8	0.6	25.1	0.6	29.8	129	3.2	142	5.6	143	1.9	157	3.8
4	41258	8.9	31.8	3.5	31.1	1.4	44.5	158	0	205	0	206	0	242	0
5	41268	4.5	5.2	2.3	10.3	2.4	12.5	59.2	0	62.3	0	76.0	0	79.6	0
6	41314	8.4	16.7	1.5	12.6	1.4	23.4	61.3	0.1	111	0	73.6	0.1	132	0
7	41316	24.4	26.7	0.6	14.6	0.5	13.3	69.1	5.8	69.7	4.7	76.7	5.3	76.4	3.7
8	41443	3.9	4.3	0.5	1.9	0.7	3.0	9.4	0	15.1	0	10.2	0	16.9	0
9	41466	74.4	72.4	0.4	30.0	0.4	29.0	171	13.2	162	12.0	185	9.5	174	7.7
10	41467	48.8	59.0	0.9	43.9	0.7	41.3	186	0	201	0	208	0	223	0
11	41468	25.8	41.1	1.0	25.8	0.9	37.0	117	0	176	0	134	0	201	0

№	Station name	Norms		Variability				1 in 100 years				1 in 200 years			
		WMO	Weight	WMO		Weight		WMO		Weight		WMO		Weight	
				Cv	σ	Cv	σ	1.0%	99%	1.0%	99%	0.5%	99.5%	0.5%	99.5%
12	41469	12.4	21.6	1.0	12.4	0.8	17.3	56.4	0	82.8	0	64.5	0	93.6	0
13	41470	157	172	0.3	47.1	0.3	51.6	266	55.6	337	82.1	277	45.2	362	77.6
14	41471	168	173	0.9	0.8	138	151	835	49.3	769	76.6	986	49.2	903	76.5
15	41472	271	270	0.5	135	0.5	135	755	70.7	711	60.1	873	65.4	782	51.8
16	41473	265	343	0.7	185	0.5	171	917	105	901	10.1	1050	105	979	0
17	41475	94.3	99.5	0.6	56.5	0.5	50	310	44.3	270	42.0	356	44.4	300	41.3
18	41476	65.9	81.2	0.4	26.4	0.4	32.5	129	0	162	14.8	135	0	172	8.8
19	41477	187	235	0.5	93.5	0.5	117	449	0	544	26.9	484	0	587	11.9
20	41478	122	162	0.5	61	0.5	81	287	11.1	401	30.4	310	3.1	437	23.9
21	41479	119	136	0.5	59.5	0.5	68	268	0	364	19.7	284	0	400	14.2
22	41480	4.6	2.4	0.9	4.1	1.7	4.1	16.4	0	18.9	0	18.1	0	22.7	0
23	41482	7.1	8.6	0.8	5.7	0.7	6.0	25.3	0	29.8	2.3	28.3	0	33.9	2.3
24	41483	83.2	111	0.8	66.5	0.6	66.6	294	0	287	0	329	0	311	0
25	41484	24.6	28.2	0.6	15.0	0.6	17.0	67.3	0	75.4	2.4	72.9	0	82.6	1.1
26	41485	9.6	17.3	1.0	9.6	0.8	13.8	41.6	0	60.9	0	46.8	0	86.3	0
Mean		70.6	83.4	1.0	37.9	6.2	47.1	220	13.7	238	14.9	250	12.6	266	12.4

From the table, the average rainfall across the Peninsula for the entire observation period is longer than the period of WMO, as well as standard deviations and quantiles, Probability of 1% and 0.5%, as in January. Received results of spatial dependence between parameters and quantiles for the period of WMO and for the entire period of observations:

$$P_{mean}\,(weight) = 1.131 P_{mean}(WMO) + 3.6 \quad R=0.99 \qquad (4.33)$$

$$\sigma\,(weight) = 0.860\sigma\,(WMO) + 14.5 \quad R=0.79 \qquad (4.34)$$

$$P_{1\%}\text{ (weight)} = 0.954P_{1\%}\text{(WMO)} + 28.2 \quad R=0.99 \tag{4.35}$$

$$P_{0.5\%}\text{ (weight)} = 0.913P_{0.5\%}\text{(WMO)} + 37.7 \quad R=0.98 \tag{4.36}$$

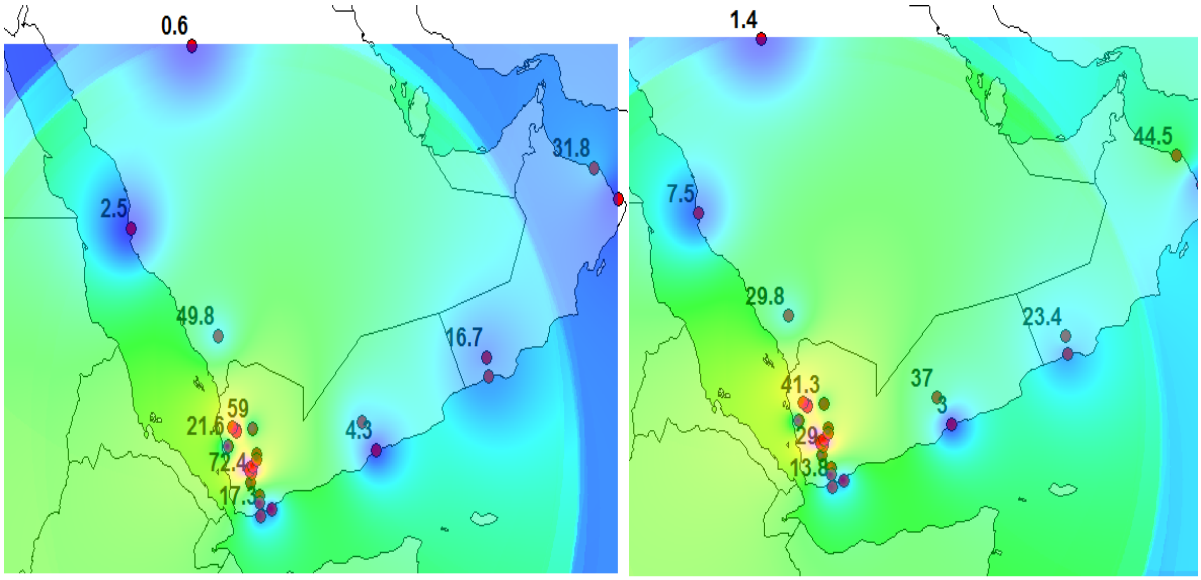

Figure 4.4.2 - Spatial distribution of norms and standard deviations of rainfall in August in the Arabian Peninsula, according to the data obtained for the long-term period (left figure – rainfall norms, right - standard deviation).

From spatial distributions rainfall is insignificant in the whole Peninsula, and all maximum are concentrated in the south-west. In general, rainfall is very unevenly distributed throughout the Peninsula and seasonal.

General information about the spatio-temporal rainfall variability, table 4.4.3. Results indicate that the average rainfall norms and their spatial monthly maximum have some annual variation with maxima in July - August and lows in December - January. At the same time the minimum monthly precipitation in the territory depict changes in the year, from 0.1 mm to 7.4 mm.

Table 4.4.3 - Spatial average rainfall norms by month in the Arabian Peninsula.

Period	Characteristics	Month											
		1	2	3	4	5	6	7	8	9	10	11	12
Weight	Mean	22.8	26.2	38.3	44.6	37.7	26.9	50.5	83.5	23.6	27.6	35.7	27.8
	Max	81.5	93.2	89.4	168.8	162	120	203	343	169	123	93	65.5
	Min.	1.2	2.2	3.5	1.9	1	0.1	0.1	0.6	0.1	0.4	1.0	4.5
WMO	Mean.	16.7	23.4	27.6	38.1	28.6	22.5	42.9	70.6	18.2	21.5	23.5	20.7
	Max.	68	80.4	71.1	168	115	132	169	271	141	73.3	70.1	63
	Min.	0.7	2.0	2.5	2.8	0.2	0.2	0.1	0.4	0.1	1.2	2.6	7.4

In general, the spatial distribution of precipitation analysis parameters (norms and standard deviation), and the following main conclusions:

- Precipitation remains practically stable;
- In the sediments of these distinct spatial relationships, as in the air temperature is not observed, although there is a tendency that the coastal, especially over the mountains parts of the Peninsula have more precipitation than in the interior;
- Variability of rainfall is greater, the greatest absolute values of precipitation in the cold period varies from 1-2 mm in the southwest to 20-40 mm in the interior and northern parts of the Peninsula, and in the warm period, from 0.1 mm in the central part to 20-40 mm in the southwest.

4.6. Spatial statistical models of air temperature and precipitation and regular properties of their coefficients over the time.

Table 4.5.1 shows the results of evaluating the effectiveness of time series models to approximate the derived parameters of spatial models A1j, A0j and SEj obtained from the dependence of (4.15) for the territory of the Arabian Peninsula, where: Δtr, Δctup - relative deviations or variations (%) trend model and model step changes in the model of a stationary sampling; Ftp, Fst - Statistics Fisher criterion to assess the statistical significance of differences from the stationary model Fst - Year of step changes, defined by a minimum of residual variances of the two parts of the time series, Tin., T. - Start and end years of observations, n-observation period (in years), R - correlation coefficient equation linear trend.

Moreover, spatial modeling was carried out for different periods: the entire observation period and the recovered data, revised from excluding non-uniform reconstructed values and the last 50 years, including 1960 -2011. In Tabl.4.12 results of modeling for the last 50-year period. In addition to the monthly average temperatures are modeled as the average temperature (Tyear) and the parameters of the model intra-oscillations (B1, B0, Se), prepared according to the method [120, 121]. Bright color in Tabl.4.5.1 allocated efficient statistical model which unlike fixed at 10% or more, as well as statistically significant estimated values of the test statistic Fisher and correlation coefficients of the linear trend.

Table 4.5.1 - The characteristics of time series models for the parameters of spatial models of air temperature on the Arabian Peninsula for the period 1960-2011.

Month	Δtr,%	Δst,%	Ftr	Fst	Tst	Tin	Tfin	n	R
A1									
1	1.6	7.2	1.03	1.16	1972	1960	2011	52	0.18
2	0.6	4.9	1.01	1.11	1980	1960	2011	52	0.11
3	0	6.7	1	1.15	2001	1960	2011	51	-0.01
4	2.9	6.5	1.06	1.14	1972	1960	2011	52	-0.24
5	0.5	2.6	1.01	1.05	2000	1960	2010	51	0.1
6	**10**	**12.4**	1.23	1.3	1994	1960	2010	51	**0.44**
7	**17.1**	**15.2**	1.46	1.39	1980	1960	2010	51	**0.56**
8	**13.9**	**25.4**	1.35	1.8	1996	1960	2010	51	**0.51**
9	0.6	2.4	1.01	1.05	1997	1960	2010	51	0.11
10	2.7	4.7	1.06	1.1	1991	1960	2010	51	-0.23
11	0.7	2.6	1.01	1.05	1971	1960	2010	51	0.12
12	1.2	5.3	1.02	1.11	1970	1960	2010	51	0.16
Тгод	0.4	5.5	1.01	1.12	1938	1928	2011	84	-0.09
B1	2.2	5.2	1.05	1.11	1951	1906	2011	100	-0.21
B0	0.7	5.4	1.01	1.12	2001	1941	2011	70	-0.12
Se	1.3	2.5	1.03	1.05	1972	1938	2011	70	-0.16
A0									
1	0.3	4.2	1.01	1.09	1972	1960	2011	52	-0.08
2	0	2.6	1	1.05	1999	1960	2011	52	-0.01
3	0.3	8.4	1.01	1.19	2001	1960	2011	51	0.07

Month	Δtr,%	Δst,%	Ftr	Fst	Tst	Tin	Tfin	n	R
4	5.8	8.8	1.13	1.2	1972	1960	2011	52	0.34
5	0.6	3.4	1.01	1.07	1988	1960	2010	51	0.11
6	5.6	7.4	1.12	1.17	1996	1960	2010	51	-0.33
7	**12.8**	**12**	1.31	1.29	1980	1960	2010	51	**-0.49**
8	8.2	**17.9**	1.19	1.48	1996	1960	2010	51	**-0.4**
9	0.1	2.1	1	1.04	1979	1960	2010	51	0.04
10	7	8.8	1.16	1.2	1991	1960	2010	51	0.37
11	0	1.4	1	1.03	1971	1960	2010	51	0.01
12	0	2	1	1.04	1970	1960	2010	51	0
Тгод	7.5	**10.7**	1.17	1.26	1998	1944	2010	64	**0.38**
B1	1.8	5.6	1.04	1.12	1963	1934	2010	73	-0.19
B0	0.2	3.5	1	1.07	1948	1934	2010	74	-0.06
Se	2.1	5.9	1.04	1.13	1993	1942	2010	69	-0.2
ASe									
1	0.5	3	1.01	1.06	1970	1960	2011	52	-0.1
2	0.1	1.7	1	1.04	2001	1960	2011	52	0.04
3	1.6	7.1	1.03	1.16	2000	1960	2011	51	0.18
4	0	3.1	1	1.06	1999	1960	2011	52	0
5	1.1	8.9	1.02	1.2	1999	1960	2010	51	0.15
6	1.9	**10.4**	1.04	1.25	1998	1960	2010	51	0.19
7	3.8	5.7	1.08	1.13	1996	1960	2010	51	**0.27**
8	2.1	6.2	1.04	1.14	1995	1960	2010	51	0.2
9	2.4	5.7	1.05	1.12	1999	1960	2010	51	0.22
10	5.6	8.5	1.12	1.19	1972	1960	2010	51	**-0.33**
11	0	2.5	1	1.05	2000	1960	2010	51	0
12	0	0.9	1	1.02	1970	1960	2010	51	0.01
Тгод	0.6	6.2	1.01	1.14	1963	1944	2010	64	-0.11
B1	6.5	**14.1**	1.14	1.35	1963	1934	2010	73	**-0.36**
B0	7.1	**13.1**	1.16	1.32	1963	1934	2010	74	**-0.37**
Se	5.1	**13**	1.11	1.32	1966	1942	2010	69	**-0.32**

From the table 4.5.1 follows that non-stationary in the parameters of spatial models takes place in the summer months and sometimes it affects the unsteadiness of average temperatures for the parameter A0 and the model coefficients for intra-oscillation parameters ASe. The

chronological time series of parameters of spatial model for the summer months, temperatures are shown in Fig.4.10 non-stationary parameters A1 to summer temperatures due to its step-increase in the early 1990s, which is especially evident for June and August to July is more in the nature around a linear trend 1980 and a significant increase in recent years. Therefore, we can assume that for the summer months in recent years, the spatial gradient of the temperature field became more. Same parameter A0 for July, which characterizes the average regional temperature, on the contrary decreased since the early 1980s, and especially its decrease took place in 2008-2010., And for June and August, he stepwise decreased in the mid-1990s. Decrease in the average regional temperature in the summer months at the same time it is compensated by an increase in April and October, which is practically little impact on the average temperature, which has a stepped growth but often at $\Delta st = 10.7\%$. The most significant non-stationary occur in the parameters of the internal field in homogeneity ASe for June, which is growing (Fig.4.10), but at the same time for the coefficients of intra-annual fluctuations unsteadiness associated with their decrease, which indicates the formation of a homogeneous field in recent years (Table .4.12).

Here it should be noted that if we construct a spatial model for the entire period of observation, including the recovered data, the number of non-stationary time series of parameters will be substantially higher due to individual extreme recovered data having a large error. If we consider the whole period, but with the adjustments, ie exclusion extreme recovered with substantial errors, the results of the evaluation of stationary parameter are almost the same as in the last period of Tabl.4.5.1 observations.

Spatial statistical models were constructed for precipitation of each month and the results of evaluation of the stationary parameters A1, A0 and Ase are given in table.4.13 for the last 50-year period.

Table 4.5.2 - The characteristics of time series models for the spatial patterns of precipitation parameters on the Arabian Peninsula for the period 1960-2011.

Month	Δtr,%	Δst,%	Ftr	Fst	Tst	Tin	Tfin	n	R
A1									
1	0.8	6	1.02	1.13	1994	1960	2005	45	0.12
2	**11.4**	**19**	1.27	1.52	1975	1961	2010	38	**-0.46**

Month	Δtr,%	Δst,%	Ftr	Fst	Tst	Tin	Tfin	n	R
3	0.1	2	1	1.04	1992	1960	2011	48	-0.05
4	0	3.4	1	1.07	1995	1960	2010	50	0.03
5	2.9	**10.2**	1.06	1.24	1997	1960	2010	49	0.24
6	0.2	0.9	1	1.02	1978	1960	1999	34	0.06
7	0	4.2	1	1.09	1973	1960	2003	39	-0.02
8	0	2.9	1	1.06	1995	1960	2010	46	0.02
9	1.8	7.4	1.04	1.17	1973	1960	1999	32	-0.19
10	7.1	**10.5**	1.16	1.25	1976	1960	2009	46	**0.37**
11	5.3	**14**	1.12	1.35	1970	1960	2009	48	**-0.32**
12	4.1	6.8	1.09	1.15	1993	1960	2009	45	0.28
A0									
1	0.8	4.2	1.02	1.09	1994	1960	2005	45	-0.12
2	**10.5**	**19.3**	1.25	1.54	1975	1961	2010	38	**0.45**
3	1	4.5	1.02	1.1	1992	1960	2011	48	0.14
4	4.6	**12.6**	1.1	1.31	1995	1960	2010	50	-0.3
5	2.6	6.9	1.05	1.15	1986	1960	2010	49	-0.23
6	1.6	1.3	1.03	1.03	1982	1960	1999	34	-0.18
7	0.6	3.2	1.01	1.07	1971	1960	2003	39	-0.11
8	0.1	1.7	1	1.04	1989	1960	2010	46	0.04
9	0.1	5.7	1	1.12	1971	1960	1999	32	0.05
10	0.1	1.2	1	1.02	1977	1960	2009	46	-0.05
11	4.4	7.8	1.09	1.18	1970	1960	2009	48	0.29
12	1.4	2	1.03	1.04	1976	1960	2009	45	-0.16
ASe									
1	0.6	4.4	1.01	1.09	1985	1960	2003	44	-0.11
2	1.8	3.6	1.04	1.08	1981	1961	2010	38	-0.19
3	0.4	1.2	1.01	1.03	1985	1960	2011	48	0.09
4	4	3.6	1.09	1.08	1984	1960	2010	50	-0.28
5	0.8	3.6	1.02	1.08	1991	1960	2010	49	-0.13
6	0.2	0.6	1	1.01	1978	1929	1999	35	0.07
7	0.2	1.6	1	1.03	1973	1960	2003	39	-0.06
8	0.2	3.5	1	1.07	1995	1960	2010	46	0.06
9	2.1	5.6	1.04	1.12	1982	1960	1999	32	-0.2

Month	Δtr,%	Δst,%	Ftr	Fst	Tst	Tin	Tfin	n	R
10	2.9	6.2	1.06	1.14	1977	1960	2009	46	0.24
11	2.5	6	1.05	1.13	1980	1960	2009	48	-0.22
12	0.4	3.5	1.01	1.07	1971	1960	2009	45	-0.09

From the results table 4.5/2 follows that the non-stationary spatial gradient of precipitation (parameter A1) takes place mainly in February and November and rainfall field during these months is more uniform. The most significant increase in the value of A0 is in February and in April; it was not as significant as stepwise decrease in the 1980s. Time series parameter ASe, associated with the heterogeneity of the precipitation field, are stationary.

Summary and conclusions:

- In addition to confirming the known patterns of climate, which in the Arabian Peninsula in winter warmer coastal areas and in the summer - the inner desert, obtained numerical values of the spatial gradient norm temperature up to 20 ° C in winter and up to 10 ° C in summer; found that the variability of long-term temperature fluctuations lowest in the south and southeast, and the highest - in the north and in the center; climate norms temperature stable for about half of the stations, although the direction of growth of the norms is the case for a small number of stations, mainly in summer;
- Slightly more precipitation in coastal, especially hilly and mountainous parts of the peninsula than inland; the territory they change during the cold period of 2 mm in the coastal areas of the south and west to 30 mm, and even up to 70 mm in the northeast, and in the warm, on the contrary, from 0.1 - 1 mm in the north and central parts 60-70 mm in the south-western coastal areas; precipitation variability depends on the magnitude and up to 50% of the norm, while the rules themselves remain practically stable precipitation;
- The analysis of stability parameters of spatial statistical models of temperature and precipitation suggests that they practically do not change over time except for the growth of the spatial gradient of the temperature field and reduce their average regional values in the summer months.

CONCLUSION

Results of the implementation of regional climate research for Yemen and around the Arabian Peninsula, the following main scientific and practical results have been achieved.

1. A regional database that includes long-term time series of observations of mean monthly air temperature at 188 meteorological stations, 36 meteorological stations- Arabian Peninsula and adjacent territories and for the monthly rainfall data at 310 weather stations (43 in the Arabian Peninsula) with a mean observation period of 45-50 (20% of the period of observation stations are over 70 years) with the inclusion of the last years of observation (2011-2012.) about 20% of the stations.

2. The analysis of the quality and consistency of information in the regional database on the basis of statistical criteria, and some cases of non-uniform extreme and non-stationarity means and variances, mainly related to the omissions and lack of long term time series. The recovering process of missing data and extension time series was carried out, result shows that that, the average period of observation for 39-41 year mean monthly air temperature in the Arabian Peninsula was increased to 96 (August) - 116 (February) years, with recovered data in the colder months of the year was more effective than in the warmer, due to the greater homogeneity of synoptic processes and better spatial distribution of winter temperatures. Precipitation data recovered worse than the air temperature and the average for the duration of the Arabian Peninsula observations Monthly precipitation was increased from 33-36 years to 73-79 years. After the restored data were analyzed, data homogeneity and base was formed for continuous long-term series for modeling, including most of the 20th century and beginning of the 21th century.

3. For Separately weather stations in Yemen and for the purpose of analyzing time series model of air temperature, the following conclusions were made:

   - The vast majority of the time series of observations at meteorological stations in Republic of Yemen are stationary;
   - Individual cases of non-stationarity, such as at the meteorological station Taiz, due to insufficient length of observation and possible errors of observations.

Only for weather station Ibb in Yemen non stationary is related to the fact that rainfall in the first part of the series is less than compared to the second part. Stepwise increase in rainfall from the early 2000s is particularly vivid in May, June and September.

4. On the basis of implementation of statistical modeling of time series by comparing model with time-varying sampling stationary model of a linear trend and stepwise functions for average monthly air temperature, it was noted that the percentage of non-stationary models varies from 0% in winter to 60% in June-August. The most effective non-stationary model is the model of stepwise functions, which differs from the fixed to the middle reaches 15-18% (with peaks up to 30-32%), while the efficiency of the linear trend model reaches 11-12% (with peaks up to 30-33 as %). In the warm period, non-stationary models are more common in the inner parts of the Peninsula and in the cold months in some coastal areas of the south and west of the Peninsula.

5. For the average annual temperature average deviation of the model stepwise functions of stationary model is 20.6% (with a maximum of up to 38%) and the percentage of effectiveness models is 95.8%. The linear trend model of the average deviation from a hundred stationary equal 17.4% and the relative number of effective non-stationary model is 62.5%.

Therefore, the average annual air temperature is much more non- stationary, than any of the mean monthly temperatures, due to the averaging procedure and formation of random components in each of the 12 cases of average monthly temperatures and selection of climate signals of the summer months. Stationary models have can be applied only along the Red Sea coast and in the far east of the Peninsula. All remained part of the Arabian Peninsula contains non-stationary model with increase of annual temperature. And in the central regions, this

increase is related to the increase in the months temperatures of the warmth half of the, and in the southern coastal - rising temperatures in the cold half of the year.

6. For the time series of averages monthly rainfall territorial deviations from the hundred-stationary models are very small and vary from 4.5% to 7.7% for the model of stepwise change and from 1.8% to 3.6% for the model of a linear trend. The number of cases of stationary varies from 0 to 4, for the model of linear trend and stepwise changes from 0 to 2. Therefore, the spatial distribution of non-stationary time series, as well as absences of non stationary appear at individual stations, located in the coastal areas south and west of the Peninsula and is determined by local factors rather than climatic factors.

7. We obtain a very close relationship between the territorial average temperature and the temperature rarely events (once in 100 and 200 years old) with correlation coefficients greater than 0.9 for most months. They are of great practical importance for climate applications, as on one hand they allow us to obtain estimates of climatic characteristics of rare events for the considered stations, and on the other hand, based on spatial interpolation of these rules and regression can be calculated for the climatic characteristics at any point in the Arabian Peninsula, where observations are missing.

8. For the time series of monthly precipitation spatial averages deviations from the hundred-stationary models are very small and varies from 4.5% to 7.7% for the model of step-change and from 1.8% to 3.6% for the model of a linear trend. The number of rows of stationary and also little varies from 0 to 4, for the model and changes stepwise from 0 to 2 and linear trend model that percentage yields up to 12% and 7% of the total number of cases. Therefore, the spatial distribution of non-stationary series, an absence, and unsteadiness manifested at individual stations, located in the coastal areas south and west of the peninsula and is determined by local rather than climatic factors..

References

1. *Abdulaziz University, Jeddah, Saudi Arabia* **6**: 203–214. Kotwicki V, Al Sulaimani Z. 2009. Climates of the Arabian Peninsula – past, present, future. *International Journal of Climate Change Strategies and Management* **1**: 297–310, DOI: 10.1108/17568690910977500.
2. About the WCRP CMIP3 Multi-Model Dataset Archive at PCMDI: http://www-pcmdi.llnl.gov/ipcc/about_ipcc.php
3. Abram, N. J., M. K. Gagan, J. E. Cole, W. S. Hantoro, and M. Mudelsee, 2008: Recent intensification of tropical climate variability in the Indian Ocean. Nature Geosci., **1**, 849–853.
4. Aikin J. E. Calculation of mean areal depth of precipitation. – J. of Hydrol., 1971, vol. 2. № 4, p. 367-386.
5. Allan, R., and B. Soden, 2008: Atmospheric warming and the amplification of precipitation extremes. Science, **321**, 1481–1484.
6. Almazroui M. 2006. *The Relationship Between Atmospheric Circulation Patterns and Surface Climatic Elements in Saudi Arabia*, PhD thesis, Climate Research Unit, University of East Anglia.
7. Almazroui M. 2012a. The life cycle of extreme rainfall events over western Saudi Arabia simulated by a regional climate model: case study of November 1996. *Atm´osfera* **25**: 23–41.
8. Almazroui M. 2012b. Temperature variability over Saudi Arabia during the period 1978–2010 and its association with global climate indices. *Journal of King Abdulaziz University: Met Env Arid Land Agric Sci*. **23**(1), DOI: 10.4197/Met.23-1.6. (In press).
9. Alory, G., S. Wijffels, and G. Meyers, 2007: Observed temperature trends in the Indian Ocean over 1960–1999 and associated mechanisms. Geophys. Res. Lett., **34**, L02606
10. AlSarmi, S., and R. Washington, 2011: Recent observed climate change over the Arabian Peninsula. J. Geophys. Res. Atmos., **116**, D11109.
11. Alyamani MS, ¸Sen A. 1993. Regional variations of monthly rainfall amounts in the Kingdom of Saudi Arabia. *Journal of King Abdulaziz University: Earth Sciences* **6**: 113–133.
12. Atmospheric Model Intercomparison Project http://www-cmdi.llnl.gov/projects/amip/index.
13. Bal, S., S. Schimanke, T. Spangehl, and U. Cubasch, 2011: On the robustness of the solar cycle signal in the Pacific region. Geophys. Res. Lett., **38**, L14809.
14. Barnes, E., J. Slingo, and T. Woollings, 2012: A methodology for the comparison of blocking climatologies across indices, models and climate scenarios. Clim. Dyn., **38**, 2467–2481.

15. Becker, A., P. Finger, A. Meyer-Christoffer, B. Rudolf, K. Schamm, U. Schneider, and M. Ziese, 2013: A description of the global land-surface precipitation data products of the Global Precipitation Climatology Centre with sample applications including centennial (trend) analysis from 1901–present. Earth Syst. Sci. Data, **5**, 71–99.

16. Benestad, R. E., and G. A. Schmidt, 2009: Solar trends and global warming. J.Geophys. Res. Atmos., **114**, D14101.

17. Black, E., J. Slingo, and K. Sperber, 2003: An observational study of the relationship between excessively strong short rains in coastal East Africa and Indian Ocean SST. Mon. Weather Rev., **131**, 74–94.

18. Chadwick, R., I. Boutle, and G. Martin, 2013: Spatial patterns of precipitation change in CMIP5: Why the rich don't get richer in the tropics. J. Clim., **26,** 3803–3822.

19. Chang, E. K. M., Y. Guo, and X. Xia, 2012: CMIP5 multimodel ensemble projection of storm track change under global warming. J. Geophys. Res. Atmos., **117**, doi: 10.1029/2012jd018578.

20. Christensen, J. H., et al., 2007: Regional climate projections. In: Climate Change 2007: The Physical Science Basis. Contribution of Working Group I to the Fourth Assessment Report of the Intergovernmental Panel on Climate Change [Solomon, S., D. Qin, M. Manning, Z. Chen, M. Marquis, K. B. Averyt, M. Tignor and H. L. Miller (eds.)] Cambridge University Press, Cambridge, United Kingdom and New York, NY, USA, pp. 847–940.

21. Climate normals (ed. Omar Baddour) World Meteorological Organization CCl/MG/2011/Doc.10, Commission for climatology item 10, Management group meeting, Denver, USA, October 2011, 8pp.

22. Edgell HS. 2006. *Arabian Deserts: Nature, Origin and Evolution*. Springer: Dordrecht, The Netherlands.

23. El Gindy, A. A. H. (1994), Seasonal and long-term changes of air and sea surface temperature and impact of the Gulf War in the Arabian Gulf and Gulf of Oman, Fresenius Environ. Bull., 3(8), 481–486.

24. Elagib NA, Abdu ASA. 2009. Development of temperature in the Kingdom of Bahrain from 1947 to 2005. *Theoretical and Applied Climatology* **101**: 269–279, DOI: 10.1007/s00704-009-0205-y.

25. El-Sabbagh MK. 1982. On the climate of Saudi Arabia. *Bulletin of Faculty of Science, King*

26. Elsner, J. B., J. P. Kossin, and T. H. Jagger, 2008: The increasing intensity of the strongest tropical cyclones. Nature, **455**, 92–95.

27. Endo, H., A. Kitoh, T. Ose, R. Mizuta, and S. Kusunoki, 2012: Future changes and uncertainties in Asian precipitation simulated by multiphysics and multi–sea surface temperature ensemble experiments with high-resolution Meteorological Research Institute atmospheric general circulation models (MRI-AGCMs). J.Geophys. Res., **117**, D16118.

28. Evan, A. T., J. P. Kossin, C. E. Chung, and V. Ramanathan, 2011: Arabian Sea tropical cyclones intensified by emissions of black carbon and other aerosols. Nature, **479**, 94–97.

29. Evans, J. P., 2009: 21st century climate change in the Middle East. Clim. Change, **92**, 417–432.

30. Feliks, Y., M. Ghil, and A. W. Robertson, 2010: Oscillatory climate modes in the eastern Mediterranean and their synchronization with the North Atlantic Oscillation. J.Clim., **23**, 4060–4079.

31. Folland, C. K., et al., 2013 High predictive skill of global surface temperature a year ahead. Geophys. Res. Lett., **40**, 761–767.

32. Ghoneim, Eman. 2009. "Remote Sensing Study of Some Impacts of Global Warming on the Arab Region" in Tolba, Mostafa and Najib Saab, eds. "Arab Environment: Climate Change." 2009 Report of the Arab Forum for Environment and Development. Highlights available online at http://www.iea.org/publications/free_new_Desc.asp?PUBS_ID=2143

33. Gillett, N. P., V. K. Arora, D. Matthews, P. A. Stott, and M. R. Allen, 2013 Constraining the ratio of global warming to cumulative CO2 emissions using CMIP5 simulations. J. Clim., doi:10.1175/JCLI-D-12–00476.1.

34. Gregory, J. M., and P. M. Forster, 2008: Transient climate response estimated from radiative forcing and observed temperature change. J. Geophys. Res. Atmos.,**113**, D23105.

35. Gutowski, W. J. et al., 2010: Regional, extreme monthly precipitation simulated by NARCCAP RCMs. J. Hydrometeorol., **11**, 1373–1379.

36. Haam, E., and K. K. Tung, 2012: Statistics of solar cycle-La Nina connection: Correlation of two autocorrelated time series. J. Atmos. Sci., **69** 2934–2939.

37. Han, W., et al., 2010: Patterns of Indian Ocean sea-level change in a warming climate. Nature Geosci., **3**, 546–550.

38. Hansen, J., M. Sato, R. Ruedy, K. Lo, D. W. Lea, and M. Medina-Elizade, 2006: Global temperature change. Proc. Natl. Acad. Sci. U.S.A., **103**, 14288–14293.

39. Hegerl, G. C., F. W. Zwiers, P. A. Stott, and V. V. Kharin, 2004: Detectability of anthropogenic changes in annual temperature and precipitation extremes. J. Clim., **17**, 3683–3700.

40. Hoerling, M. P., J. K. Eischeid, X.-W. Quan, H. F. Diaz, R. S. Webb, R. M. Dole, and D. R. Easterling, 2012: Is a transition to semipermanent drought conditions imminent in the U.S. great plains? J. Clim., **25**, 8380–8386.

41. Hoerling, M., et al., 2013: Anatomy of an extreme event. J. Clim., **26**, 2811–2832.

42. Hood, L. L., and R. E. Soukharev, 2012: The lower-stratospheric response to 11-yr solar forcing: Coupling to the troposphere-ocean response. J. Atmos. Sci., **69**, 1841–1864.

43. http://www.ipcc.ch/publications_and_data/ar4/syr/en/contents.html

44. http://www.ipcc.ch/publications_and_data/ar4/wg2/en/contents.html

45. Hu, Z. Z., 1997: Interdecadal variability of summer climate over East Asia and its association with 500 hPa height and global sea surface temperature. J. Geophys.Res. Atmos., **102**, 19403–19412.

46. Hurrell, J. W., and C. Deser, 2009: North Atlantic climate variability: The role of the North Atlantic Oscillation. J. Mar. Syst., **78**, 28–41.

47. Imbers, J., A. Lopez, C. Huntingford, and M. R. Allen, 2013: Testing the robustness of the anthropogenic climate change detection statements using different empirical models. J. Geophys. Res. Atmos., doi:10.1002/jgrd.50296.

48. Ingram, W. J., 2007: Detection and attribution of climate change, and understanding solar influence on climate. In: Solar Variability and Planetary Climates [Y. Calisesi, R.-M. Bonnet , L. Gray , J. Langen, and M. Lockwood (eds.)]. Springer Science+Business Media, New York, NY, USA, and Heidelberg, Germany, pp. 199–211.

49. IPCC (Intergovernmental Panel on Climate Change). 2001. Climate change: the scientific basis. In *Contribution of Working Group I to the Third Assessment Report of the Intergovernmental Panel on Climate Change*, Houghton JT, Ding Y, Griggs DJ, Noguer M, van der Linden PJ, Xiaosu D (eds). Cambridge University Press: Cambridge, UK, 944.

50. IPCC (Intergovernmental Panel on Climate Change: Climate Change). 2007. The physical science basis. In *Contribution of Working Group I to the Fourth Assessment Report of the Intergovernmental Panel on Climate Change*, Solomon S, Qin D, Manning M, Chen Z, Marquis, Averyt K, Tignor M, Miller H (eds). Cambridge University Press: Cambridge, p 996.

51. IPCC (Intergovernmental Panel on Climate Change: Climate Change). 2013. The physical science basis. In *Contribution of Working Group I to the Firth Assessment Report of the Intergovernmental Panel on Climate Change*, Thomas F. Stocker, Dahe Qin, Gian-Kasper Plattner, Melinda M.B. Tignor, Simon K. Allen, Judith Boschung, Alexander Nauels, Yu Xia, Vincent Bex, Pauline M. Midgley (eds). Cambridge University Press: Cambridge, p 1552.

52. IPCC Standard Output from Coupled Ocean-Atmosphere GCMs: http://www-pcmdi.llnl.gov/ipcc/standard_output.html#Experiments.

53. IPCC, 2013: Annex I: Atlas of Global and Regional Climate Projections [van Oldenborgh, G.J., M. Collins, J. Arblaster, J.H. Christensen, J. Marotzke, S.B. Power, M. Rummukainen and T. Zhou (eds.)]. In: Climate Change 2013: The Physical Science Basis. Contribution of Working Group I to the Fifth Assessment Report of the Intergovernmental Panel on Climate Change [Stocker, T.F., D. Qin, G.-K. Plattner, M. Tignor, S.K. Allen, J. Boschung, A. Nauels, Y. Xia, V. Bex and P.M. Midgley (eds.)]. Cambridge University Press, Cambridge, United Kingdom and New York, NY, USA.

54. Izumo, T., C. D. Montegut, J. J. Luo, S. K. Behera, S. Masson, and T. Yamagata, 2008: The role of the western Arabian Sea upwelling in Indian monsoon rainfall variability. J. Clim., **21**, 5603–5623.

55. J. Sowers and E. Weinthal. 2010. Climate Change Adaptation in the Middle East and North Africa: Challenges and Opportunities. Belfer Center for Science and International Affairs Harvard Kennedy School 79 JFK St., Cambridge, MA 02138 USA 21 pp.

56. Jevrejeva, S., J. C. Moore, et al. 2010. "How will sea level rise correspond to changes in natural and anthropogenic forcings by 2100?" Geophysical Research Letters 37.

57. Jones, G. S., and P. A. Stott, 2011: Sensitivity of the attribution of near surface temperature warming to the choice of observational dataset. Geophys. Res. Lett., **38**, L21702.

58. Jones, G. S., M. Lockwood, and P. A. Stott, 2012: What influence will future solar activity changes over the 21st century have on projected global near surface temperature changes ? J. Geophys. Res. Atmos., **117**, D05103.

59. Kaufmann, R. K., H. Kauppi, and J. H. Stock, 2006: Emission, concentrations, & temperature: A time series analysis. Clim. Change, **77**, 249–278.

60. Kaufmann, R. K., H. Kauppi, M. L. Mann, and J. H. Stock, 2011: Reconciling anthropogenic climate change with observed temperature 1998–2008. Proc. Natl. Acad. Sci. U.S.A., **108**, 11790–11793.

61. Kaufmann, R. K., H. Kauppi, M. L. Mann, and J. H. Stock, 2013: Does temperature contain a stochastic trend: Linking statistical results to physical mechanisms.Clim. Change, doi:10.1007/s10584–012–0683–2.

62. Kidson J.w. Index cycles in the Northern Hemisphere during Global Weather Experiment.- Month. Wea. Redv., vol. 113, 1985, p.607-623.

63. Kim, D., and H. Byun, 2009: Future pattern of Asian drought under global warming scenario. Theor. Appl. Climatol., **98**, 137–150.

64. Kwarteng, A. Y., A. S. Dorvlo, and G. T. V. Kumar (2009), Analysis of a 27-year rainfall data (1977–2003) in the Sultanate of Oman, Int. J. Climatol., 29(4), 605–617, doi:10.1002/joc.1727.

65. Landsea, C. W., R. A. Pielke, A. Mestas-Nunez, and J. A. Knaff, 1999: Atlantic basin hurricanes: Indices of climatic changes. Clim. Change, **42**, 89–129.

66. Lean, J. L., 2006: Comment on "Estimated solar contribution to the global surface warming using the ACRIM TSI satellite composite" by N. Scafetta and B. J. West. Geophys. Res. Lett., **33**, L15701.

67. Lean, J. L., and D. H. Rind, 2008: How natural and anthropogenic influences alter global and regional surface temperatures: 1889 to 2006. Geophys. Res. Lett., **35**, L18701.

68. Lean, J. L., and D. H. Rind, 2009: How will Earth's surface temperature change in future decades? Geophys. Res. Lett., **36**, L15708.

69. Levine, R. C., and A. G. Turner, 2012: Dependence of Indian monsoon rainfall on moisture fluxes across the Arabian Sea and the impact of coupled model sea surface temperature biases. Clim. Dyn., **38,** 2167-2190.

70. Lockwood, M., 2008: Recent changes in solar outputs and the global mean surface temperature. III. Analysis of contributions to global mean air surface temperature rise. Proc. R. Soc. London A, **464**, 1387–1404.

71. Lockwood, M., 2012: Solar influence on global and regional climates. Surv. Geophys., **33**, 503–534.

72. Lockwood, M., and C. Fröhlich, 2007: Recent oppositely directed trends in solar climate forcings and the global mean surface air temperature Proc. R. Soc. London A, **463**, 2447–2460.

73. Lockwood, M., and C. Fröhlich, 2008: Recent oppositely directed trends in solar climate forcings and the global mean surface air temperature: II. Different reconstructions of the total solar irradiance variation and dependence on response time scale. Proc. R. Soc. London A, **464**, 1367–1385.

74. Mansour Almazroui,a* M. Nazrul Islam,a H. Athar,a P. D. Jonesa,b and M. Ashfaqur Rahmana 2012 Recent climate change in the Arabian Peninsula: annual rainfall and temperature analysis of Saudi Arabia for 1978–2009 *International Journal of Climatology Int. J. Climatol.* **32**: 953–966.

75. Marchant, R., C. Mumbi, S. Behera, and T. Yamagata, 2007: The Indian Ocean dipole—the unsung driver of climatic variability in East Africa. Afr. J. Ecol., **45**, 4–16.

76. Meehl, G. A., J. M. Arblaster, K. Matthes, F. Sassi, and H. van Loon, 2009: Amplifying the Pacific climate system response to a small 11-747year solar cycle forcing. Science, **325** 1114–1118.

77. Min, S.-K., and A. Hense, 2006: A Bayesian assessment of climate change using multimodel ensembles. Part I: Global mean surface temperature. J. Clim., **19**, 3237–3256.

78. Min, S.-K., X. Zhang, F. W. Zwiers, P. Friederichs, and A. Hense, 2008c: Signal detectability in extreme precipitation changes assessed from twentieth century climate simulations. Clim. Dyn., **32**, 95–111.

79. Misios, S., and H. Schmidt, 2012: Mechanisms involved in the amplification of the 11-yr solar cycle signal in the Tropical Pacific ocean. J. Clim., **25**, 5102–5118.

80. Mitchell TD, Jones PD. 2005. An improved method of constructing a database of monthly climate observations and associated highresolution grids. *International Journal of Climatology* **25**: 693–712, DOI: 10.1002/joc.1181.

81. Nasrallah HA, Balling RC Jr. 1996. Analysis of recent climatic changes in the Arabian Peninsula region. *Theoretical and Applied Climatology* **53**: 245–252.

82. Nasrallah, H. A., E. Nieplova, and E. Ramadan (2004), Warm season extreme temperature events in Kuwait, J. Arid Environ., 56(2), 357–371, doi:10.1016/S0140-1963(03)00007-7.

83. Onol, B., and F. Semazzi, 2009: Regionalization of climate change simulations over the Eastern Mediterranean. J. Clim., **22**, 1944–1961.

84. Peterson, T. C., et al. (1998), Homogeneity adjustments of in situ atmospheric climate data: A review, Int. J. Climatol., 18(13), 1493–1517, doi:10.1002/(SICI)1097-0088(19981115)18:13<1493::AID-JOC329>3.0. CO;2-T.

85. Roy, I., and J. D. Haigh, 2010: Solar cycle signals in sea level pressure and sea surface temperature. Atmos. Chem. Phys., **10** 3147–3153. Roy, I., and J. D. Haigh, 2012: Solar cycle signals in the

86. Said AlSarmi1 and R. Washington (2011) Recent observed climate change over the Arabian Peninsula Journal of Geophysical Research, Vol. 116, D11109, doi:10.1029/2010JD015459, 2011

87. Scaife, A., et al., 2009: The CLIVAR C20C project: Selected twentieth century climate events. Clim. Dyn., **33**, 603–614.

88. Sen, P. K. (1968), Estimates of the regression coefficient based on Kendall's Tau, J. Am. Stat. Assoc., 63(324), 1379–1389, doi:10.2307/2285891.

89. Sowers, J., A. Vengosh, and E. Weinthal. 2009. "Climate change, water resources, and the politics of adaptation in the Middle East and North Africa." Climatic Change (published online 23 April 2010)

90. Sun, J., H. Wang, and W. Yuan, 2008: Decadal variations of the relationship between the summer North Atlantic Oscillation and middle East Asian air temperature. J. Geophys. Res. Atmos., **113**, D15107.

91. Taylor, K. E., R. J. Stouffer, and G. A. Meehl, 2011c: An overview of CMIP5 and the experiment design. Bull. Am. Meteorol. Soc., **93**, 485–498.

92. Taylor, K. E., R. J. Stouffer, and G. A. Meehl, 2012b: An overview of CMIP5 and the experiment design. Bull. Am. Meteorol. Soc., **93**, 485–498.

93. The WCRP CMIP3 Multimodel dataset – A new era in Climate change research. 12 pp http://nldr.library.ucar.edu/repository/assets/ams-pubs/ams_pubs_200083.pdf

94. Thiessen A.H. Precipitation averages for large areas. – Mon. Wea. Rev., 1911, vol. 39, № 7, p. 1082-1084.

95. Tolba, M. K. and N. W. Saab. 2009. "Arab Environment: Climate Change." Beirut, Arab Forum for Environment and Development.

96. Trewin, B (2007): The role of climatological normals in a changing climate. World Climate Data and Monitoring Program No 61, WMO-TD No 1377. 46pp. Tung, K.-K.,

and J. Zhou, 2010: The Pacific's response to surface heating in 130 yr of SST: La Nina-like or El Nino-like? J. Atmos. Sci., **67**, 2649–2657.

97. UNDP. 2007. *Human Development Report 2007/2008, Fighting Climate Change: Human Solidarity in a Divided World.* New York: UNDP.

98. van Loon, H., and G. A. Meehl, 2008: The response in the Pacific to the sun's decadal peaks and contrasts to cold events in the Southern Oscillation. J. Atmos. Sol. Terres. Phys., **70** 1046–1055

99. van Loon, H., G. A. Meehl, and D. J. Shea, 2007: Coupled air-sea response to solar forcing in the Pacific region during northern winter. J. Geophys. Res. Atmos., **112**, D02108.

100. Wang, B., S. Xu, and L. Wu, 2012a: Intensified Arabian Sea tropical storms. Nature, **489**, E1–E2.

101. Wang, X. L. (2008), Accounting for autocorrelation in detecting mean shifts in climate data series using the penalized maximal t or F test, J. Appl. Meteorol. Climatol., 47(9), 2423–2444, doi:10.1175/2008JAMC1741.1

102. White, W. B., and Z. Y. Liu, 2008: Non-linear alignment of El Nino to the 11-yr solar cycle. Geophys. Res. Lett., **35**, L19607.

103. Zhang, H. et al. 2005. "Trends in Middle East Climate Indices from 1950 to 2003." Journal of Geophysical Research 110 (D22104): 1-12.

104. Zhang, X., et al., 2005: Trends in Middle East climate extreme indices from 1950 to 2003. J. Geophys. Res. Atmos., **110**, doi: 10.1029/2005JD006181.

105. Бендат Дж. Прикладной анализ случайных данных / Дж. Бендат, А. Пирсол. – М. : Мир, 1989. – 540 с.

106. Бокс Дж., Дженкинс Г. Анализ временных рядов. - М.: Мир, 1974. - 406 с.

107. В. А. Лобанов, Омар А.А. Шукри Моделирование пространственных климатических изменений на Аравийском полуострове. Ученые записки РГГМУ, 2014 (в печати).

108. В. А. Лобанов, Омар А.А. Шукри Оценка климатических изменений температуры воздуха и осадков на Аравийском полуострове. Ученые записки РГГМУ, 2014 (в печати).

109. В.А.Лобанов, Лемешко Н.А., Жильцова Е.Л., Горлова С.А., Ренева С.А. Методы восстановления многолетних рядов температуры воздуха. Сборник работ по гидрологии, №27, 2004, С.-Петербург, Гидрометеоиздат, с.54-68.

110. В.А.Лобанов, Лемешко Н.А., Жильцова Е.Л., Горлова С.А., Ренева С.А. Восстановление многолетних рядов температуры воздуха на Европейской территории России. Метеорология и гидрология, №2, 2005 г., с.5-14.

111. Венцель Е.С., Овчаров Л.А. Теория случайных процессов и ее инженерные приложения. -М.: Наука, 1991. -379с.

112. Гандин Л.С., Каган Р.Л. Статистическая структура метеорологических полей и ее приложения. - В кн.: Современные фундаментальные и прикладные исследования ГГО, Л.: Гидрометеоиздат, 1977, с.142-150.

113. Гандин Л.С., Каган Р.Л. Статистические методы интерпретации метеорологических данных. – Л.: Гидрометеоиздат, 1976. – 365 с.

114. Дроздов О.А., Васильев В.А., Кобышева Н.В., Раевский А.Н., Смекалова Л.К., Школьный Е.П. Климатология. - Л.: Гидрометеоиздат, 1989. – 568 с.

115. Дымников В.П., Лыкосов В.Н., Володин Е.М. Моделирование климата и его изменений. - М.: Наука, 2006. – 173 с.

116. Закс Л. Статистическое оценивание. М.: Статистика, 1976. – 598 с.

117. Заявление ВМО о состоянии глобального климата в 2013 году. WMO Bul. № 1130 Chair, Publications Board World Meteorological Organization (WMO) 7 bis, avenue de la Paix P.O. Box 2300 CH-1211 Geneva 2, Switzerland ISBN 978-92-63-41130-3, 24 pp.

118. Информация о многолетних рядах среднемесячной температуры воздуха и сумм осадков за месяц // KNMI [Электронный ресурс] / The Royal Netherlands Meteorological Institute.–Амстердам, Нидерланды, 2010.–Режим доступа: http://www.knmi.nl/about_knmi/

119. Информация о многолетних рядах среднемесячной температуры воздуха и сумм осадков за месяц // KNMI [Электронный ресурс] / The Royal Netherlands Meteorological Institute.–Амстердам, Нидерланды, 2010.–Режим доступа: http://www.knmi.nl/about_knmi/

120. Каган Р.Л. Характеристика статистической структуры метеорологических полей. - В кн.: Статистическая структура метеорологических полей. - Будапешт, 1976, с. 33-47.

121. Казакевич Д. И. Основы теории случайных функций в задачах гидрометеорологии / Д. И. Казакевич. – Л. : Гидрометеоиздат, 1989. – 230 с.

122. Казакевич Д.И. Основы теории случайных функций и ее применение в гидрометеорологии. - Л.: Гидрометеоиздат, 1977. - 320 с.

123. Климатические данные // CDIAC [Электронный ресурс] / Carbon Dioxide Information Analysis Center/–Washington, USA.– Режим доступа: http://cdiac.ornl.gov/by_new/bysubjec.html#climate.

124. Кобышева Н.В.. Наровлинский Г.Я. Климатологическая обработка метеорологической информации. - Л.: Гидрометеоиздат, 1978. – 295 с.

125. Лобанов В.А., А.Е.Шадурский Выделение зон климатического риска на территории России при современном изменении климата. Монография. Санкт-Петербург, издание РГГМУ, 2013. – 164 с.

126. Лобанов В.А., Анисимов, О.А., Современные изменения температуры воздуха на территории Европы. - // Метеорология и гидрология, № 2, 2003, с. 5-14.

127. Лобанов В.А., Задорожный С.П., Молдован Н.В., Шадурский А.Е., Шукри омар А. Информация и методы для оценки устойчивости расчетных гидрометеорологических характеристик при инженерных изысканиях //Инженерные изыскания. Всероссийский научно – аналитический журнал, октябрь 10/2011, с.52-58.

128. Лобанов В.А., И.А.Смирнов. А.Е.Шадурский. Практикум по климатологии. Часть 1. (учебное пособие). Санкт-Петербург, 2011. – 144 с.

129. Лобанов В.А., И.А.Смирнов. А.Е.Шадурский. Практикум по климатологии. Часть 2. (учебное пособие). Санкт-Петербург, 2012. – 141 с.

130. Лобанов В.А., Тощакова Г.Г. Проявление современных изменений климата на территории Костромской области. Монография. ФГБУ «Костромской центр по гидрометеорологии и мониторингу окружающей среды», Кострома. 2013 – 171 с.

131. Лобанов, В.А., Анисимов, О.А., 2003 Современные изменения температуры воздуха на территории Европы. Метеорология и гидрология, № 2, с. 5-14.

132. Малинин В.Н. Статистические методы анализа гидрометеорологической информации. СПб: изд. РГГМУ, 2008. – 408 с.

133. МГЭИК 2007: Изменение климата, 2007. Обобщающий доклад. Вклад рабочих групп I, II и III в Четвертый доклад об оценке Межправительственной группы экспертов по изменению климата (Пачаури Р.К., Райзингер А. и основная группа авторов (ред.)). МГЭИК, Женева, Швейцария, 104 с.

134. Н.Дрейпер, Г.Смит Прикладной регрессионный анализ. М., Статистика, 1973. – 392 с.

135. Определение основных расчетных гидрологических характеристик [Текст]: СП 33-101-2003.–М.: Госстрой России, 2004.–73 с.

136. Переведенцев Ю.П. Теория климата. Казанский государственный университет. 2009. – 503 с.

137. Рекомендации по статистическим методам анализа однородности пространственно-временных колебаний речного стока [Текст] / ГГИ.– Л.: Гидрометеоиздат, 1984.–78 с.

138. СНиП 23-01-99 Строительная климатология. М.: Госстрой России, 1999 – 74 с.

139. Шукри Омар А.А. Современные климатические изменения температуры воздуха и осадков в Йемене и прилегающих территориях // Ученые записки РГГМУ,2011,с.86-94.

140. Шукри Омар Абдулхаким Али Климатичские сценарии и их применимость для оценки будущих изменений климата на Аравийском полуострове// Ученые записки РГГМУ, 2013,№29,С.110-124.